

AUGMENTATION OF FORCED-CONVECTION HEAT TRANSFER
IN ROPED TUBES AND INVESTIGATION OF
VARIATION OF THE HEAT TRANSFER COEFFICIENT
AND FRICTION FACTOR FOR BOTH LAMINAR
AND TURBULENT FLOW



by

Abdi KORKMAZ

B.S., in M.E., Istanbul Technical University, 1977

Submitted to the Faculty of the Graduate School
of Engineering in Partial Fulfillment of
the Requirements for the Degree of

MASTER OF SCIENCE

in

MECHANICAL ENGINEERING

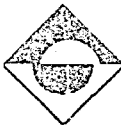
Boğaziçi University

1982

ACKNOWLEDGEMENT

I am deeply grateful to all who have been ready to help in the preparation of this work, and I wish to express my sincere thanks, in particular, to my thesis supervisors Prof. Dr. A. Rasim Büyüktür and Prof. Dr. Akin Tezel for their invaluable help and guidance, to Mr. Yahya Kemal Tayfun for providing the roped tubes, and to the members of the Heat Transfer Department of the Istanbul Technical University for their help in the construction of the experimental set up.

Special thanks are to Gülsen Karşit for her excellent typing.



ABSTRACT

Since the geometry of roped tubes and smooth tubes are different, the flow characteristics and the heat transfer coefficients associated with each tube are also different. Because of improved geometry it is possible to attain higher heat transfer coefficients in the case of roped tubes. However, the increase in the heat transfer coefficient is unavoidably associated with higher pressure drops. Therefore, the use of roped tubes with the intention of achieving high heat transfer rates is necessarily subject to justification. The intention of the present work is to determine, experimentally, the flow and the heat transfer characteristics of roped tubes selected from a representative class, to compare these characteristics with that of smooth and other profiled tubes, and thus to provide a quantitative basis for the justification of the use of such tubes to achieve high heat transfer rates with small size equipment.

ÖZET

Yivli borularla düz boruların geometrileri farklı olduğundan, her iki tip borudaki akış karakteristikleri ve ısı geçiş katsayıları da farklı olmaktadır. Değiş-tirilmiş geometri nedeniyle roped (yivli) borularda daha yüksek ısı geçiş katsayıları elde etmek mümkündür. Bununla beraber, yivli borularda, ısı geçiş katsayısındaki artışa karşılık, basınç kayıplarında da önemli bir artış meydana gelir. Bu nedenle, yüksek ısı geçişini başarmak amacıyla, yivli boruların kullanılması isteniyorsa böyle bir seçimin yerinde olup olmadığı araştırılmalıdır. Bu çalışmanın amacı, nümune olarak seçilen yivli boruların akış ve ısı geçiş karakteristiklerini elde ederek, bu karakteristikleri düz ve diğer profil boruların karakteristikleriyle karşılaştırmak ve böylece daha küçük bir tesisatla daha büyük ısı geçişi elde etmek için, yivli boruların kullanılmasının hangi koşullarda daha elverişli olduğunu belirten bir kaynak sağlamaktır.

TABLE OF CONTENTS

	Page
ACKNOWLEDGEMENT	iii
ABSTRACT	iv
ÖZET	v
1. INTRODUCTION	1
A. Roped Tubes, Description and Their Use	5
B. How to Increase Heat Transfer	14
C. Performance Evaluation Criteria	19
2. EXPERIMENTAL SET UP	23
A. Roped Tube Characteristics	31
B. Measured and Calculated Quantities and Measurements	33
3. HYDRODYNAMIC AND THERMAL ENTRY LENGTH	40
4. DETERMINATION OF HEAT TRANSFER COEFFICIENT AND FRICTION FACTOR AND RESULTS	45
A. Determination of Heat Transfer Quantities and Results	45
B. Determination of Friction Factor and Results	64
5. COMPARISON OF ROPED TUBES WITH TURBOTEC AND SPIRALLY FLUTED TUBES	90
6. CONCLUSION	99
NOMENCLATURE	103
APPENDIX A	106
APPENDIX B	115
APPENDIX C	149
REFERENCES	154

LIST OF FIGURES

	Page
FIGURE 1 Typical Roped Tubes	9
FIGURE 2 A Typical Roped Tube	10
FIGURE 3 Heat Transfer from Various Surfaces	16
FIGURE 4 Schematic Drawing of the Heat Transfer Experimental Set-Up	24
FIGURE 5 Photograph of the Heat Transfer Experimental Set-Up	27
FIGURE 6 Schematic Drawing of the Pressure Drop Experimental Set-Up	29
FIGURE 7 Photograph of the Pressure Drop Experimental Set-Up	30
FIGURE 8 Attaching Pressure Top to the Tube Wall	31
FIGURE 9 Location of the Thermometers and Thermocouples	34
FIGURE 10 Thermal Voltage - Temperature Relation of Thermocouple	36
FIGURE 11 Junction of Thermocouple	37
FIGURE 12 Schematic Drawing of the Prandtl Manometer	38
FIGURE 13 Photograph of the Inclined Manometer	39
FIGURE 14 Boundary Layer and Development of the Velocity Profile in a Tube	42
FIGURE 15 Temperature Profiles of the Test Heat Exchanger	45
FIGURE 16 Heat Transfer Results of the First Roped Tube in Transition and Turbulent Flow	55
FIGURE 17 Heat Transfer Results of the Second Roped Tube in Transition and Turbulent Flow	63

	Page
FIGURE 18 Heat Transfer Results of the Second Roped Tube in Laminar Flow	65
FIGURE 19 Friction Factor Results of Roped and Smooth Tubes in Entrance Region	77
FIGURE 20 Friction Factor Results of Roped and Smooth Tubes in Fully Developed Flow	89
FIGURE 21 Photographs of Turbotec Tube	91
FIGURE 22 Typical Tubes in the Spirally Fluted Category	92
FIGURE 23 Composite of Internal Turbulent Flow Heat Transfer Characteristics for Roped and Turbotec Tubes	93
FIGURE 24 Pressure Drop Characteristics for Roped and Turbotec Tubes	95

LIST OF TABLES

		Page
TABLE 1	How to Increase Heat Transfer	18
TABLE 2	Summary of Performance Criteria Evaluations	20
TABLE 3	Dimensions of Roped Tube	32
TABLE 4	Internal Nusselt Number and Heat Transfer Coefficient in the First Roped Tube in Turbulent Flow	50
TABLE 5	Heat Transfer Results of the First Roped Tube in Turbulent Flow	52
TABLE 6	Internal Heat Transfer Results of the First Roped Tube in Transition Flow	53
TABLE 7	External Heat Transfer Results of the First Roped Tube	54
TABLE 8	Internal Nusselt Number and Heat Transfer Coefficient of the Second Roped Tube in Turbulent Flow	57
TABLE 9	Heat Transfer Results of the Second Roped Tube in Turbulent Flow	58
TABLE 10	Heat Transfer Results of the Second Roped Tube in Transition Flow	59
TABLE 11	Heat Transfer Results of the Second Roped Tube in Laminar Flow	60
TABLE 12	External Heat Transfer Results of the Second Roped Tube	61
TABLE 13	Relations Between Friction Factor and Reynolds Number	68
TABLE 14	Friction Factor Results of the Smooth Tube in Entrance Region Laminar Flow	70
TABLE 15	Friction Factor Results of the Smooth Tube in Entrance Region Transition Flow	71

		Page
TABLE 16	Friction Factor Results of the Smooth Tube in Entrance Region Turbulent Flow	72
TABLE 17	Friction Factor Results of the Roped Tube in Entrance Region Laminar Flow	73
TABLE 18	Friction Factor Results of the Roped Tube in Entrance Region Critical Flow	74
TABLE 19	Friction Factor Results of the Roped Tube in Entrance Region Transition Flow	75
TABLE 20	Friction Factor Results of the Roped Tube in Entrance Region Turbulent Flow	76
TABLE 21	Friction Factor Results of the Smooth Tube in Fully Developed Laminar Flow	81
TABLE 22	Friction Factor Results of the Smooth Tube in Fully Developed Flow in Critical Region	82
TABLE 23	Friction Factor Results of the Smooth Tube in Fully Developed Transition Flow	83
TABLE 24	Friction Factor Results of the Smooth Tube in Fully Developed Turbulent Flow	84
TABLE 25	Friction Factor Results of the Roped Tube in Fully Developed Laminar Flow	85
TABLE 26	Friction Factor Results of the Roped Tube in Fully Developed Flow in Critical Region	86
TABLE 27	Friction Factor Results of the Roped Tube in Fully Developed Transition Flow	87
TABLE 28	Friction Factor Results of the Roped Tube in Fully Developed Turbulent Flow	88
TABLE 29	Summary of Other Tests with Spirally Fluted Tubing in Turbulent Single-Phase Internal Flow	97

1. INTRODUCTION

Over the last few years in every engineering design there has been ever increasing concern over the best method of using the world's limited resources. In particular, in the design of heat exchangers, since the cost of non-ferrous tubing is responsible for a substantial proportion of the capital cost of the overall equipment, great care has been exercised toward achieving the most economical method of using the limited resources of non-ferrous metal. This is particularly true in the case of heat exchanger equipment used in desalinization plants where the cost of non-ferrous tubes is between 15% and 20% of the total cost of the plant.

Such material saving consideration as well as the best energy utilization incentives and economic stimuli have led to expansion of efforts to produce more efficient heat transfer equipment. All of these efforts aim to improve the heat transfer performance and to reduce the size of the heat exchanger to be designed for a given heat load. The use of profiled tubes has been the most fruitful among such efforts [1].

The object of the present study is to determine, experimentally, the heat transfer coefficient and the friction factor for a representative set of roped tubes, to investigate the variation of this data with the Reynolds number, and finally to compare the performance of such tubes with that of smooth and other profiled tubes reported in the literature. The results thus obtained will provide a quantitative basis for the justification of the use of roped tubes to achieve high heat transfer rates with small size equipment.

There are various techniques of augmenting heat transfer resulting in an increase in the convective heat transfer coefficient [2]. Enhancement techniques can be classified as passive methods, which require no direct application of external power and as active schemes, which require external power [1].

Passive techniques include:

Treated surfaces

Rough surfaces

Extended surfaces

Displaced enhancement devices

Swirl flow devices

Surface tension devices

Fluid additives

The active techniques include:

Mechanical aids

Surface vibration

Fluid vibration

Electrostatic fields

Injection

Suction

Two or more of these techniques may be utilized simultaneously (compound augmentation). It is apparent that enhancement may be inherent in a heat exchange system, e.g., rough surface produced by standard manufacturing, surface vibration resulting from rotating machinery.

Compound techniques are a slowly emerging area of enhancement which hold promise for practical applications since the heat transfer coefficients can usually be increased above each of the several techniques acting alone.

Some examples [1]:

Rough tube wall with twisted tape inserts

Rough cylinder with acoustic problem

Internally finned tube with twisted tape inserts

Finned tube in fluidized beds.

The augmentation techniques were studied by various investigators and a general survey of these works

is given by A.E. Bergles [1]. Summary of tests with spirally fluted tubing in turbulent single-phase internal flow is given by A.E. Bergles [3]. Some investigations have been made with typical tubes in the spirally fluted category [4,17].

In Chapter 1, the necessity of using profiled tubes in the design of heat exchanger due to material restrictions will be emphasized, as it has always been happening in other engineering designs since the world's resources are limited. Furthermore, the intention of the present work and the practical techniques to enhance the heat transfer in tubes will be represented. Some resources for several researchers made on spirally fluted tubes including the roped tubes will be given. The roped tube which is a kind of profiled tube, its usage and its production process will be explained. The advantages and disadvantages of the roped tube will be concisely discussed. The theory of the increasing of heat transfer in tubes, specially in the roped tubes, will be discussed. Performance evaluation criteria to compare the profiled tubes with the smooth tubes and the criterion used in this project will be explained.

Two experimental set-ups to determine the values in heat transfer and pressure losses in tubes will be explained in the second chapter. The schema and the

photographs of the experiment installations and the pictures of some individual components will be presented. Finally, Chapter 2 includes the measured and calculated values in the experiments.

In Chapter 3, hydrodynamic and thermal entry length in the tubes will be explained.

In Chapter 4, the methods used to determine both the heat transfer coefficient and the friction factor will be explained, moreover the results will be tabled and plotted.

In Chapter 5, the results of the present work will be compared to the results of other experiments made using the similar tubes by other researchers.

In the last chapter, the general discussion about the conclusions of the present work will be given.

A. ROPED TUBES, DESCRIPTION AND THEIR USE

To improve the heat transfer, two different types of tubes can be used:

1. Extended surface tubes
2. Profiled tubes

As it will be explained in the next section, there are two ways of increasing heat transfer. The first way is, to provide more surfaces area per unit length of the tube. The extended surface tubes improve the heat transfer by using this fact as it can be inferred from their name. The extended surface tubes are generally produced by making some additions to the smooth tubes. The mostly used extended surface tubes are: finned tubes, integron tubes, innestar tubes, tubes with dimples, etc. Integron tubes are externally finned and their economical use requires in all cases that internal heat transfer coefficient, h_i , is significantly higher than external heat transfer coefficient, h_o . High fin integron tubes are mainly of interest when a gas or sometimes a slow-moving or highly viscous liquid flows transversely to the tube axis. Low fin integron is used predominantly in shell and tube heat exchangers and in these the external heat transfer situation is often fairly complex. Innestar tubes, containing an aluminium extrusion in the bore, are mainly used with evaporating refrigerant inside and water outside the tube.

Profiled tubes are also known as enhanced heat transfer tubes. Profiled tubes are produced modifying the shapes of smooth tubes. The profiled tubes (enhanced heat transfer tubes) mostly encountered are: roped tubes, fluted tubes, turbotec tubes.

With sufficiently high film coefficients the use of fins is uneconomical because the resistance to heat transfer through the fin becomes a factor of major importance. At some point, then, there is more incentive to increase the heat transfer coefficient, h , than the heat transfer surface, A , so that there is no significant increase in metal resistance above the plain tube value. Furthermore, because the metal content is not increased, the economical use of Enhanced Heat Transfer tubes does not require such a substantial performance advantage.

If both the external heat transfer coefficient, h_o , and the internal heat transfer coefficient, h_i , are extremely high, the resistance to heat transfer through the metal wall is significant even with plain tube and more so with Enhanced Heat Transfer tubes because of the higher film coefficients that are obtained. Metal resistance ultimately becomes a critical factor, therefore, but at much higher levels of film coefficient than is the case with finned tubes. It is therefore worth looking again at established views on choice of tube material and wall thickness, because too conservative an attitude may unnecessarily restrict the advantage that can be obtained.

There are also numerous duties with relatively

low film coefficients for which the use of "integron" is ruled out because the external heat transfer coefficient, h_o , and the internal heat transfer coefficient, h_i , are of similar magnitude. In some of these, a case may be made for external fins if an insert is used to give a compensating internal advantage, but in others an Enhanced Heat Transfer tube may be more attractive [18].

Profiled tubes (Enhanced Heat Transfer tubes) are selected for use in sea-water desalinization plant and are of potential interest in numerous other applications.

Fluted tubes are used in Vertical Tube Sea-Water Evaporators (steam condensing outside and salt water evaporating inside vertical tubes).

Roped tube is mostly uncountered profiled tubes in practice. Typically roped tubes manufactured by the Yorkshire Imperial Metals are illustrated in Figure 1 and a copper roped tube manufactured by the Kanatlı Boru Sanayi in Turkey is illustrated in Figure 2.

Roped tube as a profiled tube is manufactured by extruding the smooth tubes through the rotating three cylinders. These cylinders have so many rings on them, that these rings are precisely manufactured through lathe operations. To change the groove pitch and the groove

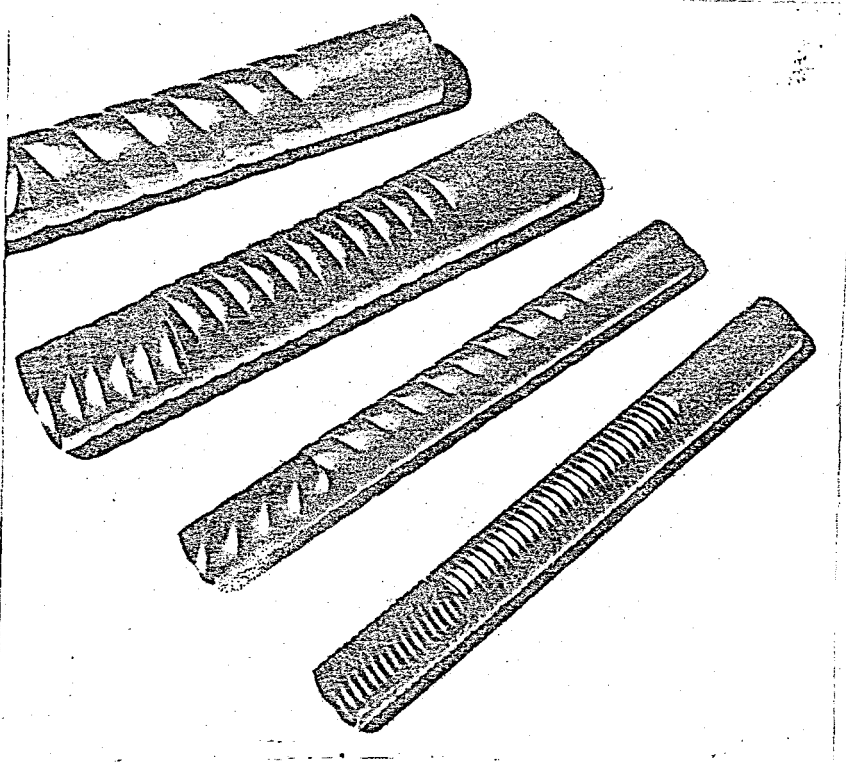


FIGURE 1. Typical Roped Tubes.

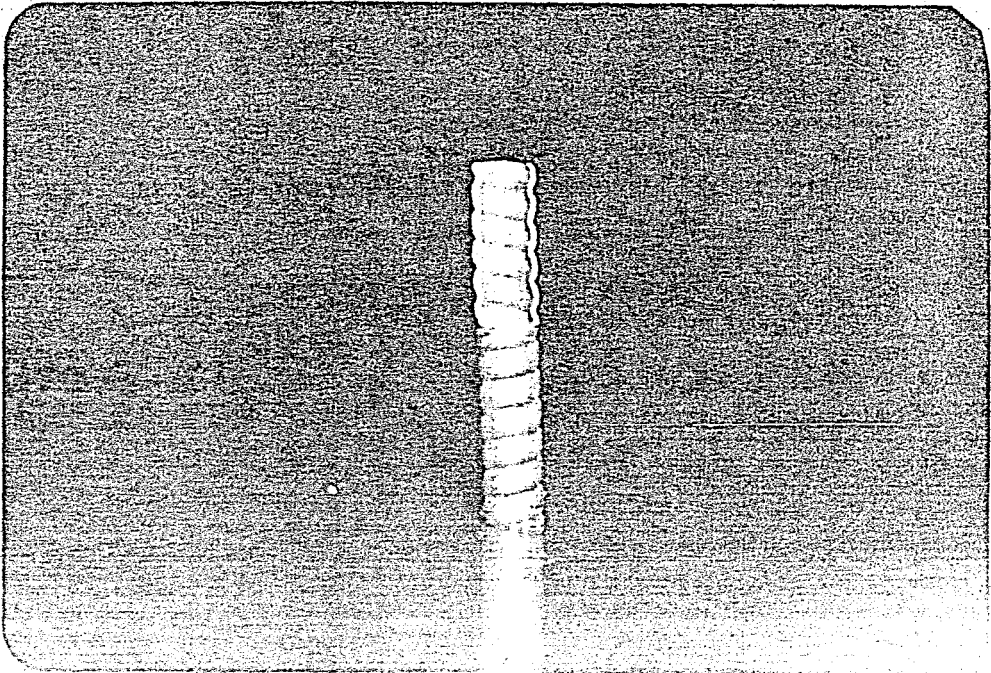


FIGURE 2. A Typical Roped Tube.

depth of the roped tube, the clearances between rings are modified. Regardless of the tube material this process can be effectively used to provide roped tubes. Roped tubes are manufactured in broadly the same range of materials as plain tubes.

Roped tubes are being used in Multi-Stage Flash pre-heaters (steam condensing outside and salt water inside horizontal tubes) associated with Vertical Tube Sea Water Evaporators. They are also being evaluated for power plant condensers. For duties of this type the performance of a wide range of profiles has been established experimentally and data are available from Yorkshire Imperial Metals [18,23]. Groove depth, groove pitch and helix angle can be varied widely to suit a diversity of applications [18].

When a roped profile is used in a steam condensing duty, the internal heat transfer coefficient, the friction factor and the condensing coefficient are all changed from the smooth (plain) tube values. A large increase in the internal heat transfer coefficient, h_i , can be obtained, but will be accompanied by a high friction factor and, where possible, the greatest benefit internally is likely to be obtained by increasing the tube diameter and using a reduced water velocity in association with a profile having a fairly high enhancement

characteristics. Externally, a suitable profile can avoid problems associated with the high surface tension in the condensate film and promote good drainage if the grooves are not too far out of vertical alignment and a much higher condensing coefficient than for a corresponding smooth tube can then be obtained. The best profile is a compromise between somewhat conflicting requirements and can give an overall gain of well over 30% with no increase in pressure drop above the smooth tube value and only a modest increase over the smooth tube cost per unit length. Tests on the most recently developed products are reported to give even better results [18].

Other profiles may be more suitable for other duties, e.g., where there are two single-phase fluids with comparable values of the heat transfer coefficient, h , as may be the case with heat transfer between two water streams or two gas streams. In such cases, roped tubes should be particularly attractive if the external fluid is in essentially longitudinal flow, as in double pipe heat exchanger or in units containing a small number of relatively long tubes.

Roped tubes may also be of interest if the external heat transfer coefficient, h_o , is much higher than the internal heat transfer coefficient, h_i , particularly

if the use of internal fins or inserts might present cleaning or pressure drop problems. In such a duty a profile that gives maximum advantage would be suggested and the overall benefit would probably not be affected much by the flow direction of the external fluid. This type of profile should also be of interest when a fluidized bed is used to improve external heat transfer and a compensating internal improvement is justified.

It is becoming increasingly clear that profiled tubes of the roped type can be effectively less costly than smooth tubes when steam condenses on the outside of horizontal tubes with cooling water in turbulent flow inside the tubes. Roped tubes are therefore of interest for applications such as multi-stage flash (MSF) sea water distillation plant and condensers for steam turbines in power stations and ships [19].

In the case of roped tubes, heat transfer rate increases as an advantage, but pressure drops also increase as a disadvantage. The advantage of roped tubes does not depend on the provision of increased surface area per unit length of tube and so metal usage is particularly economical. It is clear that, to obtain the roped tubes is a costly operation compared to the smooth tubes. However, the alternation cost of smooth tubes to get roped tubes is comparatively smaller than the total gain

obtained by using the roped tubes.

B. HOW TO INCREASE HEAT TRANSFER: TWO ALTERNATIVE APPROACHES

The rate of heat transfer, q , from a solid surface to an adjacent fluid, either stagnant or moving relative to the surface, is given as:

$$q = h A (T_s - T_\infty) \quad (1)$$

where h is the heat transfer coefficient, A is the heat transfer surface area, T_s is the surface temperature, and T_∞ is the ambient fluid temperature.

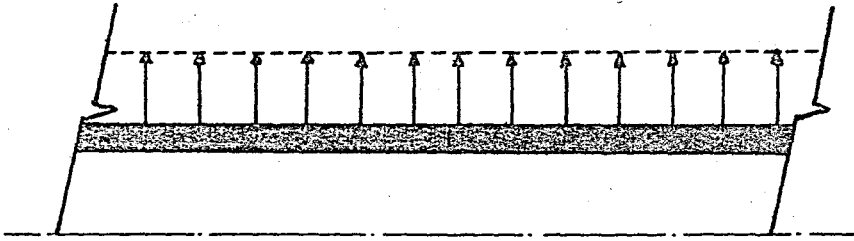
In the absence of a clear indication that there may be an economical alternative, it is natural first to consider smooth (plain) tube. Let h be the estimated plain surface heat transfer coefficient in a specified situation and A the required amount of plain surface. If a more economical solution is to be investigated, there are two basic possibilities to consider [18]:

1. Provide more surface area per unit length of tube, i.e., use of an extended surface tube and increase A .
2. Obtain more heat transfer per unit surface area, i.e., use of an Enhanced Heat Transfer

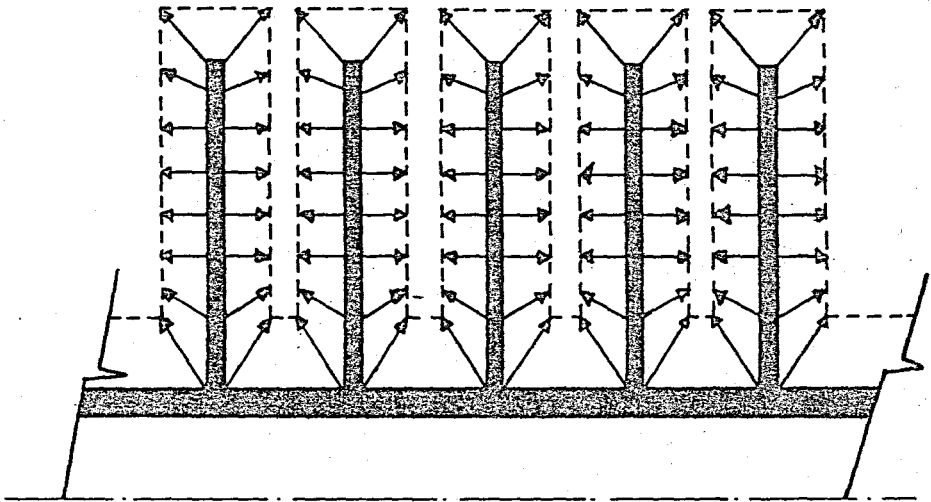
Tube and increase h .

Figure 3 illustrates the difference among various surfaces [18]. Figure 3.a represents a plain surface of unit length with a fluid boundary layer which determines a certain rate (indicated by the spacing of the arrows) of heat transfer per unit temperature difference. Figure 3.b represents a typical situation after the addition of fins, the boundary layer thickness being much the same as before (arrow spacing unchanged), however, the total heat transfer is increased because of larger surface per unit length of the tube [18].

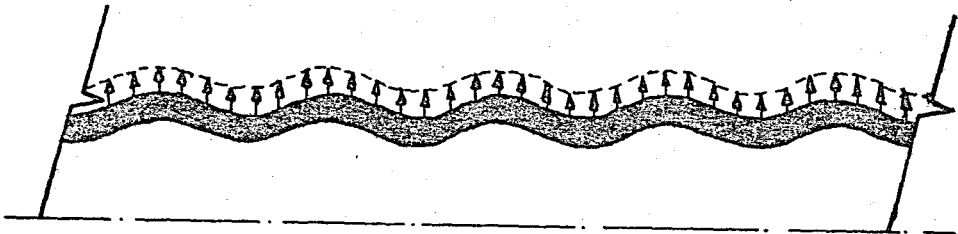
When there is a flow in a tube, starting from the entrance, the boundary layer begins to develop. At the end of the "Entry Length", the boundary layer completes its growing and the "Fully Developed Flow" occurs. Along with the forming of the "boundary layer", "laminar sublayer" develops and in laminar sublayer the flow is almost stagnant. Heat flows primarily by convection across the boundary layer and by conduction across the laminar sublayer. The rate of heat flow is, in general, inversely proportional to the laminar sublayer thickness. If the laminar sublayer thickness can effectively be reduced by changing the form of the surface, more heat will flow per unit surface area as indicated by the more closely spaced arrows in Figure 3.c. The heat transfer per



(a)



(b)



(c)

FIGURE 3. Heat Transfer from Various Surfaces [18].
(a) Heat Transfer from Plain Surface
(b) Heat Transfer from Finned Surface
(c) Heat Transfer from Corrugated Surface

unit length is increased without increasing the surface area of the tube appreciably.

In roped tubes, an account of spiral protuberances, the growing of boundary layer and laminar sublayer is disturbed. Being different in flow in smooth tubes; in roped tubes after each bulge turbulences occur, resulting in thinner laminar sublayer. Apart from this, these turbulences cause molecular movement in the fluid to increase. This means an addition increase in heat transfer coefficient.

Possible increases in the heat transfer area, A , or the heat transfer coefficient, h , can be regarded as alternative approaches to the problem, although they are not completely independent from each other. The use of an extended surface necessarily changes the geometry and therefore alters the value of h . The change of the heat transfer coefficient, however, is not substantial. Enhanced heat transfer tubes, on the other hand, change the amount of surface area per unit length of the tube, although this is of secondary importance. Tubes of intermediate types such as those having wires attached to the surface have both higher surface area, A , and heat transfer coefficient, h .

Table 1 shows the methods of increasing heat transfer.

TABLE 1
HOW TO INCREASE HEAT TRANSFER

As Alternative to Plain Tube		
Consider	Increaseing surface area, A, per unit length	Increasing film coefficient, h
Using	Extended Surface tube	Enhanced Heat Transfer Tube
Taking these factors into account	Requires relatively good heat transfer at other surface	Particularly promising with comparable h at the two surfaces
	Not effective with high h	Effective with high h
	Metal content per unit length greater than plain tube	No significant increase in metal content
	Large gain often obtainable, justifying relatively high cost	Gain of smaller magnitude justified by lower cost

C. PERFORMANCE EVALUATION CRITERIA

The recent activity in enhanced heat transfer is truly world wide. Most of the studies referred to are laboratory efforts which have established that a particular embodiment of a technique is effective in enhancing a given mode of heat transfer. However, a number of the techniques have made the transition to full-scale industrial heat exchange equipment. Numerous factors enter into the ultimate decision to use an enhancement technique: head load increas, surface area, reduction, pumping power requirements, initial cost, maintenance cost, safety, reliability, etc. Since these factors are numerous and sometimes difficult to quantize, the designer must make a decision based on the particular system and requirements. It is possible, though, to utilize a number of performance evaluation criteria for preliminary design guidance. Table 2 specifies different criteria suggested by Bergles et al. [24] which are used in evaluating relative merits of enhanced surfaces.

There is no single and absolute performance criteria for heat transfer augmentation. The two widely used are Equal Pumping Power and Equal Pressure Drop. Both criteria compare rough pipe performance to that of a smooth pipe. Comparison is made by taking the ratio of rough pipe heat transfer coefficient to the smooth

TABLE 2

SUMMARY OF PERFORMANCE CRITERIA EVALUATIONS

		CRITERION NUMBER							
		1	2	3	4	5	6	7	8
Fixed	Basic Geometry	X	X	X	X				
	Flow Rate	X						X	X
	Pressure Drop		X				X		X
	Pumping Power			X		X			
	Heat Duty				X	X	X	X	X
Objective	Increase Heat Transfer	X	X	X					
	Reduce Pumping Power				X				
	Reduce Exchange Size					X	X	X	X

pipe heat transfer coefficient as pumping power is kept constant. The latter criterion is similar to the former except this time the rough and smooth pipe performances that are compared involve equal pressure drop and not equal pumping power.

The choice as to which criterion will be used depends on the particular application. Equal pumping power consumption criterion is used more often since pumping power usually constitutes a large portion of the total cost. However, there are situations where equal pressure drop criterion becomes important as in system where pressure losses are critical.

The ratio of heat transfer coefficients for roped and smooth tubes can be written as h_{aug}/h_{smo} . Depending on which criterion is used, the subscripts P (Equal Pumping Power), ΔP (Equal Pressure Drop) or F (Equal Flow Rate) can be used. This ratio is a function of Reynolds number, Prandtl number and promoter geometry [2]. For example, when equal flow rate consumption is used:

$$\left[\frac{h_{aug}}{h_{smo}} \right]_F = f(\text{Re}, \text{Pr}, \text{promoter geometry})$$

In the present work, the first criterion in Table 2 is selected: Equal Flow Rate. The basic geometry is the same in roped and smooth tubes and equal flow rate

is considered. In that criterion, the basic geometry and flow rate are fixed and the objective is to increase heat transfer.

In heat transfer experiments, two different roped tubes were used. For both laminar and turbulent flows, the graphs that demonstrate the variation of the Nusselt number with the Reynolds number are plotted. In this particular study, no heat transfer experiments have been conducted with smooth tubes. Therefore, to compare the roped tubes with smooth tubes and to determine the variation of the Nusselt number with the Reynolds number, the empirical formulas that were obtained by other experiments, using smooth tubes under the same flow conditions (i.e., the same flow rate, Reynolds number and Prandtl number) are used in this present work. Consequently, the first criterion in Table 2 must be chosen.

2. EXPERIMENTAL SET UPS

As emphasized in the first chapter, the intention of the present work is to compare the heat transfer and pressure drop characteristics of the roped tubes and smooth tubes. Therefore, two different experimental set ups have been constructed:

1. A set up for Heat Transfer Measurements
2. A set up for Pressure Drop Measurements

In the experiments, roped tubes manufactured by "Finned Tube Company" (Kanatlı Boru Sanayi) which is a Turkish firm in Istanbul, were used.

1. Set up for Heat Transfer Measurements: The experimental heat exchanger is made up of two concentric tubes and it consists of one roped tube as the inner tube and one smooth tube as the outer tube. The first roped tube that has been tested has an inner diameter of 70 mm and an outer diameter of 76 mm. The first, outer smooth tube has an inner diameter of 81 mm and an outer diameter of 89 mm. The second roped tube has diameters of 19 and 21 mm and the outer smooth tube has diameters 54 and 60 mm. Figure 4 shows the experimental set up.

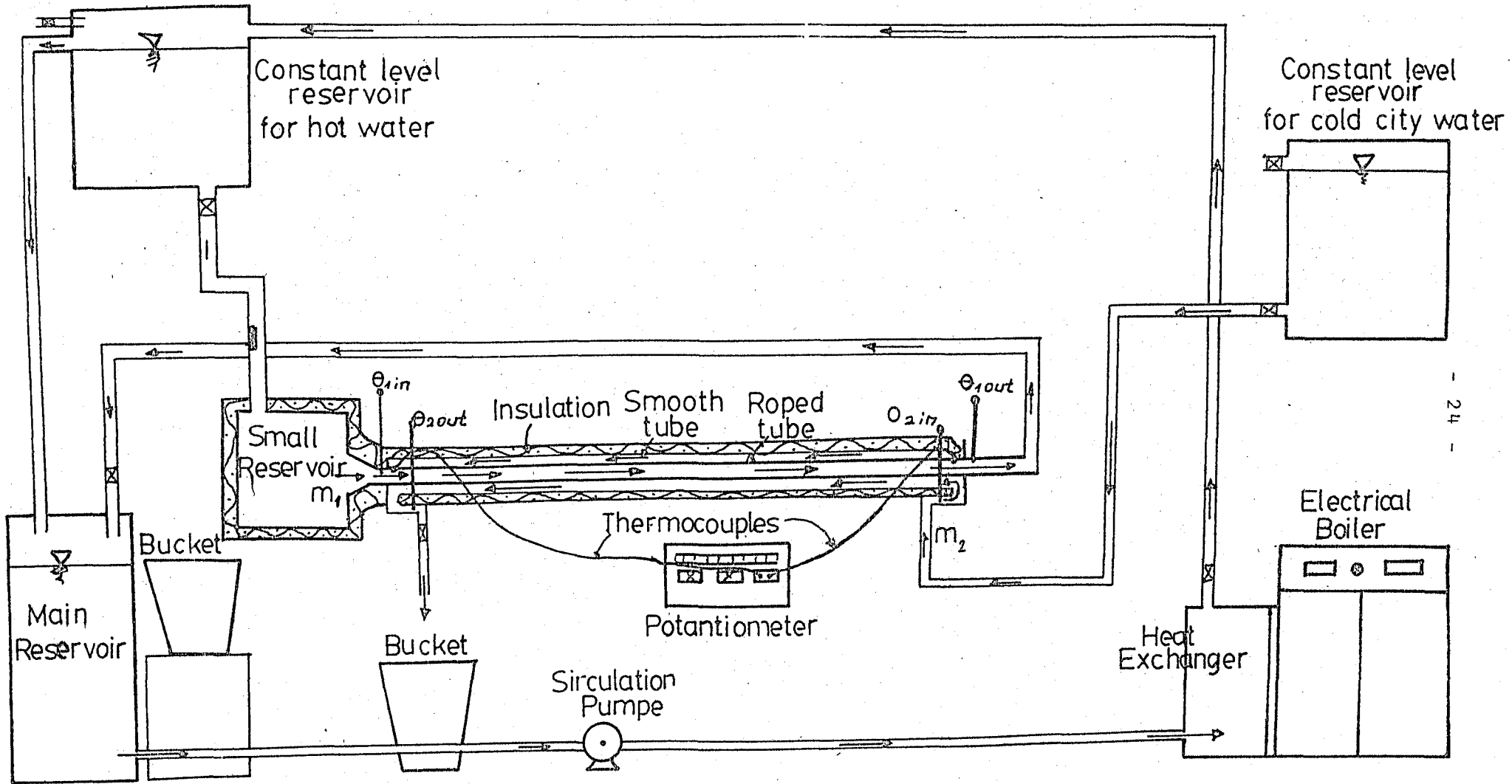


FIGURE 4. Heat Transfer Experimental Set-Up.

An electric boiler with an output of 35 Kw is used to generate steam which is used to heat the circulating water in the system through a test heat exchanger. The recirculating water is accumulated in a constant level reservoir and supplies fluid to the test heat exchanger to keep the flow rate constant. The main reservoir is below the constant level reservoir. The excess of water flows from the constant level reservoir through a pipe back into the main reservoir. Water in the main reservoir is pumped to the constant level reservoir flowing through the heat exchanger of the electric boiler. On the other hand, the hot water that flows through the roped tube also turns back to the main reservoir by a hose connection. The flow rate in the roped tube can be controlled by a valve that is placed at the end of the hose. The hose is separated from the main reservoir to measure the flow rate and water is allowed to flow into a big bucket.

Cold city water flows in the annular region. Another constant level reservoir is used for the city water in order to have constant flow rate. At the exit of that constant level reservoir, there is a valve which controls the flow rate of the city water. The flow direction of the city water in the annular region is opposite to the hot water which flows in the roped tube. The heated city water which flows from the test section

flows to a sink, and if desired it is collected in a bucket for ten minutes so that the flow rate can be measured.

In this experimental set up, there is a small reservoir before the roped tube. Hot water flows to this small reservoir from the constant level reservoir. There is a nozzle between the small reservoir and the roped tube. The aim is to obtain a uniform temperature distribution and a uniform velocity profile at the entrance of the roped tube.

The test heat exchanger is insulated with glass wool and is wrapped by cloth. The photograph of the heat transfer experimental set up is given in Figure 5.

2. Pressure Drop Experimental Set Up: In this study, a two meter long heat exchanger is built for the heat transfer experiments. A different experimental set up is constructed to measure pressure losses and to determine the variation of the friction factor with the Reynolds number. Experiments are conducted with 19 mm diameter and 6 m long roped and smooth tubes. In commercial heat exchangers, the tube length is usually two to three meters long. In the tubes tested, the length of the Entry Region for a Reynolds number of 2000, is 1.9 meters in laminar flow, so the pressure losses are mea-

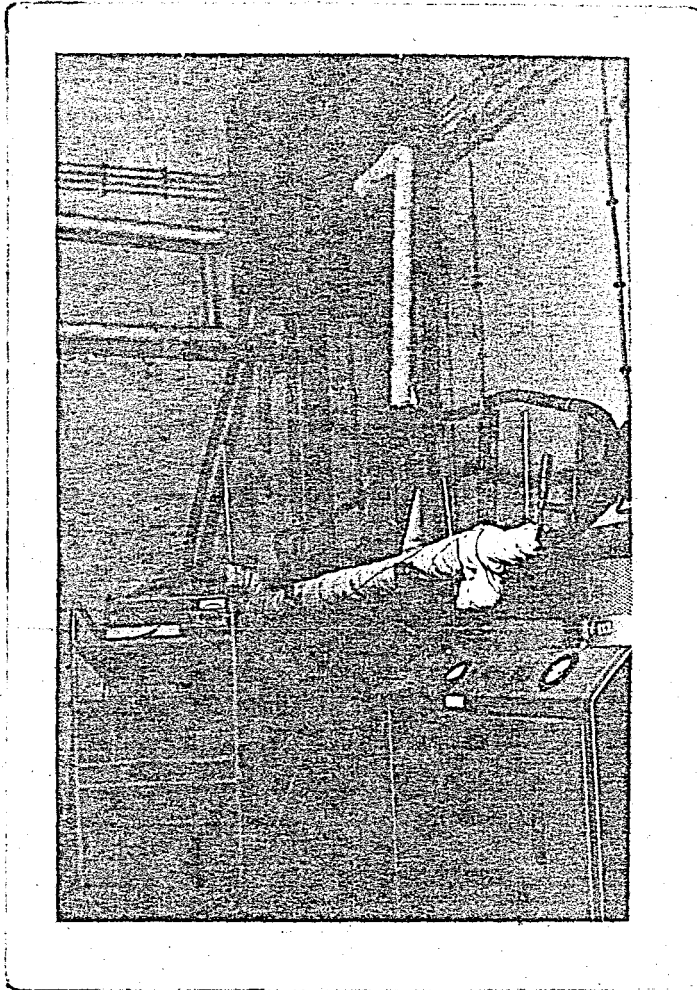


FIGURE 5. Heat Transfer Experimental Set Up.

sured both in the first 2 meter (Entry Region) and in the remaining 4 meter (Fully Developed Region). In turbulent flow, the entry length is approximately 1 m long, providing better measurements in the fully developed region. Experimental set up for measuring pressure drops is shown in Figure 6 and the photograph of the test set up is shown in Figure 7.

To attach pressure taps to the tube, plexiglass pieces are stuck to the tube and the taps are screwed into these pieces. 1.5mm holes are opened on the tube wall and the plexiglass pieces. The pressure taps are connected to a manometer by pieces of plastic hoses. Figure 8 shows the attachment of the pressure taps to the tube wall.

In the experiments, the city water at 20°C is used. The kinematic viscosity is proportional to the temperature of the water. To get high Reynolds numbers, the kinematic viscosity should be low. For this reason, water is heated to increase the Reynolds number.

Pressure Drops Experimental set up is mainly similar to the Heat Transfer Experimental set up. It should be emphasized that, the water entrance to the roped (or to the smooth tube) tube is very important to get uniform velocity profile at the tube entrance. Two nozzles

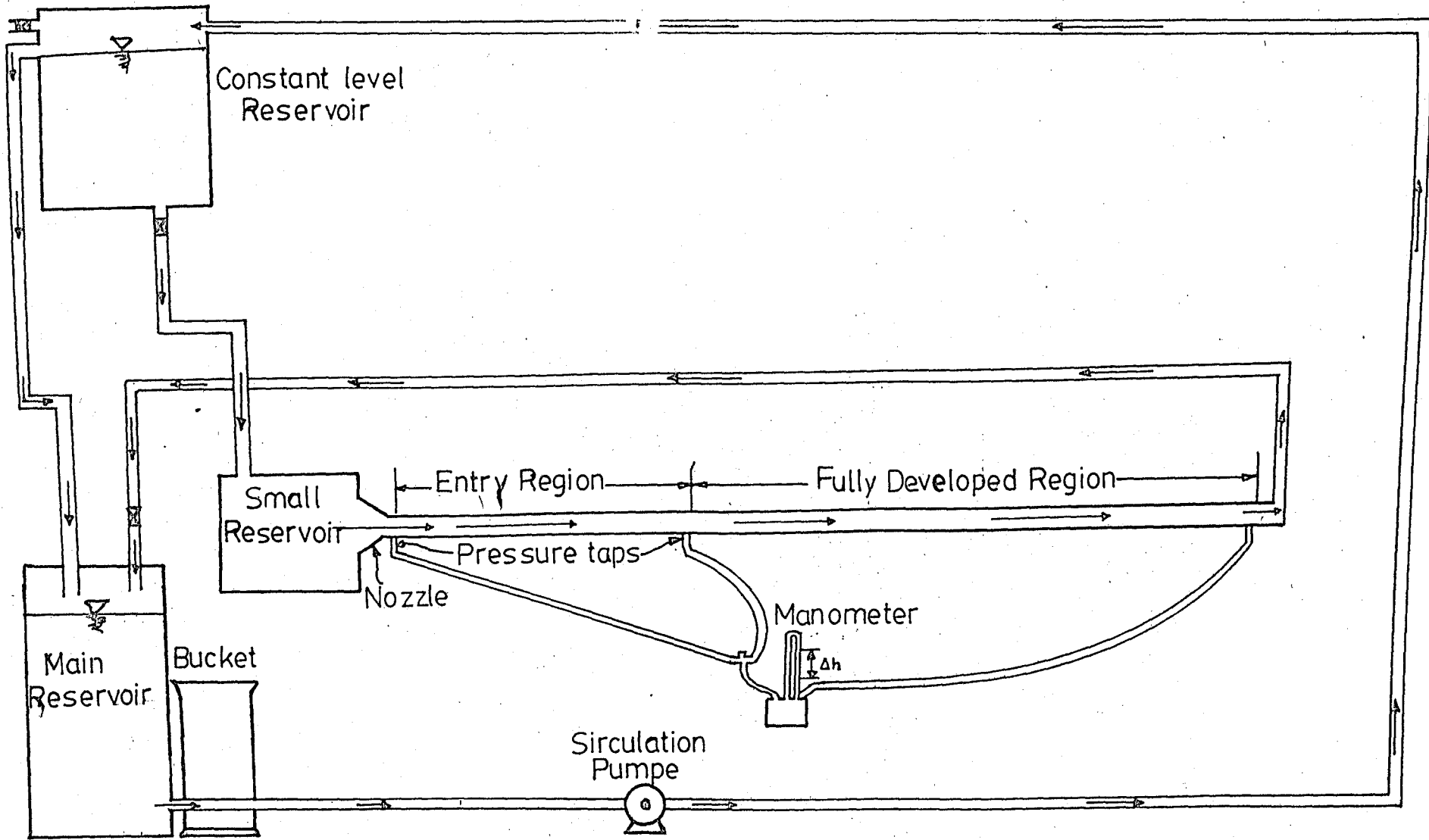


FIGURE 6. Pressure Drops Experimental Set-Up.

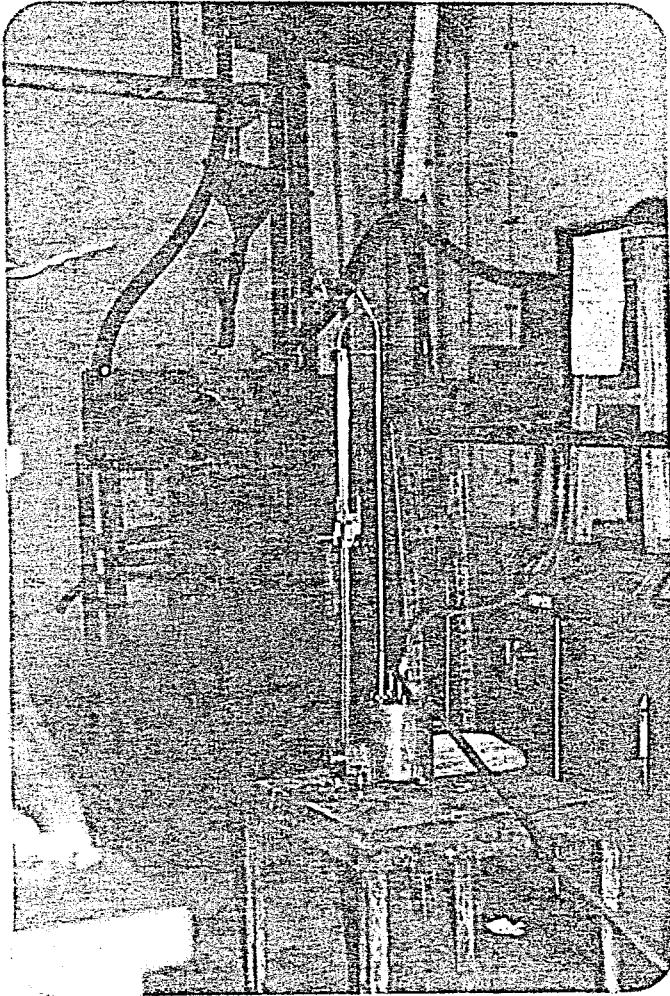


FIGURE 7. Pressure Drops Experimental Set Up.

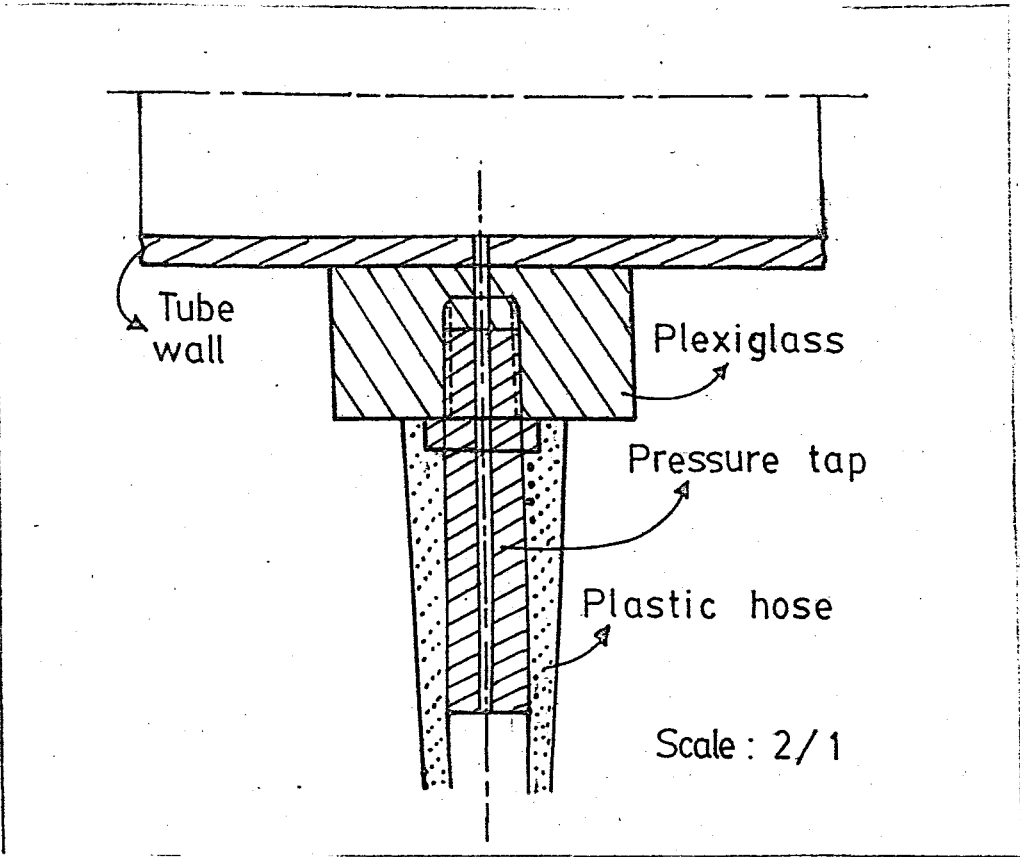


FIGURE 8. Attaching Pressure Taps to the Tube Wall.

are used to get uniform velocity profile. The steel nozzle is attached to the small reservoir with screws and nuts and welding attachment is avoided to have water enter into the tube smoothly. A plexiglass nozzle is attached to the steel nozzle and it is screwed into the tube.

A. ROPED TUBE CHARACTERISTICS

The dimensions of the roped tubes tested in the

heat transfer experiments are given in Table 3.

TABLE 3
DIMENSIONS OF ROPED TUBES

Roped Tube No.	Inside Diameter (mm)	Outside Diameter (mm)	Length (mm)	Groove Pitch (mm)	Groove Depth (mm)
1	70	76	2000	26.5	4.0
2	19	21	2000	8.5	0.5

The calculation of the cross sectional area of a roped tube is complicated. However, it can be assumed to be the same as the cross-sectional area of a smooth tube of the same dimensions. In fact, the difference between these two areas is negligible. Roped tube is manufactured from the smooth tube. In the present work, the diameters of the roped and smooth tube are assumed to be equal.

For the annular region, a hydraulic diameter:

$$D_h = \frac{4A}{P} \quad (2)$$

where A is the cross-sectional area of the annular region and P is the wetted perimeter, is used in the calculations.

B. MEASURE AND CALCULATED QUANTITIES AND MEASUREMENTS

The following quantities are measured in the experiments:

θ_{∞}	Ambient temperature ($^{\circ}\text{C}$)
$\theta_{1\text{in}}$	Inlet temperature of the hot water ($^{\circ}\text{C}$)
$\theta_{1\text{out}}$	Outlet temperature of the hot water ($^{\circ}\text{C}$)
$\theta_{2\text{in}}$	Inlet temperature of the cold water ($^{\circ}\text{C}$)
$\theta_{2\text{out}}$	Outlet temperature of the cold water ($^{\circ}\text{C}$)
ΔP	Pressure drop (mm. of water)
m_1	Mass flow rate of the water inside the roped tube (kg/h)
m_2	Mass flow rate of the water in the annular region (kg/h)
$\theta_{1\text{ts}}$	Surface temperature in the entrance of the hot water ($^{\circ}\text{C}$)
$\theta_{2\text{ts}}$	Surface temperature in the exit of the hot water ($^{\circ}\text{C}$)
θ_w	Average temperature of the water inside the tube ($^{\circ}\text{C}$)

CALCULATED QUANTITIES

The following quantities are calculated:

Q_1	Energy transferred from the hot water (Kcal)
Q_2	Energy transferred to the cold water (Kcal)
$\Delta\theta_m$	Logarithmic mean temperature difference

- h_i Internal heat transfer coefficient ($\text{Kcal/m}^2\text{h}^\circ\text{C}$)
- h_o External heat transfer coefficient ($\text{Kcal/m}^2\text{h}^\circ\text{C}$)
- v_1 Mean velocity of the water inside the roped tube (m/s)
- v_2 Mean velocity of the water in annular region (m/s)
- Re Reynolds number
- Nu Nusselt number
- f Fanning friction factor
- λ Moody-Darcy friction factor
- D_h Hydrolic diameter

The ambient temperature, the inlet and outlet temperatures of the hot and cold water streams were measured by means of thermometers calibrated to one tenth of a degree. In order to find heat transfer coefficients, the surface temperatures of the inner tube were measured at two locations by thermocouples. Figure 9 shows the location of the thermometers and the thermo-

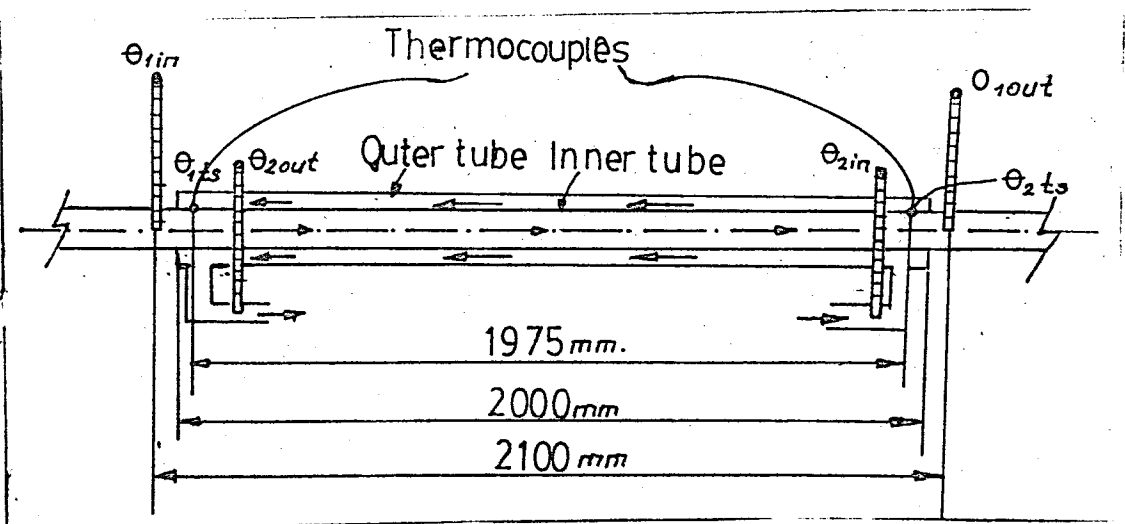


FIGURE 9. Locations of the Thermometers and Thermocouples.

couples. In the experiments, iron-constant thermocouples that were previously calibrated, were used. The variation of output voltage with temperature is given in Figure 10. As can be seen in Figure 10, when the temperature increases 1°C , the voltage increases 50 mV. Thermocouple outputs were measured by means of a special potentiometer. Readings are with respect to the ambient temperature. The thermocouples are welded to the inner tube wall such that the junctions are at the midpoint of the tube wall thickness. In the calculation of the heat transfer coefficient, it is assumed that temperature does not vary across the inner tube wall. The junction of the thermocouple is shown in Figure 11.

All the measurements are taken under steady state conditions. On the average a three hour period is necessary for the establishment of the steady state conditions. When the system reaches steady state conditions the temperatures are read in five minute intervals and the flow rates are measured in ten minute intervals and the the average values are calculated in for a one hour period.

The outlets of the test heat exchanger are accumulated in buckets for flow rates measurements.

Pressure losses along the roped and smooth tubes

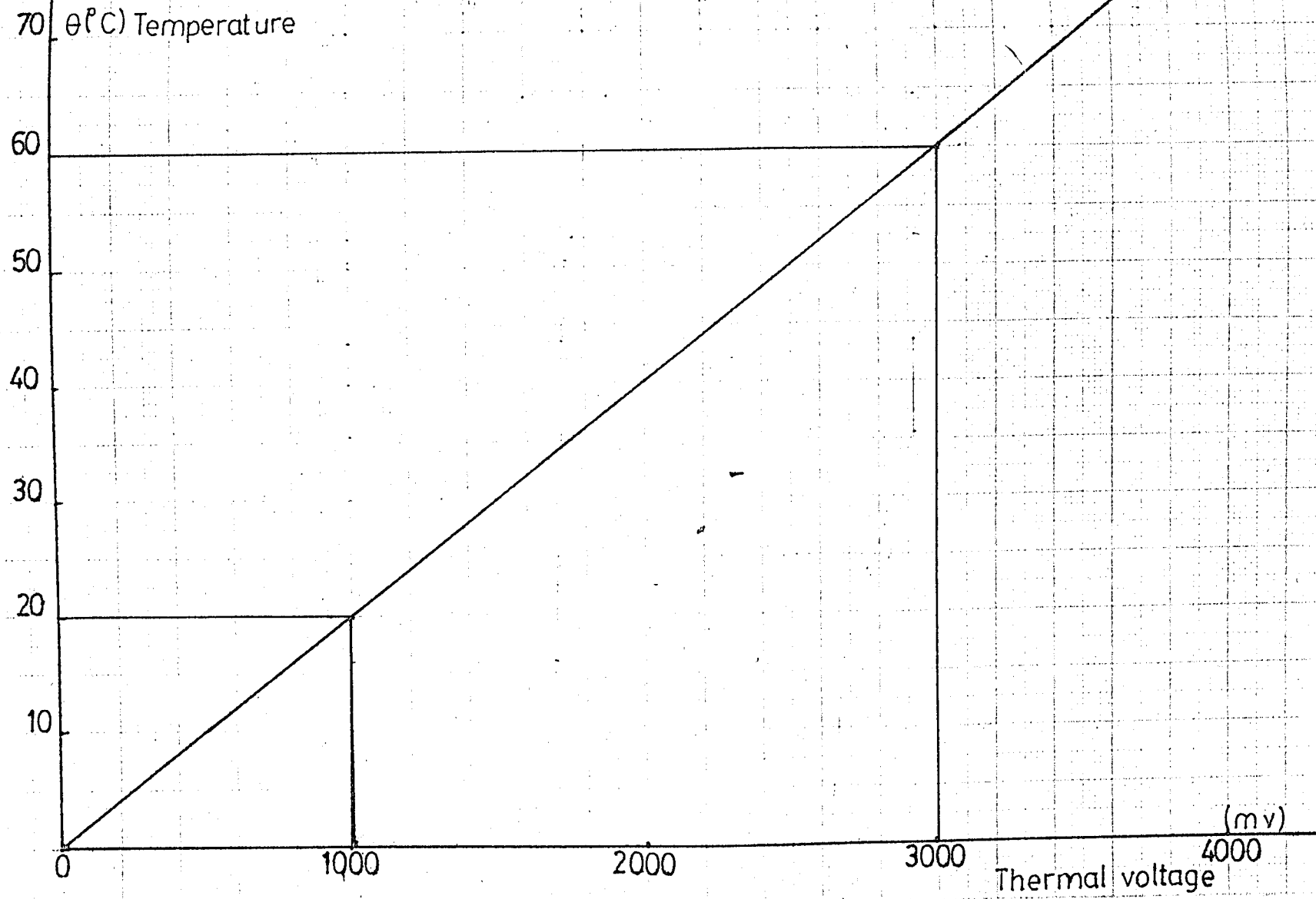


FIGURE 10. Thermal Voltage - Temperature Relation of Fe-Co Thermocouple.

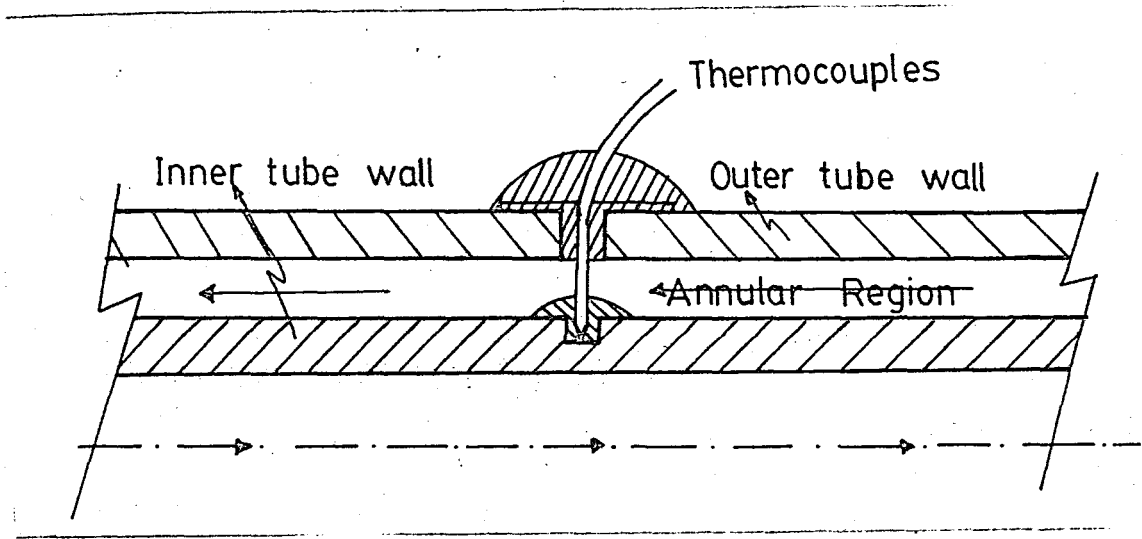


FIGURE 11. Junction of Thermocouple.

were measured by means of several manometers. In the experiments, three different manometers were used:

1. A U-type differential manometer
2. An inclined manometer
3. A Prandtl manometer.

When a U-type differential manometer is used, it is very difficult to measure the pressure losses precisely due to the fluctuations in the manometer's fluid level. Therefore, the Prandtl manometer which absorbs these fluctuations by use of capillary tubes is used. Furthermore, using Prandtl manometer, it is possible to make precise measurements up to one-twentieth of a "millimeter water column". The Prandtl manometer contains carbon

Tetrachloride inside as manometer's fluid. Carbon tetra-
chloride (CCl_4) is colored by iodine for better viewing.
The interface plane of water and CCl_4 is viewed through
lenses. Figure 12 shows the schematic drawing of the
Prandtl manometer.

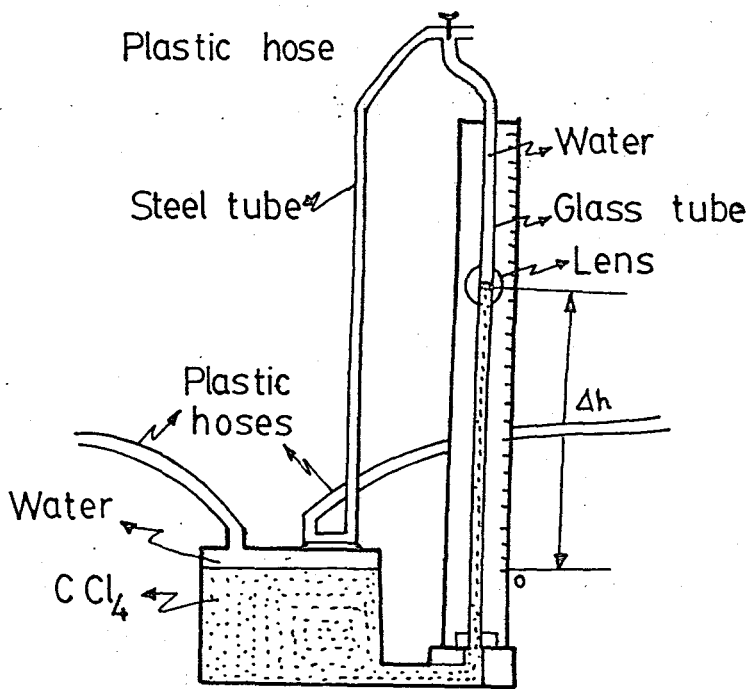


FIGURE 12. Schematic Drawing of the Prandtl Manometer.

As it will be explained in the fourth chapter, pressure losses are proportional to the square of the velocity. If the velocity increases, pressure losses increase. For high velocity, the Prandtl manometer could not be used to measure pressure losses since its height is not sufficient. For that reason, a special inclined manometer which is shown in Figure 13 is used to measure high pressure losses. Inclined manometer has mercury as the manometer fluid and its inclination can be changed.

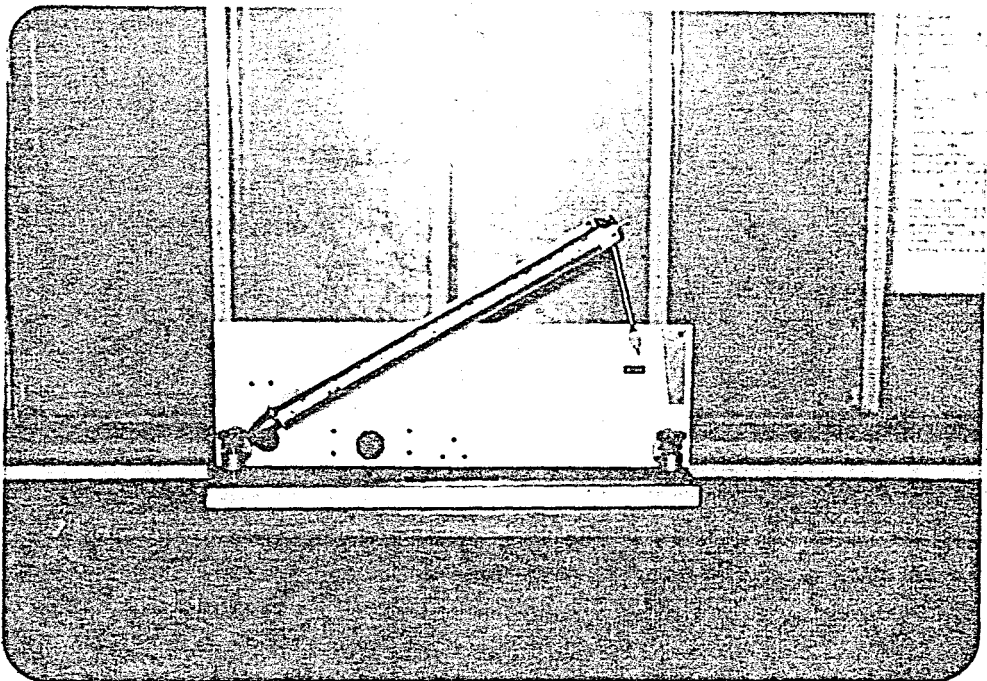


FIGURE 13. Photograph of the Inclined Manometer.

3. HYDRODYNAMIC AND THERMAL ENTRY LENGTH

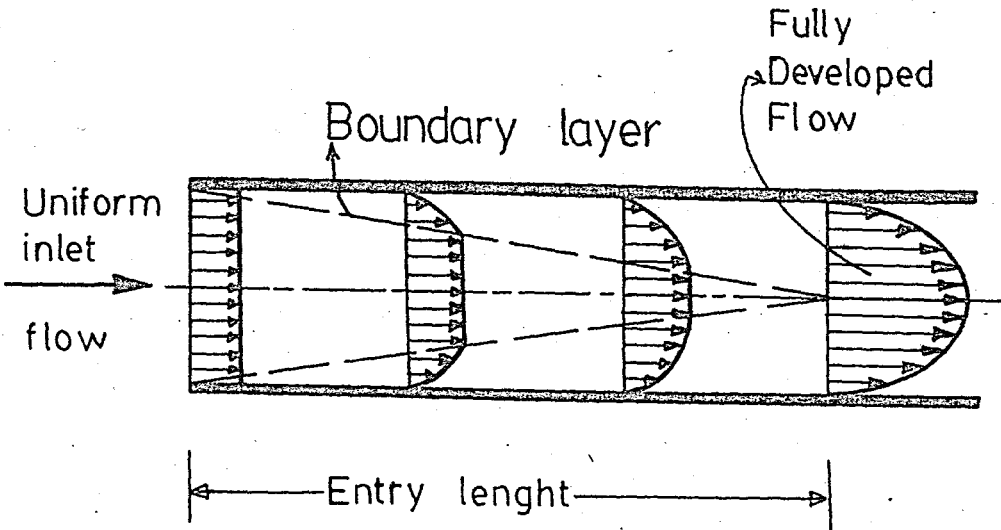
For both laminar and turbulent flow in the tubes, the wall shear stress is very large at the entrance of the tube and decreases in the direction of flow to a constant value. The magnitude of the pressure gradient dp/dx also decreases in the flow direction to a fixed value. If the tube entrance is well designed, the velocity profile is constant at the tube entrance. In the flow direction, the velocity profile changes, and eventually it becomes adjusted to a fixed profile. The wall shear stress, the pressure gradient, and the velocity profile all approach their fixed values asymptotically, and thus it is difficult to set a precise length for the Hydrodynamic Entrance Region. It could be defined as the region or length required for any one of these three quantities to reach a fixed value. [25].

On the other hand, the boundary layer will grow along the tube. At some point, the boundary layer from the wall will meet at the center of the tube. Beyond this point the velocity profile will not change its form. When the wall shear stress, the pressure gradient and

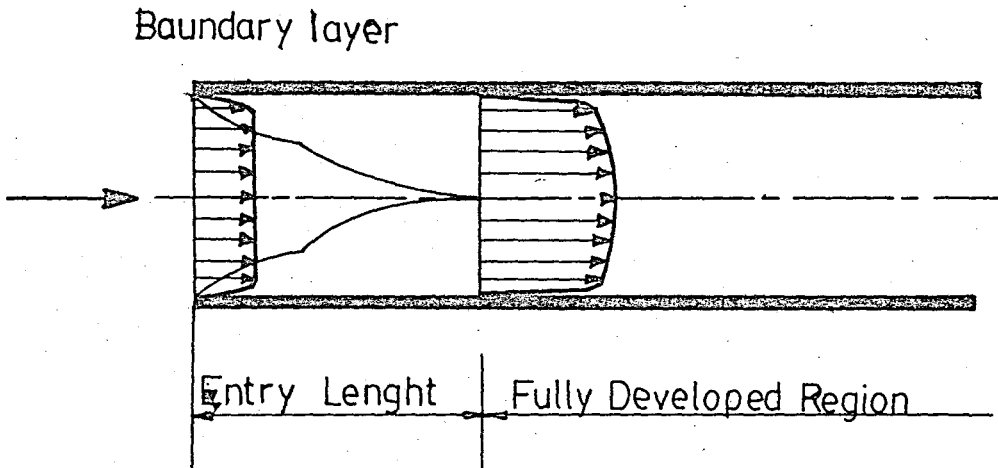
the velocity profile have reached their constant values, the flow is called "Fully Developed Flow". The development of the velocity profile and the growth of the boundary layer in the Entrance Region (Entry Length) are indicated in Figure 14.

In technical applications, one often is more concerned about the development of the hydrodynamic and thermal boundary layers together, rather than merely the hydrodynamic boundary layer alone. Thermal Entry Length (Thermal Entrance Region) can be defined as the length or region required for the temperature profile to reach its final form.

If the Prandtl number is greater than 1, it must follow that the velocity profile develops more rapidly than the temperature profile that even if both temperature and velocity are uniform at the tube entrance. Of course, the opposite also holds, and for a fluid with Pr number less than 1, the temperature profile develops more rapidly than the velocity profile. If the Pr number is 1, then heat and momentum are diffused through the fluid at the same rates, and the velocity and the temperature profiles will develop together. In the present experiments, Pr number is greater than 1, so the velocity profile develops much faster than the temperature profile.



(a)



(b)

FIGURE 14. Boundary Layer and Development of the Velocity Profile in a Tube.

- (a) In Laminar Flow
- (b) In Turbulent Flow

A good approximate formula for the length of tube necessary for the development of the laminar velocity profile is [26]:

$$\frac{x}{D} = \frac{Re}{20} \quad (3)$$

where x is the length of the Entry Region, D is the tube diameter and Re is the Reynolds number that is calculated as:

$$Re = \frac{v D}{\nu} \quad (4)$$

where v is the mean velocity, D is the tube diameter and ν is the kinematic viscosity.

A simple expression for the Entry Length, derived by Langhaar [27] in laminar tube flow is:

$$x = 0.057 Re D \quad (5)$$

So for $Re = 2000$, the highest value at which laminar flow can be conducted on, the Entry Length is about 114 times the tube diameter. For turbulent flow, the final state is reached sooner, the Entry Length is less dependent on the Reynolds number and a value of about 50 times the tube diameter is common for smooth tubes. If, however, the entry is sharp-edged or there are other

factors producing turbulence at the inlet, the Entry Length is reduced [27]. For example, the Entry Length is reduced in the roped tube since it has spiral protuberances.

In the present experiments, a roped tube which has an inner diameter of 19 mm and an outer diameter of 21 mm and 6 meters length, and a smooth tube which has the same dimensions, are tested to get the variation of friction factor as a function of the Reynolds number. For these two tubes, using formula (3), the Entry Length is found to be 1.9 meters for $Re = 2000$. In turbulent flow the Entry Length is shorter than laminar flow and it is possible to make measurements precisely in Fully Developed Region. As mentioned in Chapter 2, the pressure losses are measured in the first two meters length of the tubes and in the remaining 4 meters length of the tubes.

4. DETERMINATION OF HEAT TRANSFER COEFFICIENT, FRICTION FACTOR AND RESULTS

A. DETERMINATION OF HEAT TRANSFER QUANTITIES AND RESULTS

The inner and outer heat transfer coefficients for the roped tube and annular region can be determined by using the following relation:

$$Q = h A \Delta\theta_m \quad (6)$$

where h is the heat transfer coefficient, A is the heat transfer surface area, $\Delta\theta_m$ is the logarithmic mean temperature difference. Figure 15 shows the temperature profiles of the test heat exchanger.

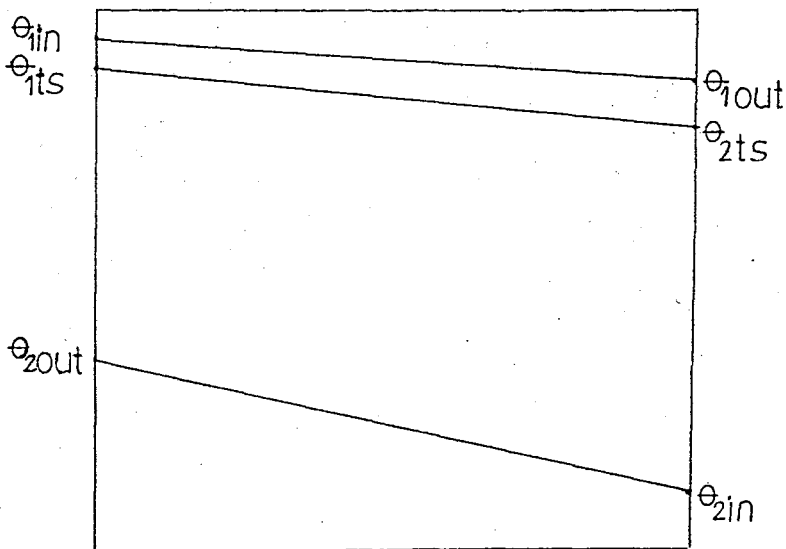


FIGURE 15. Temperature Profiles of the Test Heat Exchanger

Logarithmic mean temperature difference is calculated as

$$\Delta\theta_{m_i} = \frac{(\theta_{1in} - \theta_{1ts}) - (\theta_{1out} - \theta_{2ts})}{\ln \frac{\theta_{1in} - \theta_{1ts}}{\theta_{1out} - \theta_{2ts}}} \quad (7)$$

$$\Delta\theta_{m_o} = \frac{(\theta_{1ts} - \theta_{2out}) - (\theta_{2ts} - \theta_{2in})}{\ln \frac{\theta_{1ts} - \theta_{2out}}{\theta_{2ts} - \theta_{2in}}} \quad (8)$$

Using Equations (6), (7) and (8), the internal heat transfer coefficient, h_i , and the external heat transfer coefficient, h_o , can be written as:

$$h_i = \frac{Q_1}{A_i \Delta\theta_{m_i}} \quad (9)$$

$$h_o = \frac{Q_2}{A_o \Delta\theta_{m_o}} \quad (10)$$

Q_1 is the energy transferred from the hot water and it is calculated as:

$$Q_1 = m_1 c_1 (\theta_{1in} - \theta_{1out}) \quad (11)$$

where m_1 is the mass flow rate of the hot water inside the roped tube, c_1 is the specific heat of the hot water

at constant pressure.

Q_2 is the energy transferred to the cold water and it is calculated as:

$$Q_2 = m_2 c_2 (\theta_{2out} - \theta_{2in}) \quad (12)$$

where m_2 is the mass flow rate of the cold water in the annular, and c_2 is the specific heat of the cold water at constant pressure.

The mean velocity of the hot water inside the roped tube is:

$$v_1 = \frac{m_1}{S_1} \quad (13)$$

where S_1 is the cross-sectional area of the roped tube.

The mean velocity of the cold water in annular is:

$$v_2 = \frac{m_2}{S_2} \quad (14)$$

where S_2 is the cross-sectional area of the annular region of the test heat exchanger.

The non-dimensional quantities can be obtained as:

$$Re_i = \frac{v_1 D_i}{\nu_i} \quad (15)$$

$$Re_o = \frac{v_2 D_h}{\nu_o} \quad (16)$$

where ν_i and ν_o are kinematic viscosities of water inside the roped tube and in the annular respectively, D_i is the diameter of roped tube and D_h is the hydrolic diameter of the annular and it is calculated using Equation (2). The kinematic viscosities are taken from the table [28].

Nu numbers can be written as:

$$Nu_i = \frac{h_i D_i}{k_i} \quad (17)$$

$$Nu_o = \frac{h_o D_h}{k_o} \quad (18)$$

where k_i and k_o are thermal conductivity of water inside the roped tube and in annual respectively, and they are taken from the table [28].

To compare the roped tubes with smooth tubes, the ratio of the internal heat transfer coefficient of the roped tube to the internal heat transfer coefficient of the smooth tube should be found. This ratio (h_{roped} / h_{smooth}) shows the increment of the heat-transfer rate

in the case of roped tube. As mentioned in Chapter 1, in this particular study, no heat transfer experiments have been conducted with smooth tubes. Therefore, the empirical formulas that were given in the literature by other experiments for the smooth tubes, are used to compare the smooth tubes to the roped tubes.

On the other hand, the following ratios:

$$\frac{Nu_i}{Pr_i^{0.4}} \quad \text{or} \quad \frac{Nu_i}{Pr_i^{0.333}}$$

versus the Reynolds number are plotted in logarithmic scale to compare different tubes.

Nusselt numbers and internal heat transfer coefficients of the first roped tube and the smooth tube, and the ratio of $h_{i_{\text{roped}}}$ to the $h_{i_{\text{smooth}}}$ in the turbulent flow, are given in Table 4. As can be seen from Table 4, the ratio of $h_{i_{\text{roped}}}$ to the $h_{i_{\text{smooth}}}$ depends on the Reynolds number and average value of that ratio is 1.78. In Table 4, $Nu_{i_{\text{smooth}}}$ is calculated from [28]:

$$Nu = 0.036 Re^{0.8} Pr^{1/3} \left(\frac{D}{L}\right)^{0.055} \quad (19)$$

where L is the length of the tube and D is the tube diameter.

TABLE 4
INTERNAL NUSSELT NUMBER AND HEAT TRANSFER
COEFFICIENT IN THE FIRST ROPED
TUBE IN TURBULENT FLOW

Reynolds Number	$Nu_{i\text{ roped}}$	$Nu_{i\text{ smooth}}$	$h_{i\text{ roped}}$	$h_{i\text{ smooth}}$	$\frac{h_{i\text{ roped}}}{h_{i\text{ smooth}}}$
46417	340.0	205.17	2812	1697	1.65
41580	304	187.32	2517	1550.7	1.62
23397	194	117.67	1607	975	1.65
21896	194.6	117.0	1596	960	1.66
18906	161.9	98.35	1344	816.3	1.646
15178	170.6	88.24	1395	721.4	1.933
14442	142.8	83.46	1173	685	1.71
9817	148.37	61.7	1216	505.6	2.405
Average Value :					1.78

Internal Nusselt number, the ratio of Nu_i to the $Pr_i^{0.4}$ and the ratio of Nu_i to the $Pr_i^{0.33}$ for the first roped tube in turbulent flow are given in Table 5.

Internal Nusselt number and heat transfer coefficient, the ratio of Nu_i to the $Pr_i^{0.4}$ and the ratio of Nu_i to $Pr_i^{0.33}$ for the first roped tube in transition flow, are given in Table 6.

External Reynolds number, Nusselt number, heat transfer coefficient $Nu_o/Pr_o^{0.4}$, $Nu_o/Pr_o^{0.33}$ values are given in Table 7. The mean velocity of water in annular region is low since the cross-sectional area of the annular is very small and the height of the constant level reservoir which supplies cold water to the annular is small. The flow and heat transfer in annular region of the tested heat exchanger is not the object of the present study.

Heat transfer characteristics of the first roped tube in transition and turbulent flow (the variation of the ratio of Nu_i to $Pr_i^{0.4}$ versus Re_i) are given in Figure 16.

Nusselt numbers and internal heat transfer coefficients of the second roped tube and smooth tube, and the ratio of $h_{i\text{ roped}}$ to the $h_{i\text{ smooth}}$ in turbulent flow are

TABLE 5
HEAT TRANSFER RESULTS OF THE FIRST ROPED
TUBE IN TURBULENT FLOW

Re_i	Nu_i	$\frac{Nu_i}{Pr_i^{0.4}}$	$\frac{Nu_i}{Pr_i^{0.33}}$
46417	340.0	255.0	270.0
41580	304.0	230.0	254.0
23397	194.0	147.0	154.0
21896	194.6	140.0	147.8
18906	161.9	124.0	130.0
15178	170.6	120.0	128.2
14442	142.8	103.0	109.0
9817	148.4	106.0	112.0

TABLE 6
INTERNAL HEAT TRANSFER RESULTS FOR THE FIRST
ROPED TUBE IN TRANSITION FLOW

Re_i	h_i	Nu_i	$\frac{Nu_i}{Pr_i^{0.4}}$	$\frac{Nu_i}{Pr_i^{0.33}}$
8586	1151	141.6	97.6	104.2
7108	1065	128.8	96.0	100.9
6664	1076	130.6	95.9	101.0
4743	1013	123.3	89.3	94.3
4150	996	121.3	89.4	92.6
3352	967	117.5	85.0	90.0

TABLE 7
 EXTERNAL HEAT TRANSFER RESULTS FOR THE
 FIRST ROPED TUBE

Re_o	Nu_o	h_o	$\frac{Nu_o}{Pr_o^{0.4}}$	$\frac{Nu_o}{Pr_o^{0.33}}$
597	5.38	591.4	3.13	3.45
594	4.55	499	2.66	2.91
537	3.24	351	1.78	1.97
507	2.86	311	1.59	1.76
500	3.63	395	2.02	2.25
497	3.46	376	2.06	2.26
460	2.40	259	1.29	1.44
459	2.76	278	1.49	1.66
444	2.87	310	1.56	1.73
443	2.64	285	1.43	1.59
398	1.73	217	0.72	1.03
390	2.10	226	1.12	1.25
335	2.18	239	1.25	1.38

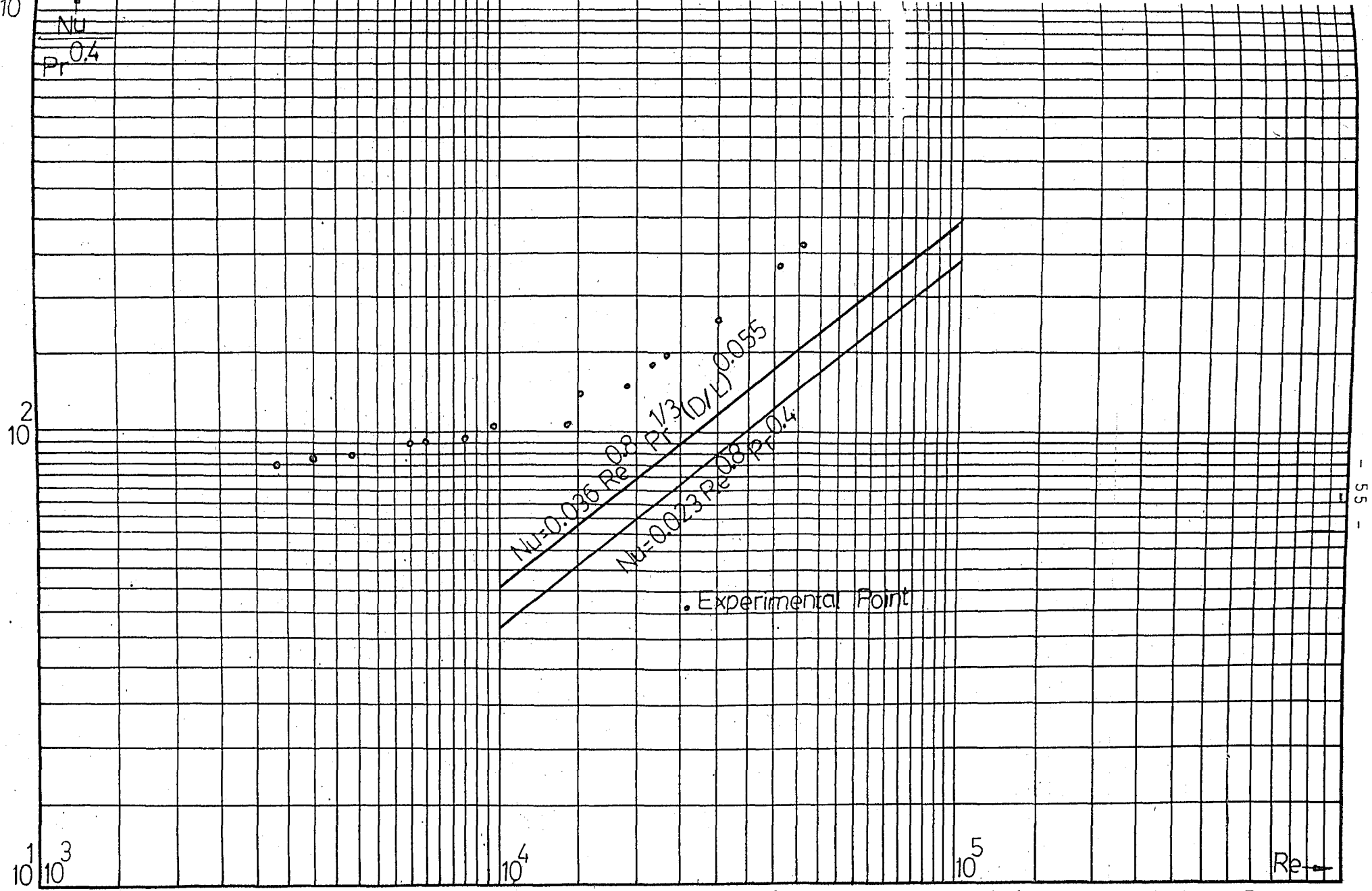


FIGURE 16. Heat Transfer Results of the First Roped Tube in Transition and Turbulent Flow.

given in Table 8. The average value of the ratio of $h_{i_{\text{roped}}}$ to $h_{i_{\text{smooth}}}$ is 1.22, i.e., the increment of the heat transfer rate is 20% in the case of roped tubes.

In table 8, $Nu_{i_{\text{smooth}}}$ is calculated using Equation (19).

Internal Nusselt number, the ratio of Nu_i to $Pr_i^{0.4}$ ($Nu_i/Pr_i^{0.4}$) and the ratio of Nu_i to $Pr_i^{0.33}$ ($Nu_i/Pr_i^{0.33}$) for the second roped tube in turbulent flow are given in Table 9.

Internal Nusselt number and heat transfer coefficient, $Nu_i/Pr_i^{0.4}$, $Nu_i/Pr_i^{0.33}$ values for the second roped tube in transition flow are given in Table 10. It should be noted that, the heat transfer results of the two roped tubes tested in the present experiment, are different. The results of the second roped tube are better than the first one.

Internal heat transfer coefficient, Nusselt number, the ratio of Nu_i to $Pr_i^{0.4}$ and the ratio of Nu_i to $Pr_i^{0.33}$ for the second roped tube in laminar flow, are given in Table 11.

External heat transfer coefficient, Nusselt number, the ratio of Nu_o to $Pr_o^{0.4}$ and the ratio of $Nu_o/Pr_o^{0.33}$ for the second roped tube (in annular region) are given in Table 12.

TABLE 8
INTERNAL NUSSELT NUMBER AND HEAT TRANSFER
COEFFICIENT OF THE SECOND ROPED TUBE
IN TURBULENT FLOW

Re_i	$Nu_{i,roped}$	$Nu_{i,smooth}$	$h_{i,roped}$	$h_{i,smooth}$	$\frac{h_{i,roped}}{h_{i,smooth}}$
35594	209.0	147.15	6383	4492	1.42
32931	181.7	141.82	5566	4344	1.28
27586	142.33	123.0	4360	3767	1.157
22193	145.0	107.8	4470	3524	1.344
20634	116.0	101.23	3424	3076	1.145
14797	84.24	75.33	2574	2301	1.118
12104	70.55	64.14	2154	1964	1.10
Average Value :					1.22

TABLE 9

HEAT TRANSFER RESULTS OF THE SECOND
ROPED TUBE IN TURBULENT FLOW

Re_i	Nu_i	$\frac{Nu_i}{Pr_i^{0.4}}$	$\frac{Nu_i}{Pr_i^{0.33}}$
35594	209.0	166.7	173.0
32931	181.7	140.6	147.0
27586	142.33	110.14	115.2
22193	145.0	106.75	112.6
20634	116.0	85.88	90.5
14797	84.24	64.6	67.7
12104	70.55	54.13	56.7

TABLE 10

INTERNAL HEAT TRANSFER RESULTS FOR THE SECOND
ROPED TUBE IN TRANSITION FLOW

Re_i	h_i	Nu_i	$\frac{Nu_i}{Pr_i^{0.4}}$	$\frac{Nu_i}{Pr_i^{0.33}}$
8866	1362	44.6	34.0	35.7
7771	1396.8	45.87	34.28	36.0
6570	1160	38	28.4	30.0
5427	1102	36.28	26.66	28.0
4675	836.8	27.5	20.0	21.46
3072	676.5	22.36	16.12	17.0

TABLE 11

INTERNAL HEAT TRANSFER RESULTS OF THE SECOND
ROPED TUBE IN LAMINAR FLOW

Re_i	h_i	Nu_i	$\frac{Nu_i}{Pr_i^{0.4}}$	$\frac{Nu_i}{Pr_i^{0.33}}$
2174	583	19.27	13.9	14.7
1776	500	16.6	11.76	12.5
1439	493	16.4	11.45	12.2
950	466	15.67	11.0	11.7
730	391	13.2	8.55	9.2
482	304	10.3	6.5	7.0
200	195	6.67	4.0	4.4

TABLE 12
EXTERNAL HEAT TRANSFER RESULTS OF
THE SECOND ROPED TUBE

Re_o	h_o	Nu_o	$\frac{Nu_o}{Pr_o^{0.4}}$	$\frac{Nu_o}{Pr_o^{0.33}}$
2532	118.8	7.49	3.12	3.64
2444	121.5	7.66	3.19	3.71
2329	195.8	9.19	3.83	4.47
2328	163.7	10.31	4.29	5.01
2292	193.0	12.16	5.26	6.10
2278	142.5	8.97	3.75	4.37
2256	168.5	10.63	4.43	5.16
2245	213.0	13.42	5.80	6.73
2185	196.0	12.35	5.19	6.04
2092	154.3	9.74	3.94	4.65
2015	180.0	11.32	4.68	5.44
2013	208.0	13.10	5.39	6.30
1988	135.0	8.52	3.49	4.08
1984	272.0	17.12	7.16	8.35
1966	240.0	15.0	6.27	7.30
1927	294.4	18.5	7.83	9.10
1778	137.0	8.59	3.58	4.19
1717	144.0	9.06	3.79	4.44
1674	355	22.50	9.23	10.78
1408	268.6	17.0	6.47	8.15

Heat transfer results of the second roped tube in transition and turbulent flow are given in Figure 17. For fully developed turbulent flow in smooth tubes the following relation is recommended by Dittus and Boelter [29]:

$$\text{Nu} = 0.023 \text{Re}^{0.8} \text{Pr}^n \quad (20)$$

The properties in this equation are evaluated at the fluid bulk temperature and the exponent n has the following values:

$$n = 0.4 \text{ for heating}$$

$$n = 0.3 \text{ for cooling.}$$

To calculate the Nusselt number of the smooth tube in Figure 17, Equation (19) and Equation (20) are used. Comparing the results obtained from Equations (19) and (20), it is possible to emphasize that, heat transfer rate in Entrance Region is higher than in the Fully Developed Region. As can be seen in Figure 17, experimental points obtained in this particular study are above the smooth tube results, i.e., heat transfer rate in turbulent flow in the roped tube is higher than in the smooth tube. It should be noted that the increment of the heat transfer rate in the roped tube due to the smooth tube, depends on the Re number. If the Re number

NO
PT 0.4

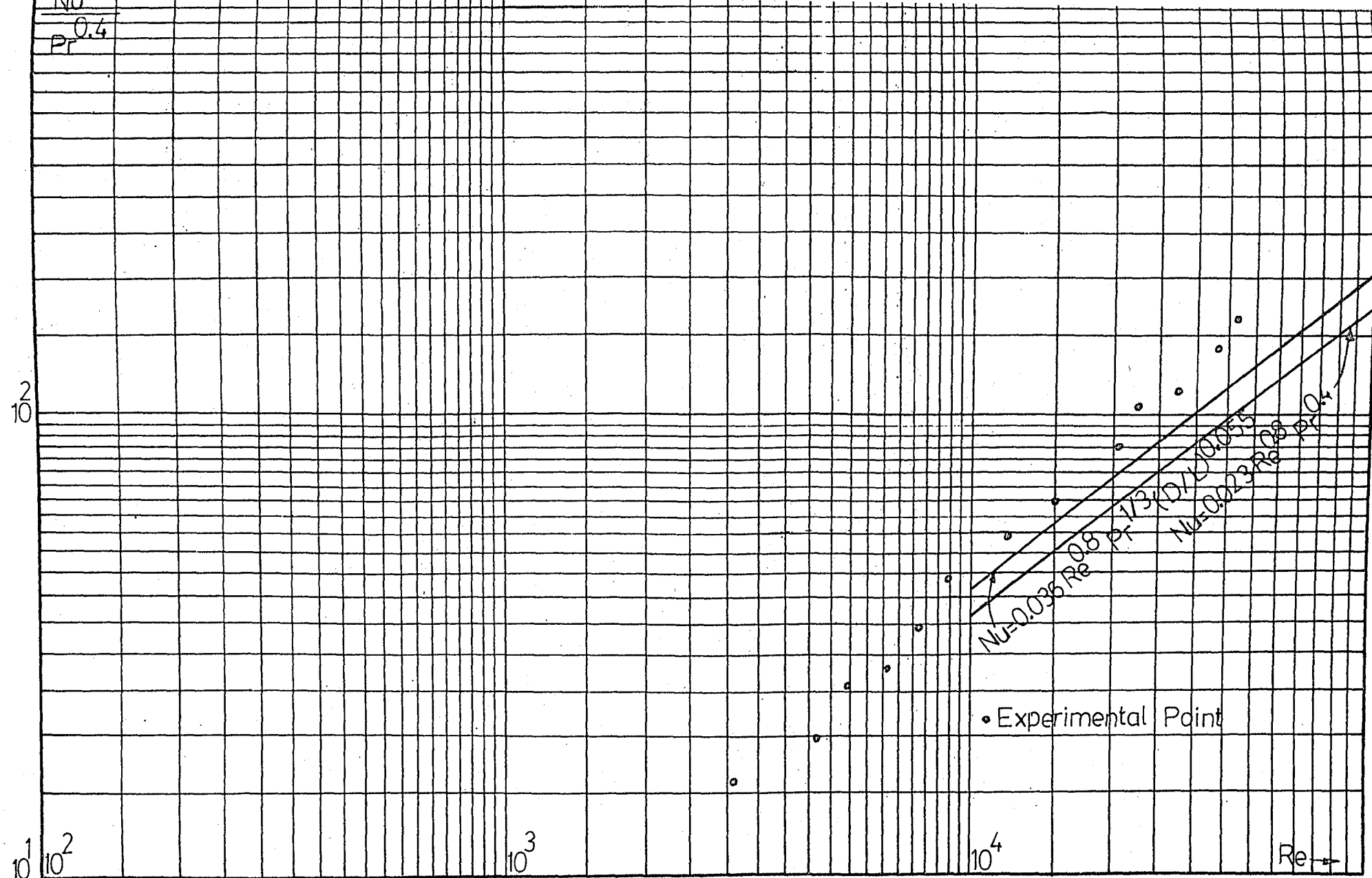


FIGURE 15 - Heat Transfer Results of the Second Roped Tube in Transition and Turbulent Flow.

increases, the ratio of the heat transfer coefficient of the roped tube to the heat transfer coefficient of the smooth tube increases.

In the literature, there are no correlation available to calculate the Nu number in transition flow in a tube, therefore, it is necessary to make experiments using both roped and smooth tube in transition flow.

Heat transfer results of the second roped tube in laminar flow are presented in Figure 18. To calculate the Nusselt number of the smooth tube, the following empirical relation presented by Housen [29] is used:

$$\text{Nu} = 3.66 + \frac{0.0668(D/L)\text{RePr}}{1 + 0.04|(D/L)\text{RePr}|^{2/3}} \quad (21)$$

B. DETERMINATION OF FRICTION FACTOR AND RESULTS

The friction coefficient f is defined by [29]

$$\Delta P = f \frac{L}{D} \rho \frac{v^2}{2g} \quad (22)$$

where ΔP is pressure drop along the tube, L is the length of the tube, D is the diameter of the tube, ρ is the fluid density (mass per unit of volume), v is the mean flow velocity and g is the acceleration of gravity.

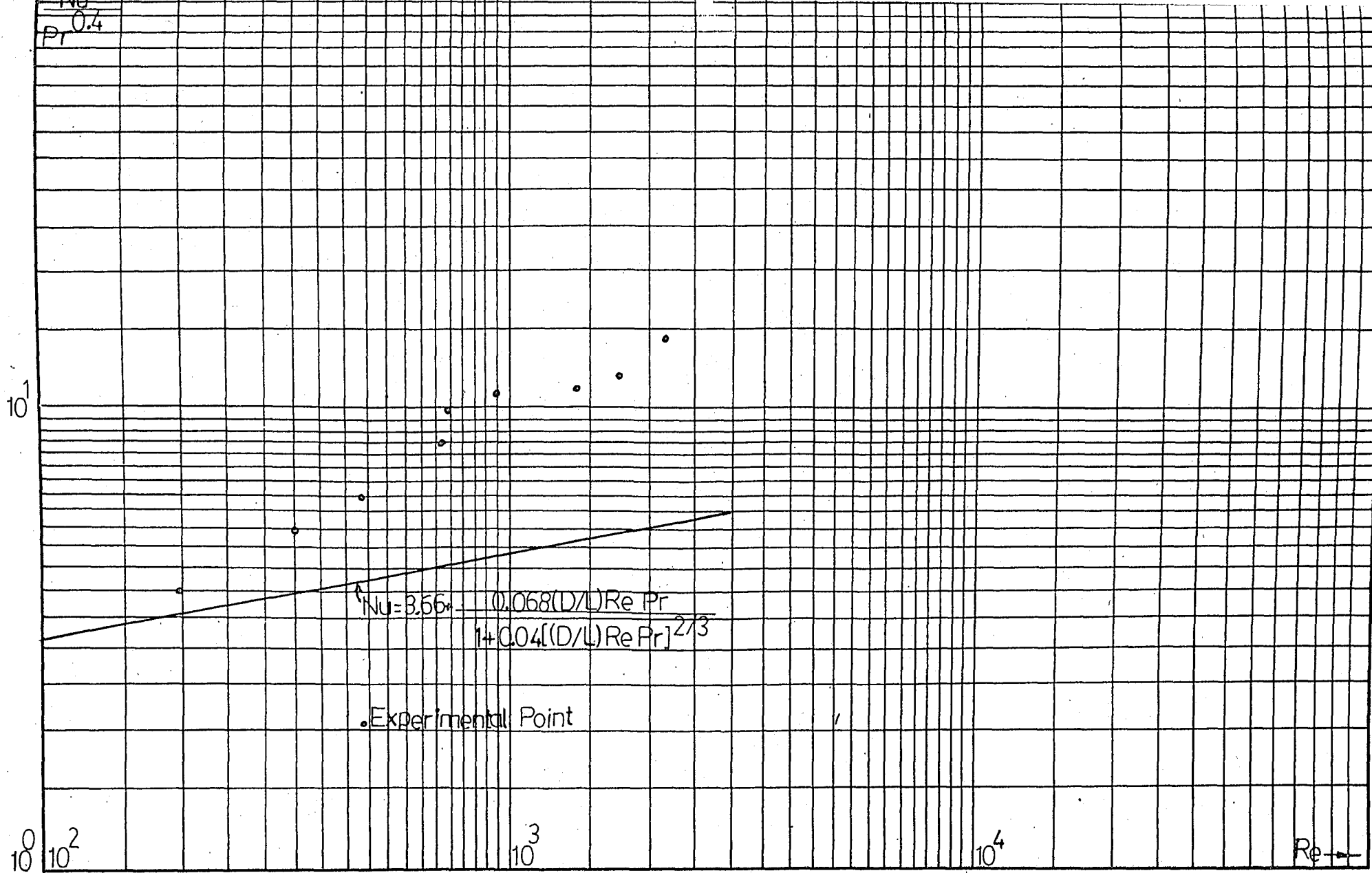


FIGURE 18. Heat Transfer Results of the Second Roped Tube in Laminar Flow.

Three friction coefficients are indicated: f , f_x , \bar{f}_{app} . The local friction coefficient is described as f_x and is based on the actual local wall shear stress at x . In computing the pressure drop in a tube, the integrated mean wall shear stress from $x=0$ to the point of interest is of more utility than the local shear stress. The mean friction coefficient from $x=0$ to x is described by f . Part of the pressure drop in the entrance region of a tube is attributable to an increase in the total fluid momentum flux, which is associated with the development of the velocity profile. Pressure drop calculations in this region must consider the variation in momentum flux as well as the effects of surface shear forces. The combined effects of surface shear and momentum flux have been incorporated in a single apparent mean friction coefficient, \bar{f}_{app} . The pressure drop from 0 to x can then be evaluated from

$$\Delta P = \bar{f}_{app} \frac{x}{D} \rho \frac{v^2}{2g} \quad (23)$$

Fanning friction factor is evaluated from

$$f = \frac{1}{2} \frac{\Delta P}{\rho} \frac{D}{L} \frac{g}{v^2} \quad (24)$$

and Moody-Darcy friction factor, λ , is about 4 times the fanning friction factor

$$\lambda = 4f \quad (25)$$

The variation of fanning friction factor as a function of Reynolds number is plotted in logarithmic scale. In the experiments, a typical roped tube and a smooth tube which has the same dimensions, are tested. The experiments are conducted both in the entrance region and the fully developed region. .

In fully developed laminar flow in circular tube, the fanning friction factor can be evaluated by the following relation [26]:

$$f = \frac{16}{Re} \quad (26)$$

The relation between friction factor and the Reynolds number can be written as [30]:

$$\lambda = a + b Re^n \quad (27)$$

where a, b and n are constants and they all are found from the experiments. In fully developed turbulent flow, the relations between friction factor and the Reynolds number in the smooth circular tube, are presented by H. Richter [30]. Some of them are given in Table 13.

A commonly used relation is given by A.E. Bergles [3]:

$$f = 0.046 Re^{-0.2} \quad (28)$$

TABLE 13

RELATIONS BETWEEN FRICTION FACTOR AND THE REYNOLDS NUMBER

Researcher	Year	Range	Fluid or Gas	Relation
Jacob	1922	$Re \leq 70000$	Water and Air	$\lambda = 0.3270 Re^{-0.254}$
Kozeny	1925	$Re \leq 400000$	Water	$\lambda = 0.00648 + 0.54 Re^{-0.333}$
Blasius	1913	$Re \leq 10^5$	Water and Air	$\lambda = 0.3164 Re^{-0.25}$
Lees	1915	$Re \leq 430000$	Water and Air	$\lambda = 0.0072 + 0.06105 Re^{-0.35}$
Hermann	1930	$Re \leq 1900000$	Water	$\lambda = 0.0054 + 0.3964 Re^{-0.300}$
Nikuradse	1932	$Re \leq 3240000$	Water	$\lambda = 0.0032 + 0.221 Re^{-0.237}$
Harris	1949	$10^5 \leq Re \leq 10^6$	Water	$\lambda = 0.0061 + 0.55 Re^{-0.333}$

Fanning friction factor data of the smooth tube in the entrance region, in laminar flow are given in Table 14. The smooth tube data in laminar flow are in good agreement with the usual correlation $f = 16/Re$.

Fanning friction factor data of the smooth tube in the entrance region in transition flow are presented in Table 15. Fanning friction factor data of the smooth tube in the entrance region in turbulent flow are presented in Table 16. Smooth tube fanning friction factor is calculated using Equation (28) and Blasius' Equation in Table 13 to compare the results obtained to the other researchers' results.

Fanning friction factor data of the roped tube in the entrance region in laminar flow are given in Table 17. Table 18 represents the results of the roped tube in the entrance region in the Critical Region. Fanning friction factor results of the roped tube in the entrance region in transition and in turbulent flow are given in Table 19 and in Table 20 respectively.

The comparison of Fanning Friction Factor Results of the roped and smooth tube is presented in Figure 19. The results given in Table 17 and Figure 19, indicate that the pressure drops with the roped tube are as much as 1.5 times the smooth tube values in laminar flow. The

TABLE 14

FRICTION FACTOR RESULTS OF THE SMOOTH TUBE IN ENTRANCE REGION LAMINAR FLOW

Re	ΔP	f_{smooth}	$\frac{f_{16}}{\text{Re}}$
1932	2.15	0.00966	0.00828
1864	2.124	0.01057	0.00858
1628	1.68	0.01063	0.0098
1520	1.59	0.0114	0.01052
1378	1.475	0.0130	0.0116
1318	1.38	0.0132	0.01213
1151	1.18	0.01473	0.0139
977	1.00	0.0155	0.1637
913	0.944	0.0184	0.0175
890	0.885	0.0182	0.0179
828	0.826	0.0194	0.0193
813	1.00	0.0185	0.0196
771	0.826	0.0196	0.0207
767	0.855	0.0195	0.0208

Re	ΔP	f_{smooth}	$\frac{f_{16}}{\text{Re}}$
661	0.708	0.0232	0.0242
663	0.737	0.0273	0.0241
647	0.708	0.0268	0.0247
632	0.796	0.0236	0.0253
546	0.560	0.0295	0.0293
502	0.501	0.03117	0.0318
442	0.472	0.0371	0.0362
411	0.442	0.040	0.0389
340	0.354	0.044	0.0470
278	0.324	0.064	0.0575
241	0.280	0.062	0.0664
205	0.236	0.073	0.078
185	0.295	0.0979	0.0865

TABLE 15
 FRICTION FACTOR DATA OF THE SMOOTH TUBE IN
 ENTRANCE REGION IN TRANSITION FLOW

Re	ΔP	f_{smooth}	Re	ΔP	f_{smooth}
9806	50.1	0.0082	4196	11.5	0.0102
9729	52.6	0.0085	4054	10.2	0.01037
8970	43.6	0.00814	3844	9.5	0.0104
8956	45.6	0.00873	3756	8.8	0.0105
7884	35.9	0.00898	3586	7.8	0.0103
7866	35.3	0.00858	3497	8.0	0.0106
7110	30.0	0.00888	3227	6.68	0.0105
6912	28.9	0.00945	3214	6.6	0.0096
6050	24.1	0.0094	3206	6.7	0.0107
5985	22.4	0.00997	3181	6.35	0.0104
5931	20.8	0.00958	3122	6.3	0.0109
5328	18.3	0.01036	2963	5.2	0.0097
5199	17.5	0.0106	2932	5.48	0.0105
5182	19.3	0.010	2728	4.4	0.0098
5148	15.6	0.00977	2568	4.0	0.0087
4778	15.5	0.01028	2487	3.2	0.0090
4656	13.1	0.0100	2301	2.74	0.0086
4549	13.0	0.0100	2275	2.97	0.0094
4287	13.9	0.0108	2154	2.47	0.00898
4282	11.4	0.0103			

TABLE 16
 FRICTION FACTOR DATA OF THE SMOOTH TUBE IN
 ENTRANCE REGION IN TURBULENT FLOW

Re	ΔP	$f = \frac{0.046}{Re^{0.2}}$	$f = \frac{0.0791}{Re^{0.25}}$	f_{smooth}
24786	243.6	0.00608	0.0063	0.00676
22770	243.4	0.0062	0.00644	0.0070
22332	237.2	0.0062	0.00647	0.00706
21354	211.9	0.00626	0.00654	0.00694
20327	212.2	0.00632	0.00662	0.00663
20254	207.0	0.00633	0.00663	0.00697
19274	179.0	0.0064	0.00671	0.00723
19048	199.5	0.0064	0.00673	0.0068
18036	156.2	0.00648	0.00682	0.00725
17826	175.5	0.0065	0.00684	0.00705
16960	139.6	0.00656	0.00693	0.00737
14845	111.6	0.00673	0.00716	0.0077
14834	122.3	0.00673	0.00716	0.00772
14528	115.8	0.00676	0.0072	0.00775
14300	126.0	0.00678	0.00723	0.00758
14078	113.6	0.0068	0.00726	0.00763
13610	102.2	0.00685	0.00732	0.00783
13139	99.4	0.0069	0.00739	0.00791
13073	101.3	0.0069	0.00739	0.0076
12658	88.7	0.00695	0.00745	0.00804
11380	71.3	0.0071	0.00765	0.00795
10242	59.3	0.00725	0.00786	0.00844

TABLE 17
 FANNING FRICTION FACTOR DATA OF THE ROPED TUBE IN
 ENTRANCE REGION IN LAMINAR FLOW

Re	$f = \frac{16}{Re}$	f_{roped}	$\frac{f_{roped}}{f \frac{16}{Re}}$
2013	0.00795	0.01230	1.54
1994	0.00802	0.01280	1.59
1974	0.00810	0.01280	1.58
1963	0.00815	0.01449	1.77
1830	0.00874	0.01467	1.68
1825	0.00876	0.01262	1.44
1667	0.00959	0.01433	1.49
1657	0.00965	0.01515	1.57
1539	0.01039	0.01437	1.38
1410	0.01134	0.01546	1.36
1365	0.01172	0.01610	1.37
1237	0.01293	0.01857	1.43
1158	0.01381	0.01900	1.37
972	0.01646	0.02317	1.40
969	0.01651	0.02555	1.54
872	0.01834	0.02600	1.42
840	0.01900	0.02760	1.45
792	0.02020	0.03025	1.49
718	0.02228	0.03100	1.39
663	0.02413	0.03695	1.53
642	0.02490	0.03534	1.42
534	0.02979	0.04970	1.66
456	0.03508	0.04550	1.30
445	0.03595	0.05018	1.39
416	0.03846	0.05106	1.32
288	0.05555	0.07293	1.33
277	0.05776	0.08300	1.43
272	0.05882	0.08757	1.48
215	0.07440	0.08195	1.10
200	0.08000	0.11063	1.37
180	0.08888	0.12610	1.42

TABLE 18

FANNING FRICTION FACTOR RESULTS OF THE ROPED
TUBE IN ENTRANCE REGION IN
CRITICAL REGION

Re	f_{roped}		Re	f_{roped}
2145	0.01183		2325	0.01763
2225	0.01825		2665	0.03605
2314	0.01532		2800	0.03556

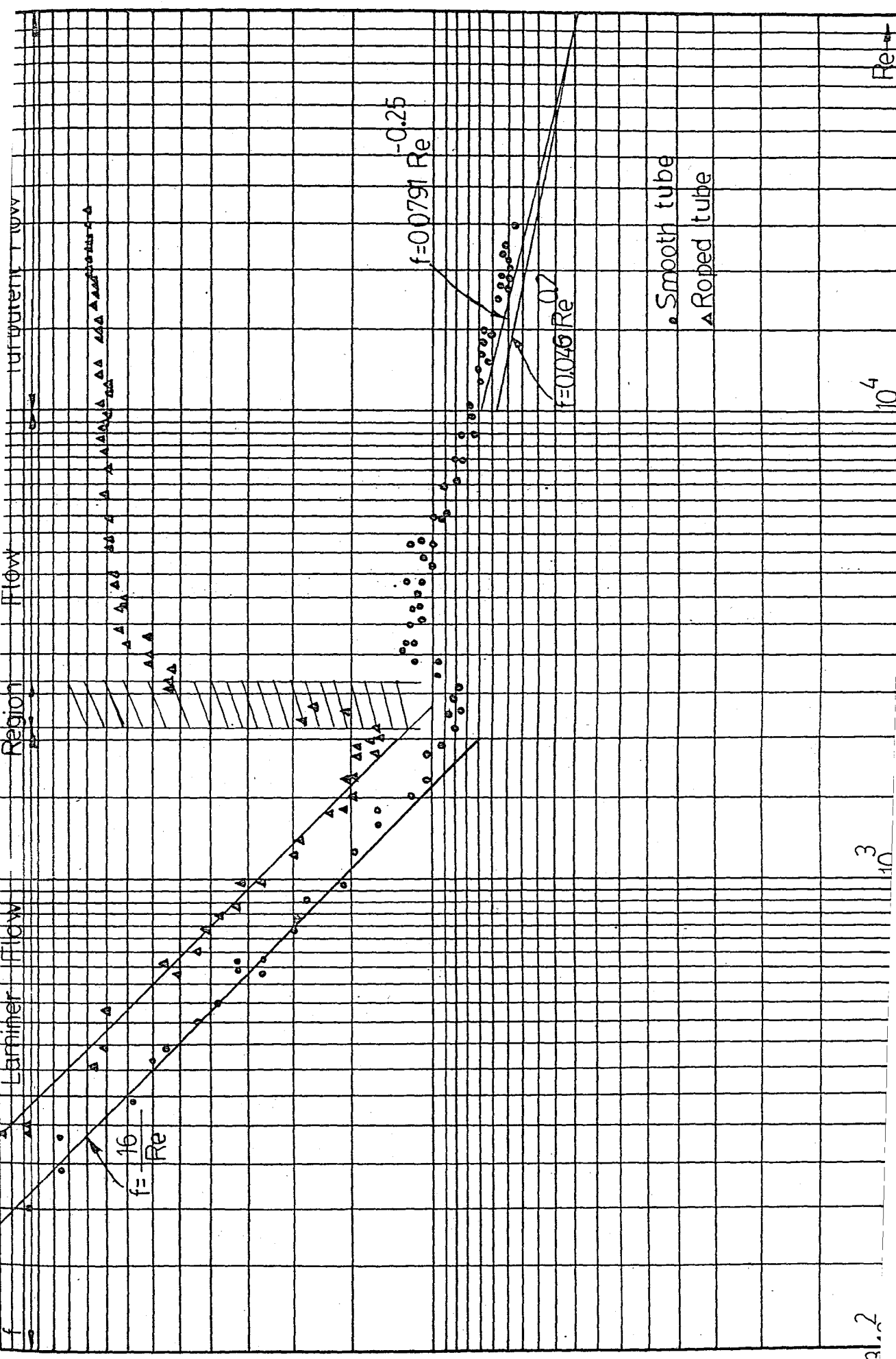
TABLE 19

FANNING FRICTION FACTOR RESULTS OF THE ROPEd TUBE
IN ENTRANCE REGION, IN TRANSITION FLOW

Re	f_{roped}		Re	f_{roped}
9896	0.04965		4300	0.04747
9220	0.05047		4015	0.04533
8676	0.05094		3911	0.04518
8210	0.05000		3797	0.04628
7573	0.04940		3426	0.04625
6624	0.05032		3328	0.04033
6550	0.05050		3208	0.04567
5952	0.04928		3041	0.04028
5109	0.04950		2933	0.04000
5052	0.04927		2861	0.03566
4534	0.04773		2665	0.03605

TABLE 20
 FANNING FRICTION FACTOR RESULTS OF THE ROPED TUBE
 IN ENTRANCE REGION IN TURBULENT FLOW

Re	f_{smooth} $f = 0.0791/Re^{0.25}$	f_{roped}	$\frac{f_{roped}}{f_{smooth}}$
26028	0.00622	0.05460	8.77
24943	0.00629	0.05434	8.64
23154	0.00641	0.05386	8.40
22403	0.00646	0.05404	8.36
21970	0.00649	0.05400	8.32
21319	0.00654	0.05373	8.21
20170	0.00663	0.05431	8.19
19431	0.00669	0.05474	8.18
19032	0.00673	0.05240	7.86
18303	0.00680	0.05264	7.74
17595	0.00686	0.05237	7.63
16537	0.00697	0.05285	7.58
15328	0.00712	0.05169	7.26
14620	0.00719	0.05139	7.14
13795	0.00729	0.05158	7.07
12468	0.00748	0.05163	6.90
11981	0.00756	0.05118	6.77
11678	0.00761	0.05019	6.59
11237	0.00768	0.04946	6.44
10926	0.00773	0.04923	6.38
10223	0.00786	0.05100	6.48



roped tube results are in good agreement with the following correlation:

$$f = \frac{24}{Re} \quad (29)$$

If the Reynolds number is between 2100 and 2600, the manometer's fluid fluctuates for both tubes, especially in the roped tube and it is not possible to measure pressure drop as a constant value. For that reason, for every 15 second interval, the manometer's fluid is observed, and the average value of the pressure drop is calculated. Friction factor of the smooth tube decreases in transition flow, in the roped tube, however, it increases and reaches a constant value. The friction factor of the roped tube is about 5 times the smooth tube friction factor in transition flow. Friction factor of the smooth tube also decreases in turbulent flow. Experimental results of the smooth tube in turbulent flow are in good agreement with the Blasius equation in Table 13. In the case of the roped tube, water is heated to obtain a high Reynolds number. If the temperature of the water is increased, the kinematic viscosity of water decreases and the Reynolds number increases. It should be noted that, friction factor of the roped tube is almost constant in turbulent flow, and it is about 6-9 times the smooth tube friction factor.

Fanning friction factor results of the smooth tube in fully developed laminar flow are given in Table 21. The smooth tube results in fully developed laminar flow are in good agreement with the usual correlation $f=16/Re$. The results in critical region are given in Table 22.

Fanning friction factor results of the smooth tube in fully developed transition flow and in fully developed turbulent flow are given in Tables 23 and 24 respectively.

Fanning friction factor results of the roped tube in fully developed laminar flow, critical region, transition flow and turbulent flow are given in Tables 25, 26, 27 and 28 respectively.

The comparison of Fanning Friction Factor Results of the roped tube and smooth tube in fully developed flow is presented in Figure 20. The smooth tube results in fully developed laminar flow are in good agreement with the usual correlation $f = 16/Re$. The results given in Table 25 and Figure 20 indicate that pressure drops with the roped tube in fully developed laminar flow are as much as 1.6 times the smooth tube values. The roped tube results are in good agreement with the following correlation:

$$f = \frac{25.6}{Re} \quad (30)$$

The smooth tube friction factor in fully developed transition and turbulent flow decreases if the Reynolds number increases. However, the roped tupe friction factor in fully developed turbulent flow is almost constant and it is about 6-9 times the smooth tube friction factor.

TABLE. 21

FRICTION FACTOR RESULTS OF THE SMOOTH TUBE IN
FULLY DEVELOPED LAMINAR FLOW

Re	f_{smooth}	$\frac{f_{16}}{\text{Re}}$	Re	f_{smooth}	$\frac{f_{16}}{\text{Re}}$
2091	0.00764	0.00765	1071	0.01355	0.01493
2080	0.00752	0.00770	1015	0.01413	0.01576
2051	0.00834	0.00780	959	0.01623	0.01668
1868	0.00901	0.00856	904	0.01820	0.01770
1813	0.00940	0.00880	796	0.01964	0.02010
1805	0.00857	0.00886	708	0.02127	0.02260
1693	0.00950	0.00945	696	0.02000	0.02298
1626	0.01000	0.00984	579	0.02421	0.02760
1610	0.01058	0.00993	451	0.03680	0.03547
1559	0.01154	0.01020	377	0.03900	0.04244
1439	0.01130	0.01110	308	0.04950	0.05194
1390	0.01180	0.01150	274	0.06220	0.05839
1270	0.01175	0.012598	254	0.07016	0.06299

TABLE 22

FRICTION FACTOR RESULTS OF THE SMOOTH TUBE IN
FULLY DEVELOPED CRITICAL REGION

Re	ΔP	f_{smooth}
2907	10.4	0.01157
2905	6.1	0.00686
2878	8.96	0.00880
2765	7.6	0.00770
2662	8.5	0.01160
2584	7.14	0.00800
2554	7.8	0.00910
2445	4.78	0.00656
2424	4.7	0.00750

TABLE 23

FRICITION FACTOR RESULTS OF THE SMOOTH TUBE IN
FULLY DEVELOPED TRANSITION FLOW

Re	f_{smooth}		Re	f_{smooth}
9752	0.00872		4832	0.00990
9080	0.00884		4442	0.01024
8470	0.00918		4435	0.01100
7842	0.00910		4424	0.01120
7212	0.00950		4237	0.01000
7070	0.00920		4045	0.01160
6231	0.00963		3690	0.01300
5866	0.00970		3672	0.01200
5741	0.01000		3600	0.01220
5656	0.01040		3352	0.01079
5346	0.01000		3315	0.01200
5166	0.01040		3296	0.01230
5149	0.01000		3191	0.01110
5125	0.01060		3142	0.01140

TABLE 24
 FRICTION FACTOR RESULTS OF SMOOTH TUBE IN
 FULLY DEVELOPED TURBULENT FLOW

Re	$f = \frac{0.046}{Re^{0.2}}$	$f = \frac{0.0791}{Re^{0.25}}$	f_{smooth}
22929	0.00617	0.00642	0.00685
21135	0.00627	0.00656	0.00730
20710	0.00630	0.00660	0.00730
20323	0.00632	0.00662	0.00737
19541	0.00637	0.00669	0.00728
19245	0.00640	0.00671	0.00735
18266	0.00646	0.00680	0.00740
17772	0.00650	0.00685	0.00740
16958	0.00656	0.00693	0.00765
15672	0.00666	0.00707	0.00770
14532	0.00676	0.00720	0.00749
14290	0.00678	0.00723	0.00760
14090	0.00680	0.00726	0.00800
13200	0.00690	0.00738	0.00782
12591	0.00696	0.00746	0.00817
12272	0.00700	0.00751	0.00804
11701	0.00706	0.00760	0.00847
11462	0.00709	0.00764	0.00824
10614	0.00720	0.00779	0.00847
10498	0.00722	0.00781	0.00847

TABLE 25
 FRICTION FACTOR RESULTS OF THE ROPEDED TUBE IN
 FULLY DEVELOPED LAMINAR FLOW

Re	$f = \frac{16}{Re}$	f_{roped}	$\frac{f_{roped}}{f \frac{16}{Re}}$
1740	0.00919	0.01518	1.65
1709	0.00936	0.01539	1.64
1640	0.00975	0.01693	1.73
1584	0.01010	0.01625	1.60
1570	0.01019	0.01648	1.62
1504	0.01063	0.01820	1.71
1433	0.01116	0.01856	1.66
1384	0.01199	0.01870	1.56
1332	0.01201	0.02029	1.69
1272	0.01257	0.02063	1.64
1262	0.01267	0.02031	1.60
1247	0.01283	0.02021	1.57
1161	0.01378	0.02212	1.60
1101	0.01453	0.02272	1.56
945	0.01693	0.02546	1.50
887	0.01803	0.03150	1.74
843	0.01897	0.03043	1.60
842	0.01900	0.03046	1.60
722	0.02216	0.03852	1.74
674	0.02374	0.03600	1.51
601	0.02662	0.04668	1.75
556	0.02871	0.04396	1.53
427	0.03747	0.06199	1.65
361	0.04432	0.06880	1.55
298	0.05369	0.08311	1.55
225	0.07111	0.01910	1.53
159	0.10062	0.17252	1.71

TABLE 26
FRICTION FACTOR RESULTS OF THE ROPED TUBE IN
FULLY DEVELOPED FLOW IN CRITICAL
REGION

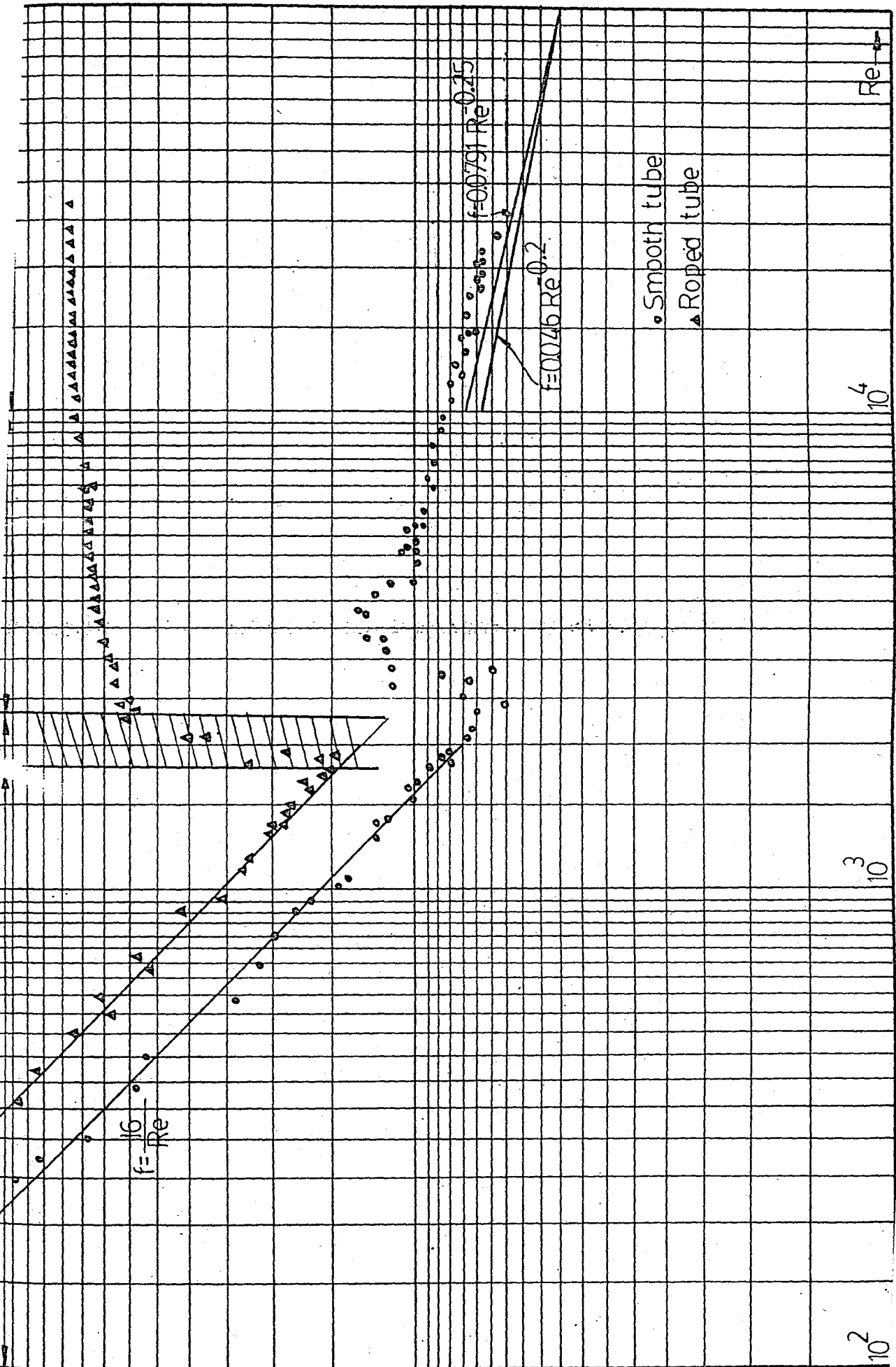
Re	f_{roped}
2070	0.02760
2067	0.03000
1926	0.01865
1881	0.01462
1819	0.01568
1786	0.02340

TABLE 27
FRICTION FACTOR RESULTS OF THE ROPED TUBE IN
FULLY DEVELOPED TRANSITION FLOW

Re	f_{roped}		Re	f_{roped}
9736	0.05191		4634	0.04744
8847	0.05118		4348	0.04735
7633	0.04915		4071	0.04690
6987	0.04794		3860	0.04652
6867	0.05040		3607	0.04560
6783	0.05030		3288	0.04500
6513	0.04871		3070	0.04411
6380	0.04877		2829	0.04309
6206	0.04913		2647	0.04243
5959	0.04892		2498	0.04033
5941	0.04831		2452	0.04240
5572	0.04815		2395	0.03941
5280	0.04825		2256	0.04080
4965	0.04815			

TABLE 28
 FRICTION FACTOR RESULTS OF THE ROPED TUBE IN
 FULLY DEVELOPED TURBULENT FLOW

Re	$f = \frac{0.0791}{Re^{0.25}}$	f_{roped}	$\frac{f_{roped}}{f_{smooth}}$
26347	0.00620	0.05284	8.52
23517	0.00638	0.05300	8.30
22273	0.00647	0.05275	8.15
20844	0.00658	0.05314	8.07
19200	0.00671	0.05315	7.92
18685	0.00676	0.05353	7.91
18195	0.00681	0.05300	7.78
17309	0.00689	0.05349	7.76
16995	0.00692	0.05278	7.62
16572	0.00697	0.05275	7.56
16023	0.00703	0.05300	7.54
15289	0.00711	0.05260	7.39
14688	0.00718	0.05241	7.23
14129	0.00725	0.05219	7.19
13431	0.00734	0.05260	7.16
12561	0.00747	0.05199	6.95
11896	0.00757	0.05203	6.87
11211	0.00768	0.05175	6.73
10542	0.00780	0.05176	6.63



Results of Tests on Smooth Tube and Roped Tube in Fully Developed Flow

5. COMPARISON OF ROPED TUBES WITH TURBOTEC AND SPIRALLY FLUTED TUBES

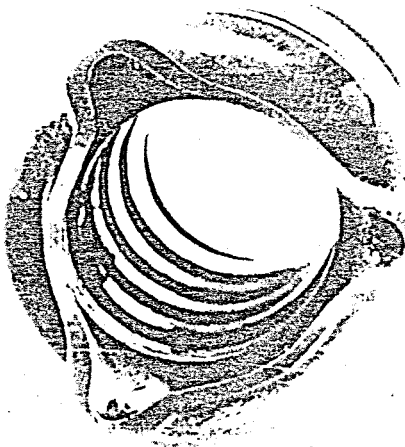
The mostly encountered profiled tubes (enhanced heat transfer tubes) in heat exchanger equipment are roped tubes, turbotec tubes, and fluted tubes. Turbotec tubes are part of a class of tubes which have multiple-start spiral corrugations along the tube length. Created by various manufacturing process, tubes within this class are referred to by such terms as "spirally fluted", "Convolute", "corrugated", "helically fluted", "spirally grooved". Their common characteristic is that both sides of the tube are geometrically modified so that, in the usual application of a two-fluid heat exchanger, there is potential enhancement of the heat transfer coefficient on either side.

Roped tubes are compared with turbotec and spirally fluted tubes. Lengthwise and axial photographs of a typical turbotec tube are shown in Figure 21. Several spirally fluted tubes are shown in Figure 22.

Heat transfer characteristics of the roped tubes and turbotec tubes are compared in Figure 23. Curve 1



a. Lengthwise view.



b. Axial view.

FIGURE 21. Photographs of Turbotec Tubes.

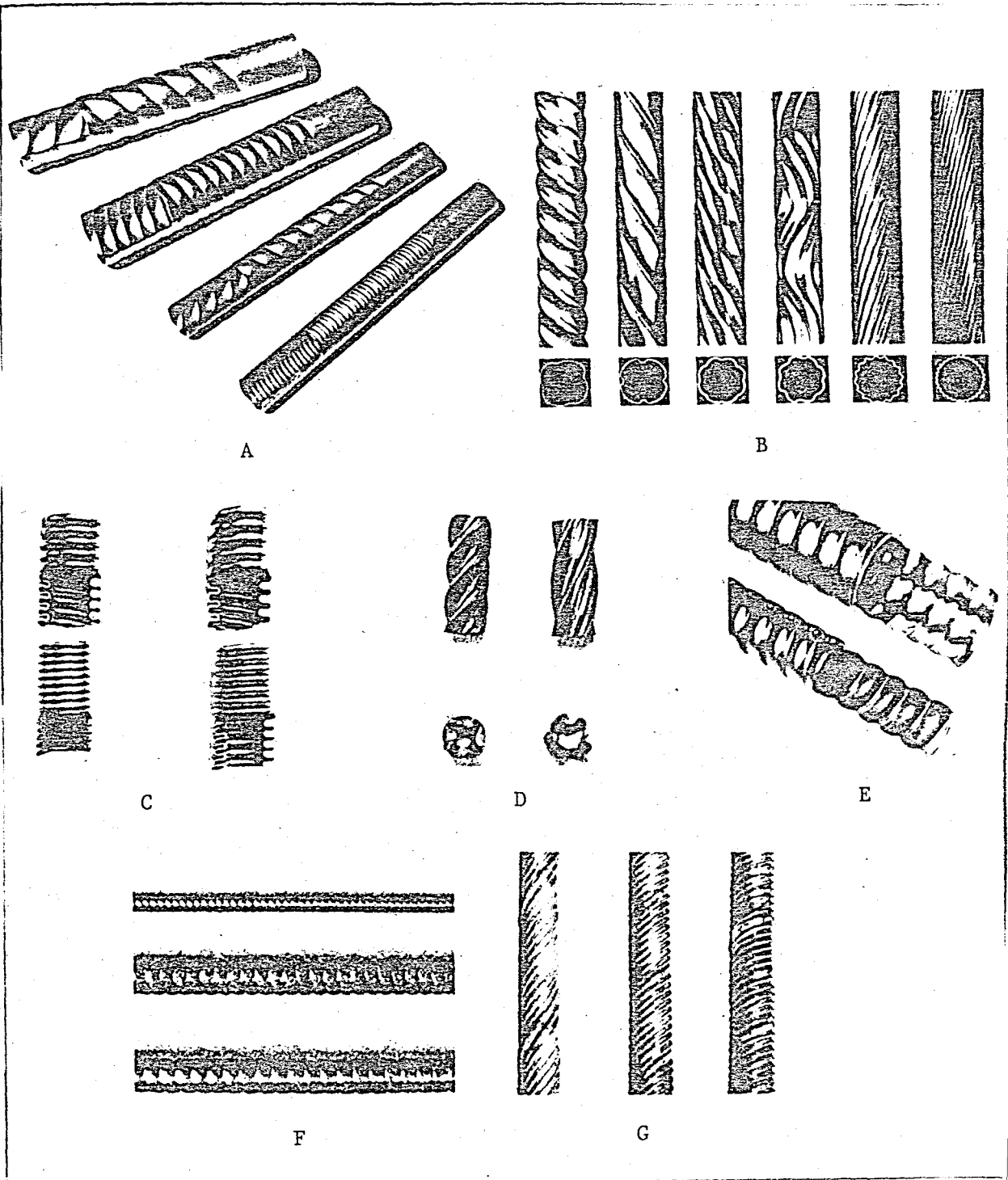


FIGURE 22. Typical Tubes in the Spirally Fluted Category.

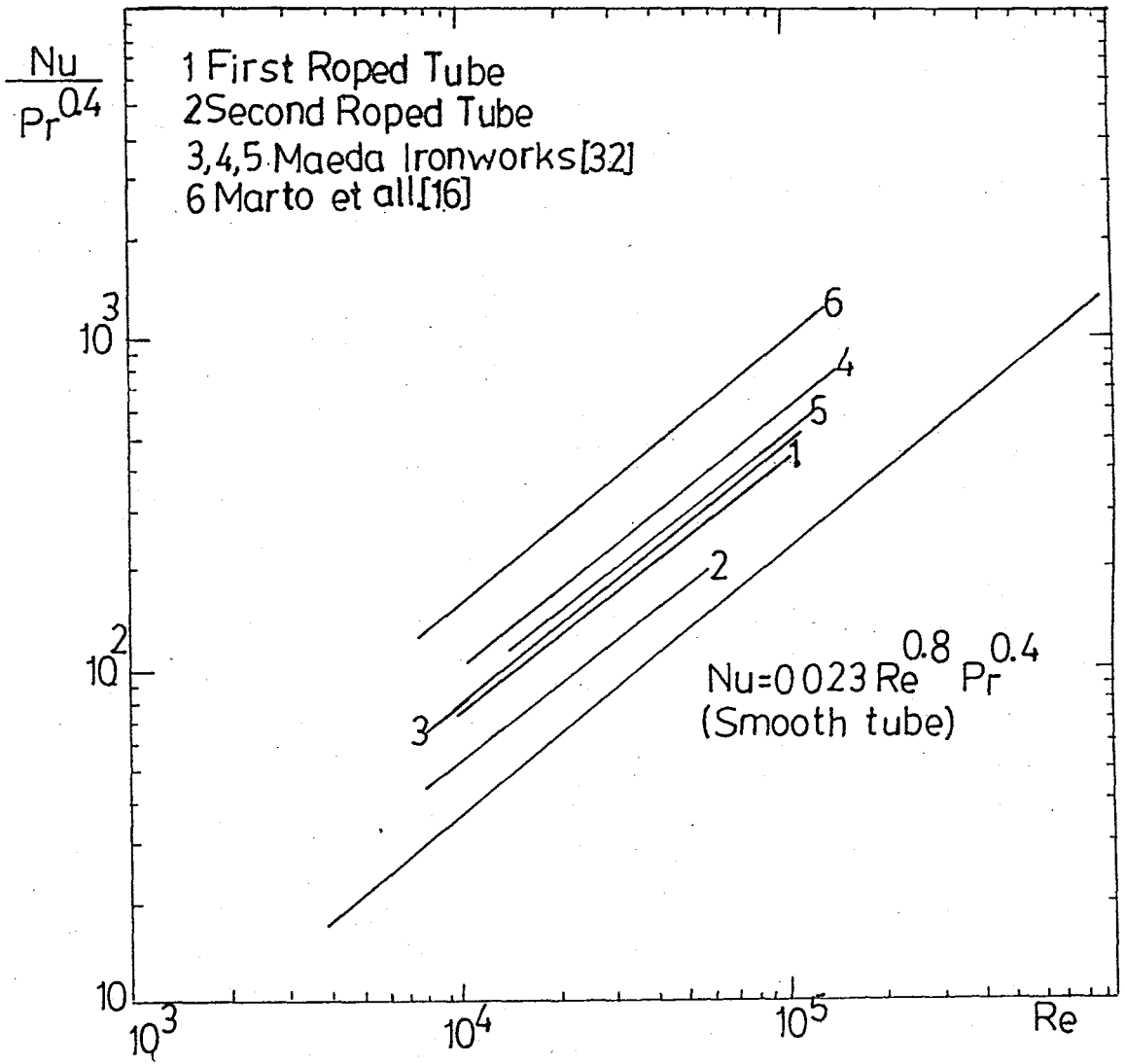


FIGURE 23. Composite of Internal, Turbulent Flow Heat Transfer Characteristics for Roped and Turbotec Tubes.

and Curve 2 indicate heat transfer characteristics of the first and second roped tube tested in the present study. Three turbotec tubes tested by Maeda Ironworks Co. [32] exhibit Nusselt numbers which are 75-125% above the smooth tube values, and their heat transfer characteristics are indicated by Curves 3, 4 and 5. Marto et al. [16] have conducted the most recent study of turbotec tubes and Curve 6 indicates that the Nusselt number of turbotec tube tested by Marto et al. is as much as 400% above the smooth tube results. It should be noted that, no direct comparison is possible since no tubes are identical in studies. Heat transfer improvement depends on the groove depth, the groove pitch of the tubes.

Pressure drop characteristics of the roped and turbotec tubes are compared in Figure 24. T-1, T-2, T-3 and T-4 present different turbotec tubes tested by Marto et al. [16]. Pressure drops with turbotec tubes are as much as 4-15 times the smooth tube values. A-1 presents the roped tube tested in the present study and pressure drop with roped tube is above 7 times the smooth tube values.

Numerous studies have considered the augmentation of single-phase turbulent flow in spirally fluted tubes. Since a detailed comparison is not within the scope of the present work, only a tabular summary of the available

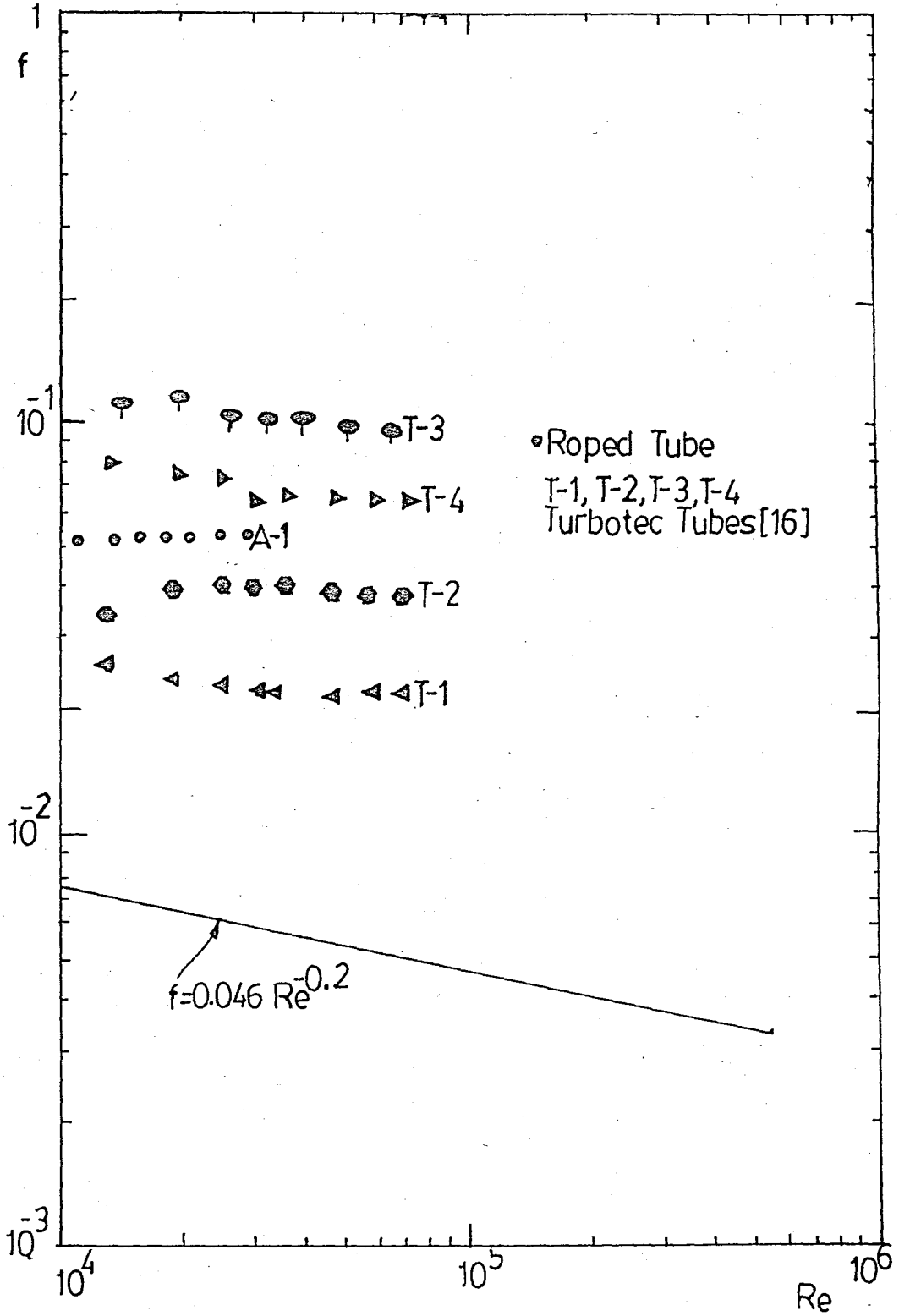


FIGURE 24. Pressure Drop Characteristics for Roped and Turbotec Tubes in Fully Developed Turbulent Flow.

information derived from the bibliography in Ref. [34] will be given. Table 29 indicates the type of tubing, test fluid, test procedure and approximate improvement in heat transfer coefficient. There are many spirally fluted tubes which exhibit improvements in turbulent heat transfer coefficient of the order of 100%, that is, the same order of magnitude in coefficient displayed by the turbotec and roped tubes in Figure 23. A full comparison, of course, requires consideration of such factors as pressure drop, fouling potential and cost.

SUMMARY OF OTHER TESTS WITH SPIRALLY FLUTED TUBING IN TURBULENT SINGLE-PHASE INTERNAL FLOW

Study	Tube Designation	Fluid	Improvement in Heat Transfer Over Smooth Tube	Designation in Figure 22
Lawson et al 4	Spirally indented	Heating of Water	100%	-
Blumenkrantz et al. 5	Spirally grooved	Heating of Air, Water & Light Oil	40% for Water	D
Kidd 6	Spirally corrugated	Air	Up to 90%	-
Withers and Young 7	Corrugated	Heating of Water	Up to 173%	E
Kalinin and Yorkho 8	Annular Diaphragms	Heating of Water	Up to 150%	-
Kramer and Gater 9	Helical and Annular convoluted	Heating of Water	300%	C
Newson and Hodgson 10	Swaged or roped helical, multifiuted	Heating of Water	Up to 150%	B
Robles 11	Helical convoluted	Heating & Cooling of Water	400% for Heating, less for cooling	C

TABLE 29 (Continued)

Study	Tube Designation	Fluid	Improvement in Heat Transfer Over Smooth Tube	Designation in Figure 22
Hitachi [12]	Circumferential groove, corrugated	Heating of Water	Up to 133%	-
		Heating of Water	Up to 173%	-
Watkinson et al. [13]	Spirally indented	Heating of Water	Up to 75%	D
Yoshitomi et al. [14]	Embossed spiral	Heating of Water	Up to 130%	F
Cunninham and Milne [15]	Roped (Yorkshire)	Heating of Water	Up to 70%	A
Marto et al. [16]	Corrugated	Heating of Water	Up to 160%	E
		Heating of Water	Up to 228%	
Mahta and Rao [17]	Spirally enhanced	Heating of Water	Up to 150%	G

6. CONCLUSION

On the basis of the present work, the following conclusions can be reached:

1. The heat transfer rate and pressure losses in the roped tubes are much greater than the smooth tube.

2. The improvement of the heat transfer rate depends on the groove depth and groove pitch of the roped tube. As the groove depth increases and the groove pitch decreases, the heat transfer rate increases. The two roped tubes with different groove depth and groove pitch are tested in the experiments. In the first roped tube with the inner diameter of 70 mm and outer diameter of 76 mm, the groove depth is much greater than the second roped tube with the inner diameter of 19 mm and the outer diameter of 21 mm. As can be seen from Table 4, the average value of the ratio of the internal heat transfer coefficient in the first roped tube to the internal heat transfer coefficient in the smooth tube, is 1.78 in turbulent flow.

Table 8 shows that the average value of the ratio of the internal heat transfer coefficient in the second

roped tube to the internal heat transfer coefficient in the smooth tube is 1.22 in turbulent flow. Figure 18 shows that the heat transfer coefficient of the roped tube in laminar flow is about 1.5 - 2.5 times the smooth tube heat transfer coefficient. For very low Reynolds number in laminar flow, internal heat transfer coefficients of the roped and smooth tube are almost equal. If the Reynolds number increases, the ratio $h_{\text{roped}}/h_{\text{smooth}}$ increases.

3. Pressure losses experiments have been conducted with a roped tube and a smooth tube. The two tubes tested have the same diameter and length. Friction factor results of the smooth tube for both in Entrance Region Laminar flow and fully developed laminar flow, are in good agreement with the usual correlation $f = 16/Re$. Friction factor results of the smooth tube for both the Entrance Region turbulent flow, are in good agreement with Blasius' equation and the other researchers' results.

4. Fanning friction factor of the roped tube in entrance region laminar flow is above 1.5 times the fanning friction factor of the smooth tube. Friction factor of the roped tube in the entrance region turbulent flow are as much as 6-9 times the smooth tube values.

Fanning friction of the roped tube in fully deve-

loped laminar flow is 1.6 times above the smooth tube value and in fully developed turbulent flow is 6-9 times above the smooth tube value.

5. Figure 19 and Figure 20 show that laminar flow in roped tubes is disturbed for smaller Reynolds number than in smooth tubes, in other words, transition flow occurs at lower Reynolds number in the case of roped tube due to turbulence in it.

6. Fanning friction factor of the roped tube for both the entrance region and fully developed turbulent flow is almost constant. Due to laboratory conditions, high Reynolds numbers could not be reached. It would be very interesting to examine the trend of friction factor for high Reynolds numbers.

7. The most convenient spirally fluted tube should be chosen for a specified heat duty considering pressure drop, fouling potential, cost, etc.

8. Alternative designs on smooth and roped tubes for a specified duty will lead to heat exchangers of different length and diameters. For example, with a single passe unit, if the tube diameter can not be varied, the roped tube design will be of somewhat larger shell diameter but significantly shorter length than the smooth

tube. However, if circumstances permit, it is usually good practice to increase the tube diameter when changing from smooth to roped tubes.

NOMENCLATURE

English letter symbols

A	Heat transfer surface area, m^2
c	Specific heat at constant pressure, $Kcal/Kg^{\circ}C$
D	Diameter, m
D_h	Hydrolic diameter, m
f	Fanning friction factor
F	Heat transfer surface area, m^2
g	Gavitational acceleration, m/S^2
h	Convective heat transfer coefficient, $Kcal/m^2h^{\circ}C$
k	Thermal conductivity, $Kcal/mh^{\circ}C$
L	Length, m
m	Mass flow rate
m_1	Mass flow rate of water in tube, Kg/h
m_2	Mass flow rate of water in annular region, Kg/h
P	Pressure
P	Wetted perimeter, m
Q	Heat transfer rate, $Kcal/h$
Q_1	Energy transferred from hot water ($Kcal/h$)
Q_2	Energy transferred to cold water ($Kcal/h$)
S	Cross sectional area, m^2
v	Mean velocity, m/s
v_1	Mean velocity of water inside the roped tube, m/s

v_2 Mean velocity of water in the annular region, m/s
 x Length of entry region, m

Greek letter symbols

Δ Difference
 ΔP Pressure losses, mm. water column
 $\Delta\theta_m$ Logarithmic mean temperature difference
 θ Temperature, °C
 θ_∞ Ambient temperature, °C
 θ_{1in} Inlet temperature of hot water, °C
 θ_{1out} Outlet temperature of hot water, °C
 θ_{2in} Inlet temperature of cold water, °C
 θ_{2out} Outlet temperature of cold water, °C
 θ_{1ts} Surface temperature at the inlet of hot water, °C
 θ_{2ts} Surface temperature at the outlet of hot water, °C
 λ Moody-Darcy friction factor
 μ Dynamic viscosity, Kg/ms
 ν Kinematic viscosity, m²/S
 ρ Fluid density, mass per unit of volume, Kg/m³

Subscripts

aug Augmented
i Inner or internal condition
in Evaluated at inlet of the tube or annular region
o Outer or external condition
out Evaluated at the outlet of the tube or annular region

rop Roped tube
s Evaluated at surface
smo smooth

Dimensionless Groups

Re Reynolds number = $\frac{V \cdot D}{\nu}$

Nu Nusselt number = $\frac{h \cdot D}{k}$

Pr Prandtl number = $\frac{c \cdot \mu}{k}$

$\Delta\theta_{m_i}$ Inner logarithmic mean temperature difference

$$\Delta\theta_{m_i} = \frac{(\theta_{1in} - \theta_{1ts}) - (\theta_{1out} - \theta_{2ts})}{\ln \frac{\theta_{1in} - \theta_{1ts}}{\theta_{1out} - \theta_{2ts}}}$$

$\Delta\theta_{m_o}$ Outer logarithmic mean temperature difference

$$\Delta\theta_{m_o} = \frac{(\theta_{1ts} - \theta_{2out}) - (\theta_{2ts} - \theta_{2in})}{\ln \frac{\theta_{1ts} - \theta_{2out}}{\theta_{2ts} - \theta_{2in}}}$$

APPENDIX A

EXAMPLE OF CALCULATION OF THE HEAT TRANSFER COEFFICIENTS, FRICTION FACTOR AND THE OTHER QUANTITIES

A. Calculation of the Heat Transfer Coefficients:

The test data during a typical experiment are:

$$\theta_{\infty} = 15.0^{\circ}\text{C}, \theta_{1\text{in}} = 86^{\circ}\text{C}, \theta_{1\text{out}} = 77.65^{\circ}\text{C}, \theta_{2\text{in}} = 6.5^{\circ}\text{C},$$
$$\theta_{2\text{out}} = 14.1^{\circ}\text{C}, m_1 = 409.5 \text{ Kg/h}, m_2 = 458.0 \text{ Kg/h},$$
$$\theta_{1\text{ts}} \div 3230\text{mv}, \theta_{2\text{ts}} \div 3200\text{mv}.$$

Using the calibration curve of the potentiometer that has been used to record the temperature data, $\theta_{1\text{ts}}$ and $\theta_{2\text{ts}}$ are found as follows:

$$\theta_{1\text{ts}} \div 3230\text{mv} \rightarrow \theta_{1\text{ts}} = 61 + \theta_{\infty} = 61 + 15 \theta_{1\text{ts}} = 76.0^{\circ}\text{C}$$

$$\theta_{2\text{ts}} \div 3200\text{mv} \rightarrow \theta_{2\text{ts}} = 60.5 + \theta_{\infty} = 60.5 + 15 \theta_{2\text{ts}} = 75.5^{\circ}\text{C}$$

The temperature profiles of that typical experiment are shown below:

The heat quantity that the inner heat transfer fluid released in the roped tube is calculated as follows:

$$Q_1 = m_1 c_1 (\theta_{1in} - \theta_{1out})$$

$$Q_1 = 409.5 (86.0 - 77.65)$$

$$Q_1 = 3420 \text{ Kcal/h}$$

The heat quantity that the outer heat transfer fluid absorbed in the annular region is calculated as follows:

$$Q_2 = m_2 c_2 (\theta_{2out} - \theta_{2in})$$

$$Q_2 = 458.0 (14.1 - 6.5)$$

$$Q_2 = 3390 \text{ Kcal/h}$$

Inner Logarithmic mean temperature difference of this experiments:

$$\Delta\theta_{m_i} = \frac{(\theta_{1in} - \theta_{1ts}) - (\theta_{1out} - \theta_{2ts})}{\ln \frac{\theta_{1in} - \theta_{1ts}}{\theta_{1out} - \theta_{2ts}}}$$

$$\Delta\theta_{m_i} = \frac{(86.0 - 76.0) - (77.65 - 75.5)}{\ln \frac{86.0 - 76.0}{77.65 - 75.5}}$$

$$\Delta\theta_{m_i} = 5.1$$

Outer Logarithmic mean temperature difference:

$$\Delta\theta_{m_o} = \frac{(\theta_{1ts} - \theta_{2out}) - (\theta_{2ts} - \theta_{2in})}{\ln \frac{\theta_{1ts} - \theta_{2out}}{\theta_{2ts} - \theta_{2in}}}$$

$$\Delta\theta_{m_o} = \frac{(76.0 - 14.1) - (75.5 - 6.5)}{\ln \frac{76.0 - 14.1}{75.5 - 6.5}}$$

$$\Delta\theta_{m_o} = 65.3$$

The heat quantities can be written as:

$$Q_1 = h_i F_i \Delta\theta_{m_i}$$

$$Q_2 = h_o F_o \Delta\theta_{m_o}$$

The inner and outer heat transfer surfaces are:

$$F_i = \pi D_i L$$

$$F_i = 3.14 \times 0.019 \times 2.0 = 0.119 \text{ m}^2$$

$$F_o = \pi D_o L$$

$$F_o = 3.14 \times 0.021 \times 2.0 \approx 0.132 \text{ m}^2$$

$$F_o = 0.132 \text{ m}^2$$

Internal heat transfer coefficient can be found as follows:

$$h_i = \frac{Q_1}{F_i \Delta\theta_{m_i}}$$

$$h_i = \frac{3420}{0.15 \times 5.1}$$

$$h_i = 4770 \text{ Kcal/m}^2\text{h}^\circ\text{C}$$

External heat transfer coefficient can be calculated as follows:

$$h_o = \frac{Q_2}{F_o \Delta\theta_{m_o}}$$

$$h_o = \frac{3390}{0.16 \times 65.3}$$

$$h_o = 355 \text{ Kcal/m}^2\text{h}^\circ\text{C}$$

Calculation of the inner Nusselt number:

$$Nu_i = \frac{h_i D_i}{k_i} \quad Nu_i = \frac{4470 \times 0.019}{0.586} \quad Nu_i = 145.0$$

where $k_i = 0.586$ for $\theta = 81.8$ [28].

Calculation of the hydrolic diameter of the annular region:

$$D_h = \frac{4 A}{P}$$

where A is the cross sectional area of the annular region and P is the wetted perimeter.

Cross-sectional area of the annular region

$$A = \frac{\pi}{4} (0.053^2 - 0.021^2) \quad A = 0.00185888 \text{ m}^2$$

Wetted perimeter

$$P = \pi (0.053 + 0.021) \quad P = 0.2323 \text{ m.}$$

Hydrolic diameter:

$$D_h = \frac{4 \times 0.00185888}{0.02323} \quad D_h = 0.032 \text{ m.}$$

Calculation of the outer Nusselt number:

$$Nu_o = \frac{h_o D_o}{k_o} = \frac{355 \times 0.032}{0.505} \quad Nu_o = 22.5$$

$$k_o = 0.505 \text{ for } \theta = 10.3 \text{ [28]}.$$

The non-dimensional quantities:

$$\frac{Nu_i}{Pr_i^{0.4}} = \frac{145.0}{2.15^{0.4}} \quad \frac{Nu_i}{Pr_i^{0.4}} = 106.75 \quad \frac{Nu_i}{Pr_i^{0.33}} = 112.6$$

$$\frac{Nu_o}{Pr_o^{0.4}} = \frac{22.5}{9.28^{0.4}} \quad \frac{Nu_o}{Pr_o^{0.4}} = 9.23 \quad \frac{Nu_o}{Pr_o^{0.33}} = 10.78$$

The velocity of water in the roped tube is calculated as follows:

$$v_1 = \frac{m_1}{S_1} = \frac{409.5}{970.515 \times 3600 \times 0.0002834}$$

where S_1 is the cross-sectional area of the roped tube and is calculated as:

$$S_1 = \frac{\pi D_i^2}{4} = \frac{3.14 \times (0.019)^2}{4} \quad S_1 = 0.00028339 \text{ m}^2$$

and $\rho = 970.515 \text{ kg/m}^3$ for $\theta = 81.8 |28|$.

$$v_1 = 0.4135 \text{ m/s}$$

The velocity of water in annular region is calculated as follows:

$$v_2 = \frac{m_2}{S_2}$$

where S_2 is the cross sectional area of the annular region and it is calculated as:

$$S_2 = \frac{\pi}{4} (0.053^2 - 0.021^2) \quad S_2 = 0.00185888 \text{ m}^2$$

Then v_2 can be calculated as:

$$v_2 = \frac{458.0}{1000 \times 36000 \times 0.00185888} \quad v_2 = 0.068 \text{ m/s}$$

Inner Reynolds number is calculated as:

$$Re_i = \frac{v_1 D_i}{\nu_i}$$

where ν_i is kinematic viscosity of water in roped tube and is taken from [28]

$$\nu_i = 0.355 \times 10^{-6} \text{ m}^2/\text{s} \quad \text{for } \theta = 81.8^\circ\text{C}$$

Then:

$$Re_i = \frac{0.4135 \times 0.019}{0.355} \times 10^6 \quad Re_i = 22193$$

Outer Reynolds number is calculated as:

$$Re_o = \frac{\nu_2 D_h}{\nu_o}$$

where ν_o is kinematic viscosity of water in annular region and is taken from [28]. $\nu_o = 1.3 \times 10^{-6} \text{ m}^2/\text{s}$ for $\theta = 10.3^\circ\text{C}$.

$$Re_o = \frac{0.068 \times 0.032}{1.3} \times 10^6 \quad Re_o = 1674$$

Nusselt number of the smooth tube is calculated as follows:

$$Nu_{i \text{ smooth}} = 0.036 Re^{0.8} Pr^{0.333} \left(\frac{D}{L}\right)^{0.055}$$

$$Nu_{i \text{ smooth}} = 0.036 \times 22193^{0.8} \times 2.15^{0.333} \left(\frac{0.019}{2}\right)^{0.055}$$

$$Nu_{i \text{ smooth}} = 107.8$$

Internal heat transfer coefficient of the smooth tube can be found as follows:

$$h_{i \text{ smooth}} = \frac{\text{Nu}_i \cdot k_i}{D_i \text{ smooth}}$$

$$k_i = 0.586 \text{ Kcal/mh}^\circ\text{C for } \theta = 81.8 |28|.$$

$$h_{i \text{ smooth}} = \frac{107.8 \times 0.586}{0.019}$$

$$h_{i \text{ smooth}} = 3324 \text{ Kcal/m}^2\text{h}^\circ\text{C}$$

The ratio of the internal heat transfer coefficient of the roped tube to the internal heat transfer coefficient of the smooth tube is:

$$\frac{h_{i \text{ roped}}}{h_{i \text{ smooth}}} = \frac{4470}{3324} = 1.34$$

B. Calculation of the Fanning Friction Factor:

Test data during a typical experiment are:

$$\Delta P = 365.0 \text{ mm.w.c. } \theta = 17.5^\circ\text{C} \quad m = 440.625 \text{ kg/h}$$

$$\rho = 998.65 \text{ Kg/m}^3, \quad v = 1.0765 \times 10^{-6} \text{ m}^2/\text{s for}$$

$$\theta = 17.5^\circ\text{C } |28|.$$

The velocity of the water inside the roped tube is calculated as:

$$v = \frac{m}{S}$$

where m is the mass flow rate of the water and S is the cross sectional area of the roped tube. $S = 0.002834 \text{ m}^2$

$$v = \frac{440.625}{998.65 \times 3600 \times 0.002834}$$

$$v = 0.432467 \text{ m/S}$$

Reynolds number can be calculated as follows:

$$Re = \frac{v D}{\nu} = \frac{0.432467 \times 0.018}{1.0765} \cdot 10^6$$

$$Re = 7633$$

Fanning Friction Factor is calculated as:

$$f = \frac{1}{2} \frac{\Delta P}{\rho} \frac{D}{L} \frac{g}{v^2}$$

$$f = \frac{1}{2} \frac{365.0}{998.650} \frac{0.019}{3.7} \frac{9.8}{(0.432467)^2}$$

$$f = 0.04917$$

APPENDIX B

A. HEAT TRANSFER DATA FOR THE FIRST ROPED TUBE

Time (min)	θ_{∞} (°C)	θ_{lin} (°C)	θ_{lout} (°C)	θ_{2in} (°C)	θ_{2out} (°C)	m_1 (kg/h)	m_2 (kg/h)	θ_{lts} (m.volt)	θ_{2ts} (m.volt)
TEST NO. 1									
0	23.3	84.7	70.5	21	49.7				
5	23.4	85	71	21	49.6	297.1	126.0	3075	2040
10	23.5	85.5	70.5	21	49.6			3080	
15	23.5	85.8	71	21	49.8	297.0	126.5	3090	2050
20	23.5	85.8	71.2	21	49.7				
25	23.8	84.8	70.5	21	49.4	297.5	127.0	3020	2000
30	23.8	83.9	70	21	49.1				
35	23.9	84	69	21	48.5	301		3000	2000
40	23.9	83.9	69	21	48				

Time (min)	θ_{∞} ($^{\circ}\text{C}$)	θ_{lin} ($^{\circ}\text{C}$)	θ_{lout} ($^{\circ}\text{C}$)	$\theta_{2\text{in}}$ ($^{\circ}\text{C}$)	$\theta_{2\text{out}}$ ($^{\circ}\text{C}$)	m_1 (kg/h)	m_2 (kg/h)	θ_{1ts} (m.volt)	θ_{2ts} (m.volt)
TEST NO. 2									
0	24.0	87.1	72.3	21	52.4				
5	24.1	87.2	71.3	21	52.2	337.5	132.32	3050	1680
10	24.2	87.1	71.7	21	52.5				
15	24.5	86.5	71.5	21	52.2	337	132.12	3000	1600
20	24.2	86.0	71.0	21	52.0			2970	1540
25	24.0	86.1	71.0	21	52.5	336	131.0	2960	1610
30	24.0	86.2	71.5	21	52.6			2920	1510

Time (min)	θ_{∞} (°C)	θ_{1in} (°C)	θ_{1out} (°C)	θ_{2in} (°C)	θ_{2out} (°C)	m_1 (kg/h)	m_2 (kg/h)	θ_{1ts} (m.volt)	θ_{2ts} (m.volt)
TEST NO. 3									
0	24.8	92.5	69.5	21.0	55.7			3270	1350
5	24.8	92.6	69.8	21.0	55.3			3240	1360
10	24.8	92.7	69.9	21.0	55.0	231.75	135.06	3260	1370
15	24.8	92.8	69.9	21.0	54.7			3270	
20	24.8	92.6	69.5	21.0	54.2				1370
25	24.7	92.2	69.5	21.0	54.0	230.21	135.96	3280	
30	24.7	92.1	69.5	20.9	53.6				1370
35	24.7	92.1	68.9	20.9	53.3			3250	
40	24.7	92.0	68.8	20.8	52.9	231.0	137.0		1380
45	24.5	92.0	68.8	20.8	52.5			3240	
50	24.4	91.9	69.0	20.8	52.5	229.0	138.66		1400
55	24.2	91.8	69.0	20.8	52.5			3250	1400
60	24.4	91.8	68.8	20.8	52.2				

Time (min)	θ_{∞} (°C)	θ_{lin} (°C)	θ_{lout} (°C)	θ_{2in} (°C)	θ_{2out} (°C)	m_1 (kg/h)	m_2 (kg/h)	θ_{1ts} (m.volt)	θ_{2ts} (m.volt)
TEST NO. 4									
0	23.2	91.8	76.9	21.9	57.9			3270	1590
5	23.2	91.6	76.6	21.8	57.4	470.3		3260	1630
10	23.3	91.5	78.0	21.7	57.5		152.8		
15	23.3	91.2	76.8	21.7	57.0			3230	1620
20	23.3	90.6	76.0	21.6	56.8	477.0		3220	1620
25	23.4	90.4	77.0	21.5	56.3			3210	1580
30	23.6	90.4	76.0	21.4	55.7		154.0		
35	23.6	89.8	75.8	21.3	55.3	470.0		3180	1580
40	23.6	89.5	76.5	21.2	55.3		154.3	3170	1575
45	23.7	89.7	75.6	21.1	55.2				
50	23.7	89.2	75.5	21.1	55.1	471.0		3150	1570
55	23.7	89.0	76.3	21.0	55.0		154.0		

Time (min)	θ_{∞} ($^{\circ}\text{C}$)	θ_{lin} ($^{\circ}\text{C}$)	θ_{lout} ($^{\circ}\text{C}$)	$\theta_{2\text{in}}$ ($^{\circ}\text{C}$)	$\theta_{2\text{out}}$ ($^{\circ}\text{C}$)	m_1 (kg/h)	m_2 (kg/h)	θ_{1ts} (m.volt)	θ_{2ts} (m.volt)
TEST NO. 5									
0	24.0	88.3	74.3	20.9	54.0		142.2	3080	1540
5	24.0	88.3	74.8	20.9	54.3			3080	1540
10	24.0	88.1	75.0	20.9	54.1	452.6	142.5		
15	24.1	88.2	75.5	20.9	54.3			3110	1550
20	24.3	88.3	74.8	20.8	54.0			3120	1540
25	24.1	88.3	75.9	20.8	54.0	454.0	141.8		
30	24.1	88.5	75.3	20.7	54.0			3110	1510
35	24.3	88.3	75.0	20.7	53.7		142.0		
40	24.2	88.2	74.0	20.7	53.2			3090	1540
45	24.3	88.2	75.0	20.7	53.3	456.3			
50	24.5	88.5	74.8	20.7	53.3				
55	24.6	88.5	74.8	20.7	53.2		141.5	3120	1540
60	24.5	88.7	75.0	20.7	53.2	454.0		3140	1560
65	24.5	88.8	75.0	20.7	53.2				

Time (min)	θ_{∞} (°C)	θ_{lin} (°C)	θ_{lout} (°C)	θ_{2in} (°C)	θ_{2out} (°C)	m_1 (kg/h)	m_2 (kg/h)	θ_{1ts} (m.volt)	θ_{2ts} (m.volt)
TEST NO. 6									
0	25.6	92.4	88.2	21.1	67.1		91.0	3430	2510
5	25.6	92.7	88.9	21.1	67.5	1155.0		3460	2500
10	25.6	92.5	88.6	21.3	67.8				
15	25.7	92.2	88.5	21.2	67.2		92.0	3430	2470
20	25.6	92.7	88.7	21.1	68.1	1156.0			
25	25.5	82.8	88.8	20.9	67.8			3460	2500
30	25.5	93.2	88.8	20.8	67.5		90.0		
35	25.4	93.1	88.2	20.8	67.5	1154.0		3490	2510
40	25.3	92.8	83.8	20.8	67.3				
45	25.2	92.8	88.9	20.8	67.2			3450	2500

Time (min)	θ_{∞} (°C)	θ_{lin} (°C)	θ_{lout} (°C)	θ_{2in} (°C)	θ_{2out} (°C)	m_1 (kg/h)	m_2 (kg/h)	θ_{1ts} (m.volt)	θ_{2ts} (m.volt)
						TEST NO. 7			
0	24.7	90.6	86.5	20.7	59.5		146.7	3380	2140
5	24.8	90.5	86.0	20.7	59.0	1472.5		3370	2140
10	24.9	90.6	86.2	20.6	59.0			3360	2100
15	24.9	90.4	86.3	20.5	59.1		148.0	3370	2110
20	25.1	90.6	86.3	20.5	59.1				
25	25.3	89.8	85.7	20.5	58.5	1475.0		3330	2070
30	25.3	89.8	85.6	20.5	58.5				
35	25.4	90.0	86.0	20.5	58.7		146.2	3380	2060
40	25.4	90.0	85.8	20.5	59.4			3330	2080
45	25.5	90.1	86.2	20.5	59.6	1476.5			
50	25.6	89.5	85.8	20.5	59.5		147.8	3300	2140
55	25.7	89.8	86.0	20.6	60.2			3310	2110
60	25.5	90.0	86.2	20.6	60.4				
65	25.4	90.1	86.2	20.6	60.2	1480.5		3350	2140
70	25.3	89.9	86.0	20.6	59.7		148.0	3330	2110
75	25.3	89.3	85.8	20.6	58.7				
80	25.4	89.6	85.5	20.6	58.5	1477.5		3310	2140
85	25.4	89.9	85.6	20.6	58.6		148.2	3330	2110
90	25.3	90.0	86.0	20.5	58.6			3330	2100

Time (min)	θ_{∞} (°C)	θ_{lin} (°C)	θ_{lout} (°C)	θ_{2in} (°C)	θ_{2out} (°C)	m_1 (kg/h)	m_2 (kg/h)	θ_{lts} (m.volt)	θ_{2ts} (m.volt)
TEST NO. 8									
0	24.8	88.6	85.5	20.7	72.9			3320	2080
5	24.8	88.4	85.0	20.7	72.9	2655.0			
10	24.8	88.1	85.0	20.5	72.3		158.0	3300	2080
15	24.6	88.9	85.5	20.5	72.5				
20	24.6	88.6	85.0	20.4	72.1	2653.0		3330	2060
25	24.6	88.4	85.1	20.4	72.0		157.0	3320	2080

Time (min)	θ_{∞} (°C)	θ_{lin} (°C)	θ_{lout} (°C)	θ_{2in} (°C)	θ_{2out} (°C)	m_1 (kg/h)	m_2 (kg/h)	θ_{lts} (m.volt)	θ_{2ts} (m.volt)
TEST NO. 9									
0	24.5	87.8	84.8	20.8	70.9		157.5	3290	2110
5	24.6	87.7	84.7	20.7	70.8	3002			
10	24.7	87.7	84.7	20.7	70.9			3290	2090
15	24.9	87.7	84.7	20.7	70.9		157.3	3280	2100
20	24.9	87.8	84.9	20.7	71.4	3000			
25	24.9	87.6	84.7	20.7	71.4			3270	2100
30	25.1	87.6	84.6	20.7	71.3	3001	157.3		
35	25.2	87.5	84.5	20.7	71.3			3260	2090
40	25.4	87.7	84.5	20.7	71.3		157.2		
45	25.5	87.6	84.5	20.7	71.3	3000		3250	2100
50	25.6	87.5	84.4	20.7	71.1			3240	2060
55	25.7	87.5	84.5	20.7	71.1		157.3	3230	2080
60	25.7	87.5	84.5	20.7	71.0			3230	2050

Time (min)	θ_{∞} (°C)	θ_{lin} (°C)	θ_{lout} (°C)	θ_{2in} (°C)	θ_{2out} (°C)	m_1 (kg/h)	m_2 (kg/h)	θ_{1ts} (m.volt)	θ_{2ts} (m.volt)
TEST NO. 10									
0	23.8	78.2	76.0	21.5	58.0		145.0		
5	23.8	78.5	76.0	21.5	58.4	1580.0		2720	1790
10	23.9	78.9	75.8	21.5	59.0			2730	1730
15	24.0	78.2	75.8	21.5	59.4		146.1		
20	24.1	78.0	76.0	21.5	58.4	1584.0		2730	1680
25	24.1	79.0	76.0	21.5	58.0		146.0	2730	1680
30	24.2	79.3	76.0	21.5	58.4	1584		2730	1670
35	24.5	79.1	75.8	21.5	89.0			2730	1660
40	24.8	79.0	75.6	21.5	59.4			2700	1680
45	24.9	79.1	76.0	21.5	60.3		144.0		
50	25.0	79.0	75.5	21.5	60.0	1580		2650	1700
55	25.3	79.0	75.5	21.5	60.0			2660	1670
60	25.4	78.9	75.6	21.5	60.1		145.0		
65	25.4	78.8	75.0	21.5	59.5	1582		2680	1670

Time (min)	θ_{∞} (°C)	θ_{1in} (°C)	θ_{1out} (°C)	θ_{2in} (°C)	θ_{2out} (°C)	m_1 (kg/h)	m_2 (kg/h)	θ_{1ts} (m.volt)	θ_{2ts} (m.volt)
TEST NO. 11									
0	25.3	81.0	73.5	21.6	61.0		110.0	2670	1550
5	25.4	81.2	73.0	21.7	61.3	715.0			
10	25.5	81.5	73.5	21.7	61.8			2710	1530
15	25.5	80.7	73.0	21.7	61.4	713.1	109.5	2720	1550
20	25.5	80.5	72.0	21.7	61.0			2710	1510
25	25.5	80.8	72.5	21.7	60.8		108.2	2740	1520
30	25.6	80.0	73.5	21.7	61.0	713.0		2700	1510
35	25.5	80.0	72.0	21.7	60.8			2720	1530
40	25.5	80.0	73.5	21.7	61.0		109.2	2700	1520
45	25.5	80.0	73.0	21.7	61.0	711.0			

Time (min)	θ_{∞} (°C)	θ_{lin} (°C)	θ_{lout} (°C)	θ_{in} (°C)	θ_{2out} (°C)	m_1 (kg/h)	m_2 (kg/h)	θ_{1ts} (m.volt)	θ_{2ts} (m.volt)
TEST NO. 12									
0	25.1	83.2	72.5	21.8	51.5		557.0	2800	1550
5	25.3	83.1	72.0	21.8	51.4	149.9		2750	1530
10	25.2	83.0	72.1	21.8	51.6				
15	25.3	83.0	72.0	21.8	51.5	149.1	556.0	2730	1540
20	25.1	82.9	71.9	21.8	51.6				
25	25.2	82.9	71.8	21.8	51.4		558.0	2710	1520
30	25.2	83.0	71.7	21.8	51.5	150.3	x	2720	

Time (min)	θ_{∞} (°C)	θ_{lin} (°C)	θ_{lout} (°C)	θ_{2in} (°C)	θ_{2out} (°C)	m_1 (kg/h)	m_2 (kg/h)	θ_{1ts} (m.volt)	θ_{2ts} (m.volt)
TEST NO. 13									
0	25.4	77.0	72.5	21.8	53.5		136.5	2590	1690
5	25.4	77.8	72.6	21.8	53.4	1135.1		2600	1650
10	25.5	78.0	72.5	21.8	53.2			2580	1680
15	25.4	77.3	72.8	21.9	53.2	1130.2	136.6	2540	1650
20	25.2	77.0	72.5	21.9	53.1				
25	25.4	77.0	72.0	21.9	53.0	1131.1		2530	1640
30	25.3	77.0	72.5	21.9	53.1		136.7		
35	25.5	76.7	72.8	22.0	53.4	1129.0		2560	1630
40	25.4	76.5	72.3	22.0	53.2		136.6		
45	25.4	76.2	72.5	22.0	53.2	1131.1		2520	1650

Time (min)	θ_{∞} (°C)	θ_{lin} (°C)	θ_{lout} (°C)	θ_{2in} (°C)	θ_{2out} (°C)	m_1 (kg/h)	m_2 (kg/h)	θ_{lts} (m.volt)	θ_{2ts} (m.volt)
TEST NO. 14									
0	25.3	80.7	75.2	21.7	56.5	1030.4		2720	1620
5	25.4	80.9	75.8	21.7	56.7		147.6	2710	1600
10	25.5	80.7	75.2	21.7	56.5	1031.7			
15	25.5	80.7	75.1	21.7	56.5		147.7	2700	1580
20	25.5	80.6	75.3	21.7	56.5	1030.7		2700	1600
25	25.6	80.5	75.8	21.7	56.5		147.9		
30	25.7	80.5	75.2	21.7	56.3			2680	1600

Time (min)	θ_{∞} (°C)	θ_{lin} (°C)	θ_{lout} (°C)	θ_{2in} (°C)	θ_{2out} (°C)	m_1 (kg/h)	m_2 (kg/h)	θ_{1ts} (m.volt)	θ_{2ts} (m.volt)
TEST NO. 15									
0	25.4	74.7	67.8	21.7	48.2		131.2	2420	1880
5	25.4	74.9	67.9	21.7	48.3	663.6		2430	1860
10	25.4	75.0	68.0	21.7	48.4		130.8	2430	1860
15	25.5	75.2	67.5	21.8	48.5	671.1			
20	25.5	74.9	67.9	21.8	48.1			2450	1850
25	25.6	75.0	68.0	21.8	48.2		130.0		
30	25.7	75.1	68.0	21.8	48.0	665.7		2450	1890
35	25.8	75.3	68.2	21.8	47.7		129.5		
40	25.9	75.2	67.9	21.8	47.6			2430	1850
45	25.9	75.0	68.0	21.8	47.5	666.0			

B. HEAT TRANSFER DATA FOR THE SECOND ROPED TUBE

Time (min)	θ_{∞} (°C)	θ_{1in} (°C)	θ_{1out} (°C)	θ_{2in} (°C)	θ_{2out} (°C)	m_1 (kg/h)	m_2 (kg/h)	θ_{1ts} (m.volt)	θ_{2ts} (m.volt)
TEST NO. 1									
0	15.0	86.0	77.9	14.1		410.4		3230	3200
5	15.0	86.1	77.8	14.1			459.4	3240	2190
10	15.0	86.2	77.7	14.1				3230	3200
15	15.0	86.0	77.8	14.1		409.0	455.0		
20	14.7	86.0	77.5	14.1				3250	3200
25	14.8	86.0	77.4	14.1		409.5	455.7		
30	15.0	86.0	77.8	14.1				3220	3200
35	15.0	86.0	77.5	14.1			458		
40	15.1	86.0	77.5	14.1		408.7		3230	3200

Time (min)	θ_{∞} ($^{\circ}\text{C}$)	θ_{lin} ($^{\circ}\text{C}$)	θ_{lout} ($^{\circ}\text{C}$)	θ_{2in} ($^{\circ}\text{C}$)	θ_{2out} ($^{\circ}\text{C}$)	m_1 (kg/h)	m_2 (kg/h)	θ_{1ts} (m.volt)	θ_{2ts} (m.volt)
TEST NO. 2									
0	15.6	86.4	79.0	6.8	13.7	383.0		3210	3150
5	15.7	86.4	79.0	6.7	13.7		377.1	3190	3160
10	15.6	86.6	79.2	6.8	13.6	383.0			
15	15.4	86.4	79.2	6.8	13.9		376.0	3210	3190
20	15.4	86.4	79.2	6.8	13.9	383.0		3230	3160
25	15.6	86.8	79.4	6.8	13.9		376.0		
30	15.7	86.7	79.3	6.8	13.9	382.0		3260	3160
35	15.6	86.9	79.4	6.8	13.9		375.0		
40	15.6	86.0	79.8	6.8	13.8			3290	3190
TEST NO. 3									
0	21.5	95.8	89.5	9.5	17.0	534.8		3480	3510
5	21.7	95.8	89.6	9.5	17.0		486.2	3500	3490
10	21.8	95.3	89.3	9.5	17.2	538.6			
15	21.8	94.8	88.9	9.5	17.0			3400	3450
20	21.8	94.6	88.4	9.4	16.5		488.4		
25	21.8	94.6	88.4	9.3	16.0	538.6		3390	3450
30	21.8	94.8	88.5	9.1	16.0		489.2	3460	3460
35	21.9	94.9	88.7	9.1	16.0	539.9		3400	3480
40	21.9	95.1	88.8	9.1	16.0		489.1	3440	3470
45	21.9	95.3	89.1	9.1	16.0			3440	3470

Time (min)	θ_{∞} (°C)	θ_{lin} (°C)	θ_{out} (°C)	θ_{2in} (°C)	θ_{2out} (°C)	m_1 (kg/h)	m_2 (kg/h)	θ_{1ts} (m.volt)	θ_{2ts} (m.volt)
TEST NO. 4									
0	21.3	95.0	88.2	9.1	15.2	452.4		3390	3450
5	21.3	95.1	88.2	9.1	15.2		502.8		
10	21.3	95.2	88.4	9.0	15.2	451.6		3450	3470
15	21.3	95.3	88.6	9.0	15.0		504.0		
20	21.1	95.5	88.7	9.0	15.0	451.1		3440	3500
25	21.3	95.4	88.8	9.0	15.0		505.5		
30	21.4	95.3	88.7	9.0	15.0	450.0		3440	3470
35	21.3	95.3	88.8	9.0	15.0		506.0		
40	21.3	95.3	88.8	9.0	15.0	449.8		3410	3500
45	21.3	95.3	88.9	9.0	15.0				
TEST NO. 5									
0	21.3	91.0	86.3	9.3	14.9	603.7		3240	3310
5	21.4	91.0	86.4	9.2	14.8		513.4		
10	21.5	91.1	86.4	9.1	14.5	603.7		3260	3300
15	21.6	91.1	86.5	9.0	14.3		516.0	3240	3280
20	21.6	91.2	86.9	8.9	14.2	603.7		3230	3290
25	21.5	91.0	86.3	8.9	14.0		516.7		
30	21.6	90.8	86.0	8.9	14.0	603.7		3220	3280
35	21.5	90.4	86.1	8.9	14.0		519.0	3220	3250

Time (min)	θ_{∞} (°C)	θ_{1in} (°C)	θ_{1out} (°C)	θ_{2in} (°C)	θ_{2out} (°C)	m_1 (kg/h)	m_2 (kg/h)	θ_{1ts} (m.volt)	θ_{2ts} (m.volt)
TEST NO. 6									
0	22.1	95.8	86.1	9.8	13.8	201.3		3150	3190
5	22.2	95.9	86.4	9.7	13.7		539.0	3200	3190
10	22.2	95.7	86.3	9.6	13.5	200.0			
15	22.2	95.3	86.3	9.5	13.4			3170	3160
20	22.3	95.0	85.0	9.4	13.2		540.0		
25	22.3	95.2	85.3	9.4	13.1	205.1		3130	3200
30	22.3	95.1	85.4	9.3	13.2				
35	22.3	95.1	85.4	9.3	13.0		538.0	3130	3140
40	22.3	95.0	85.3	9.3	13.0	200.0			
45	22.3	95.0	85.3	9.3	13.0			3120	3190
50	22.3	95.0	85.8	9.2	13.0		539.0		
55	22.4	95.0	85.8	9.2	12.5			3140	3160

Time (min)	θ_{∞} (°C)	θ_{lin} (°C)	θ_{lout} (°C)	θ_{2i} (°C)	θ_{2out} (°C)	m_1 (kg/h)	m_2 (kg/h)	θ_{lts} (m.volt)	θ_{2ts} (m.volt)
TEST NO. 7									
0	21.8	93.2	84.3	8.8	13.0	253.2		3190	3220
5	21.8	93.2	85.2	8.8	13.0		534.7		
10	21.8	93.2	85.1	8.8	13.0	253.1		3190	3200
15	21.8	93.2	84.8	8.8	13.0		534.9		
20	21.8	93.2	84.2	8.8	13.0	253.3		3170	3190
25	21.8	93.2	83.8	8.8	13.0		534.8		
30	21.8	93.2	83.5	8.8	13.0			3110	3140

Time (min)	θ_{∞} ($^{\circ}\text{C}$)	θ_{lin} ($^{\circ}\text{C}$)	θ_{lout} ($^{\circ}\text{C}$)	$\theta_{2\text{in}}$ ($^{\circ}\text{C}$)	$\theta_{2\text{out}}$ ($^{\circ}\text{C}$)	m_1 (g/h)	m_2 (kg/h)	θ_{1ts} (m.volt)	θ_{2ts} (m.volt)
TEST NO. 8									
0	22.3	94.3	83.0	9.1	12.0	152.8		2990	3030
5	22.3	94.3	83.0	9.0	12.0		568.6		
10	22.3	94.4	83.3	9.0	12.0	150.4		3000	2990
15	22.3	94.3	83.2	9.0	12.0		568.8		
20	22.3	94.1	83.1	9.0	12.0	150.0		2970	3030
25	22.3	94.1	83.1	9.0	12.0		568.7		
30	22.3	94.2	82.2	9.0	12.0	150.8		3000	3000
35	22.3	94.3	83.3	9.0	12.0		568.7		
40	22.3	94.3	83.6	9.0	12.0	148.0		3000	3050
45	22.3	94.4	83.2	9.0	12.0				

Time (min)	θ_{∞} (°C)	θ_{1in} (°C)	θ_{1out} (°C)	θ_{2in} (°C)	θ_{2out} (°C)	m_1 (kg/h)	m_2 (kg/h)	θ_{1ts} (m.volt)	θ_{2ts} (m.volt)
TEST NO. 9									
0	21.8	91.5	76.8	10.3	13.9	136.6		2760	2670
5	21.8	91.6	76.7	10.3	13.8	*	582.4	2790	2640
10	21.9	91.7	77.1	10.2	13.7	138.1			
15	22.0	92.1	77.3	10.1	13.7		583.0	2780	2680
20	22.1	92.0	77.3	10.1	13.6	138.3			
25	22.0	92.3	77.6	10.1	13.6		585.8	2820	2640
30	22.3	92.5	77.9	10.1	13.6	138.5		2820	2690
35	22.2	92.4	78.3	10.1	13.5		582.0	2810	2680
40	22.4	92.3	78.5	10.1	13.5	139.7		2800	2670

Time (min)	θ_{∞} (°C)	θ_{lin} (°C)	θ_{lout} (°C)	θ_{2in} (°C)	θ_{2out} (°C)	m_1 (kg/h)	m_2 (kg/h)	θ_{lts} (m.volt)	θ_{2ts} (m.volt)
TEST NO. 10									
0	22.9	91.8	74.1	10.3	12.9	84.8		2490	2360
5	22.9	91.7	74.1	10.2	12.7		588.0	2500	2340
10	22.8	91.7	73.7	10.2	12.8	85.3			
15	22.8	91.8	74.1	10.2	12.8		586.4	2500	2370
20	22.8	91.9	74.2	10.2	12.8	85.3			
25	22.8	91.7	74.2	10.2	12.8		586.4	2510	2360
30	22.8	91.6	74.2	10.2	12.8	85.8			
35	22.8	91.6	74.4	10.2	12.8		584.8	2500	2360
40	22.7	91.7	74.1	10.2	12.8				

Time (min)	θ_{∞} (°C)	θ_{lin} (°C)	θ_{lout} (°C)	θ_{2in} (°C)	θ_{2out} (°C)	m_1 (kg/h)	m_2 (kg/h)	θ_{1ts} (m.volt)	θ_{2ts} (m.volt)
TEST NO. 11									
0	22.8	93.2	77.3	10.2	13.2	117.3		2710	2600
5	22.8	93.1	77.2	10.2	13.3		597.8	2710	2570
10	22.8	93.0	77.2	10.2	13.3	116.8		2710	2600
15	22.8	92.9	77.2	10.2	13.4		594.2		
20	22.8	92.9	77.4	10.2	13.3	116.8		2730	2580
25	22.8	92.6	77.2	10.2	13.3		594.2	2680	2580
30	22.8	92.6	77.2	10.2	13.4	116.4			
35	22.8	92.7	77.3	10.2	13.3		588.6	2710	2580
40	22.8	92.7	77.4	10.2	13.2			2720	2580

Time (min)	θ_{∞} (°C)	θ_{lin} (°C)	θ_{lout} (°C)	θ_{2in} (°C)	θ_{2out} (°C)	m_1 (kg/h)	m_2 (kg/h)	θ_{1ts} (m.volt)	θ_{2ts} (m.volt)
TEST NO, 12									
0	22.4	90.0	72.6	11.1	14.3	100.4		2580	2400
5	22.4	90.0	72.9	11.0	14.1		562.0		
10	22.4	90.0	73.0	10.8	14.4	100.0		2590	2360
15	22.5	90.0	73.0	10.6	14.1		563.0		
20	22.4	90.0	73.0	10.8	13.9	100.2		2570	2390
25	22.5	90.0	73.0	10.8	14.0		562.0		
30	22.7	90.0	73.2	10.7	13.8	100.1		2570	2380
35	22.6	90.0	73.3	10.7	13.7		561.0		
40	22.5	90.0	73.2	10.7	13.6			2550	2360

Time (min)	θ_{∞} (°C)	θ_{lin} (°C)	θ_{lout} (°C)	θ_{2in} (°C)	θ_{2out} (°C)	m_1 (kg/h)	m_2 (kg/h)	θ_{lts} (m.volt)	θ_{2ts} (m.volt)
TEST NO. 13									
0	22.5	89.0	66.9	10.6	12.7	59.9		2290	1970
5	22.6	89.1	67.2	10.6	12.7		608.4	2290	1980
10	22.6	89.1	66.9	10.6	12.7	60.3		2290	1940
15	22.7	89.1	66.8	10.6	12.7		608.6		
20	22.7	89.0	66.9	10.6	12.7	59.6		2260	1960
25	22.7	89.0	67.0	10.6	12.7		608.2		
30	22.7	89.0	67.2	10.6	12.7	59.9		2320	2040
35	22.7	89.0	67.9	10.6	12.7				
40	22.7	89.0	67.9	10.6	12.7		608.4	2290	1980

Time (min)	θ_{∞} (°C)	θ_{1in} (°C)	θ_{1out} (°C)	θ_{2in} (°C)	θ_{2out} (°C)	m_1 (kg/h)	m_2 (kg/h)	θ_{1ts} (m.volt)	θ_{2ts} (m.volt)
TEST NO. 14									
0	21.7	90.0	60.6	11.2	13.0	35.4		2250	1650
5	21.7	90.0	60.5	11.2	13.0		589.0	2210	1640
10	21.7	90.0	60.8	11.2	13.0	35.7			
15	21.7	89.9	60.6	11.2	13.0		591.6	2200	1620
20	21.7	84.8	60.7	11.2	13.0	35.7		2190	1640
25	21.7	89.8	60.8	11.2	13.0		591.0		
30	21.7	89.8	60.9	11.2	13.0	35.7		2230	1670
35	21.7	89.7	60.8	11.2	13.0		593.0		
40	21.7	89.7	60.9	11.2	13.0	36.0		2230	1680

Time (min)	θ_{∞} ($^{\circ}\text{C}$)	θ_{1in} ($^{\circ}\text{C}$)	θ_{1out} ($^{\circ}\text{C}$)	θ_{2in} ($^{\circ}\text{C}$)	θ_{2out} ($^{\circ}\text{C}$)	m_1 (kg/h)	m_2 (kg/h)	θ_{1ts} (m.volt)	θ_{2ts} (m.volt)
TEST NO. 15									
0	21.7	80.6	44.3	11.0	12.3	22.1		1710	970
5	21.7	80.7	44.4	11.0	12.3		608.9	1730	970
10	21.7	80.7	44.5	11.0	12.3	22.3		1730	980
15	21.7	80.7	44.7	11.0	12.3		612.4		
20	21.7	80.8	44.9	11.0	12.3	22.1		1740	980
25	21.7	80.9	44.9	11.0	12.3		608.0		
30	21.7	81.0	45.3	11.0	12.3	22.5		1740	1010
35	21.7	81.1	45.4	11.0	12.3		605.4		
40	21.7	81.3	45.7	11.0	12.3			1760	1030

Time (min)	θ_{∞} (°C)	θ_{1in} (°C)	θ_{1out} (°C)	θ_{2in} (°C)	θ_{2out} (°C)	m_1 (kg/h)	m_2 (kg/h)	θ_{1ts} (m.volt)	θ_{2ts} (m.volt)
TEST NO. 16									
0	21.8	76.8	38.5	11.0	12.3	12.8		1510	630
5	22.1	76.6	88.5	11.0	12.3		520.5		
10	22.2	76.3	38.3	11.0	12.2	12.2		1510	610
15	22.1	76.1	38.2	11.0	12.2		520.5		
20	22.2	76.0	38.0	11.0	12.2	12.8		1480	610
25	22.3	75.8	37.8	11.0	12.2		521.2		
30	22.3	75.7	37.8	11.0	12.2	13.4		1480	580
35	22.3	75.6	37.6	11.0	12.2		519.9	1460	560
40	22.4	75.5	37.6	11.0	12.1				

Time (min)	θ_{∞} (°C)	θ_{1in} (°C)	θ_{1out} (°C)	θ_{2in} (°C)	θ_{2out} (°C)	m_1 (kg/h)	m_2 (kg/h)	θ_{1ts} (m.volt)	θ_{2ts} (m.volt)
TEST NO. 17									
0	22.7	87.6	57.0	11.0	13.0	29.9		2110	1480
5	22.7	87.7	57.1	11.0	13.0		470.1	2100	1520
10	22.7	87.8	57.2	11.0	13.0	30.0		2100	1530
15	22.7	87.8	57.5	11.0	13.0		470.2	2090	1530
20	22.7	87.8	57.3	11.0	13.0	29.8			
25	22.7	87.9	57.5	11.0	13.0		471.1	2110	1530
30	22.7	87.9	57.3	11.0	13.0	29.9		2120	1550
35	22.7	87.9	57.7	11.0	13.0		473.4		
40	22.7	88.0	57.7	11.0	13.0			2120	1560

Time (min)	θ_{∞} (°C)	θ_{lin} (°C)	θ_{lout} (°C)	θ_{2in} (°C)	θ_{2out} (°C)	m_1 (kg/h)	m_2 (kg/h)	θ_{1ts} (m.volt)	θ_{2ts} (m.volt)
TEST NO. 18									
0	22.4	90.8	64.5	11.1	13.5	41.6		2380	1920
5	22.4	91.0	64.9	11.1	13.5		449.0		
10	22.4	91.0	65.0	11.1	13.5	41.8		2390	1920
15	22.4	91.1	65.3	11.1	13.5		445.0	2380	1940
20	22.4	91.1	65.2	11.1	13.5	41.8		2390	1930
25	22.4	91.2	65.7	11.1	13.5		444.0		
30	22.4	91.3	65.7	11.1	13.5	42.1		2400	1970
35	22.4	91.3	65.9	11.1	13.5		441.3		
40	22.4	91.3	65.7	11.1	13.5			2400	1960

Time (min)	U_{∞} (°C)	θ_{lin} (°C)	θ_{lout} (°C)	θ_{2in} (°C)	θ_{2out} (°C)	m_1 (kg/h)	m_2 (kg/h)	θ_{1ts} (m.volt)	θ_{2ts} (m.volt)
TEST NO. 19									
0	20.2	78.6	41.8	11.3	12.2	17.8		1670	920
5	20.2	78.7	41.8	11.3	12.2		663.6		
10	20.2	78.8	42.1	11.2	12.1	17.9		1690	910
15	20.2	78.8	42.1	11.2	12.1		664.0	1670	920
20	20.2	78.8	42.0	11.2	12.1	17.9			
25	20.2	78.8	42.0	11.2	12.1		662.0	1640	930
30	20.2	78.9	42.0	11.2	12.1	18.0			
35	20.2	78.9	42.0	11.1	12.1		663.8	1680	920
40	20.2	78.9	42.0	11.1	12.1			1680	920

Time (min)	θ_m (°C)	θ_{lin} (°C)	θ_{lout} (°C)	θ_{2in} (°C)	θ_{2out} (°C)	m_1 (kg/h)	m_2 (kg/h)	θ_{1ts} (m.volt)	θ_{2ts} (m.volt)
TEST NO. 20									
0	20.3	77.3	29.6	11.1	11.8	5.7		1420	280
5	20.5	76.6	28.4	11.1	11.8		646.8		
10	20.4	76.1	28.5	11.1	11.8	5.6		1440	280
15	20.4	76.1	28.1	11.1	11.8		640.8		
20	20.4	76.1	28.2	11.1	11.8	5.5		1450	290
25	20.4	76.2	28.3	11.1	11.8		643.3		
30	20.3	76.3	28.2	11.1	11.8	5.4		1430	270
35	20.4	76.4	28.2	11.1	11.8		640.2		
40	20.4	76.6	28.2	11.1	11.8			1430	280

APPENDIX C

A. CALCULATED QUANTITIES FOR THE FIRST ROPED TUBE

Test No	Q_1 $(\frac{\text{kcal}}{\text{h}})$	Q_2 $(\frac{\text{kcal}}{\text{h}})$	$\Delta\theta_{m_i}$	$\Delta\theta_{m_o}$	h_i $(\frac{\text{kcal}}{\text{m}^2\text{h}^\circ\text{C}})$	h_o $(\frac{\text{kcal}}{\text{m}^2\text{h}^\circ\text{C}})$	v_1 $(\frac{\text{m}}{\text{s}})$	v_2 $(\frac{\text{m}}{\text{s}})$	Re_i	Nu_i
1	4336	4330	8.7	32.1	996	226	0.021	0.056	4056	121.3
2	5253	5200	10.3	31.6	1013	259	0.024	0.059	4600	128.3
3	5280	5150	10.9	31.4	967	285.5	0.016	0.061	3200	117.5
4	6625	6600	12.4	30.4	1063	351	0.034	0.069	6879	128.8
5	6112	6015	11.3	31.3	1076	298.4	0.032	0.064	5700	130.6
6	4618	4540	6.8	35.5	1344	239	0.083	0.041	18126	161.9
7	5900	5723	7.3	36.8	1607	311	0.10	0.06	22484	194
8	8760	8680	6.9	26.9	2517	499	0.19	0.07	40119	304
9	9000	8888	6.4	27.3	2812	591.4	0.21	0.071	44786	340
10	5380	5368	6.7	27.2	1596	395	0.114	0.065	20176	194.6
11	5351	5312	8.8	23.5	1216	366	0.05	0.049	9572	148.3
12	6070	5960	10.4	33.3	1158	267	0.04	0.067	7500	141.2
13	5090	4875	7.3	27.6	1395	310	0.081	0.061	14804	170.6
14	5356	5143	9.1	27.3	1173	376	0.074	0.066	14071	142.8
15	4732	4503	4.4	31.3	2151	217.4	0.048	0.058	8215	264.6

Test No	θ_{in} ave. ($^{\circ}C$)	θ_{out} ave ($^{\circ}C$)	$10^6 v_i$ (m^2/S)	$10^6 v_o$ (m^2/S)	k_i ($\frac{kcal}{mh^{\circ}C}$)	k_o ($\frac{kcal}{mh^{\circ}C}$)	Pr_i	Pr_o
1	78.1	35.3	0.370	0.728	0.574	0.537	2.27	4.80
2	78.4	36.6	0.370	0.705	0.575	0.539	2.24	4.67
3	80.7	37.3	0.365	0.695	0.576	0.5397	2.20	4.60
4	83.4	33.7	0.348	0.647	0.577	0.541	2.08	4.44
5	81.6	37.2	0.355	0.697	0.576	0.5396	2.16	4.61
6	90.7	44.3	0.322	0.611	0.581	0.547	1.94	3.98
7	88.0	39.8	0.330	0.656	0.580	0.543	2.12	4.30
8	86.8	46.4	0.334	0.589	0.579	0.549	2.02	3.82
9	86.1	45.9	0.337	0.594	0.579	0.549	2.02	3.85
10	77.1	40.0	0.375	0.656	0.574	0.543	2.30	4.30
11	76.7	41.4	0.376	0.641	0.573	0.555	2.31	4.29
12	77.5	36.6	0.373	0.705	0.574	0.539	2.28	4.67
13	74.7	37.5	0.386	0.692	0.572	0.540	2.37	4.57
14	78.1	39.1	0.370	0.669	0.574	0.542	2.44	4.4
15	71.5	35	0.409	0.728	0.569	0.538	2.53	4.84

B. CALCULATED QUANTITIES FOR THE SECOND ROPED TUBE

Test No	Q_1 ($\frac{\text{kcal}}{h}$)	Q_2 ($\frac{\text{kcal}}{h}$)	$\Delta\theta_{m_i}$	$\Delta\theta_{m_o}$	h_i ($\frac{\text{kcal}}{m^2 h^\circ C}$)	h_o ($\frac{\text{kcal}}{m^2 h^\circ C}$)	v_1 ($\frac{m}{S}$)	v_2 ($\frac{m}{S}$)	Re_i	Nu_i
1	3420	3480	5.10	65.3	4470	355.0	0.40	0.068	21408	145
2	2707	2580	5.12	66.5	3524	268.6	0.368	0.057	19977	116
3	3340	3268	4.0	74.0	5566	294.4	0.527	0.072	31740	181.7
4	3022	3020	4.62	74.0	4360	272.0	0.442	0.075	26587	142.3
5	2777	2738	5.56	76.0	6383	240.0	0.591	0.077	38064	209
6	1933	1920	6.95	70.9	1854	180.0	0.197	0.080	11641	60.6
7	2283	2215	5.77	71.0	2574	208.0	0.248	0.080	14453	84.2
8	1670	1590	8.17	68.7	1362	154.3	0.147	0.085	8590	44.6
9	2003	1980	9.56	62.0	1397	213.0	0.135	0.087	7535	45.8
10	1500	1466	11.95	58.0	837	168.5	0.083	0.087	4500	27.5
11	1835	1780	10.54	61.5	1160	193.0	0.114	0.088	6370	38.0
12	1707	1686	10.32	57.3	1102	196.0	0.098	0.084	5266	36.3
13	1307	1277	12.88	52.0	676	163.7	0.058	0.090	3013	22.3
14	1041	1005	13.88	47.0	500	142.5	0.035	0.088	1727	16.6
15	801	791	11.45	36.2	466	145.8	0.022	0.091	917	15.6
16	487	424	10.66	30.7	304	135.0	0.012	0.077	482	10.3
17	910	943	12.30	45.6	493	137.0	0.029	0.070	1405	16.4
18	1080	1113	12.34	51.5	583	144.0	0.041	0.066	2108	19.3
19	660	597	11.24	33.5	391	118.8	0.017	0.099	708	13.2
20	266	250	9.10	24.7	195	121.5	0.005	0.096	200	6.6

Test No	$\theta_{\text{ave.}}^{\text{in}}$ (°C)	$\theta_{\text{ave.}}^{\text{out}}$ (°C)	$10^6 v_i$ (m ² /S)	$10^6 v_o$ (m ² /S)	k_i ($\frac{\text{kcal}}{\text{mh}^\circ\text{C}}$)	k_o ($\frac{\text{kcal}}{\text{mh}^\circ\text{C}}$)	Pr _i	Pr _o
1	81.8	10.3	0.355	1.300	0.576	0.505	2.15	9.28
2	82.9	10.3	0.350	1.300	0.577	0.505	2.12	9.28
3	92.0	13.0	0.316	1.210	0.582	0.509	1.89	8.58
4	92.0	12.0	0.316	1.240	0.582	0.508	1.89	8.81
5	88.7	11.7	0.327	1.253	0.580	0.507	1.76	8.88
6	90.4	11.2	0.322	1.270	0.581	0.507	1.94	9.05
7	89.0	11.0	0.326	1.270	0.580	0.506	1.94	9.28
8	88.7	10.5	0.327	1.300	0.580	0.505	1.96	9.28
9	85.0	12.0	0.341	1.240	0.578	0.507	2.07	8.11
10	83.0	11.5	0.350	1.240	0.577	0.507	2.12	8.93
11	85.0	12.0	0.341	1.240	0.578	0.507	2.07	8.11
12	81.5	12.4	0.355	1.240	0.577	0.508	2.16	8.72
13	78.0	11.6	0.370	1.230	0.574	0.507	2.26	8.90
14	75.0	12.1	0.385	1.250	0.572	0.507	2.36	8.81
15	63.0	11.6	0.453	1.240	0.565	0.507	2.40	8.90
16	57.0	11.6	0.495	1.250	0.560	0.507	3.14	8.90
17	72.6	12.6	0.397	1.250	0.571	0.507	2.45	8.81
18	78.2	12.3	0.370	1.240	0.574	0.508	2.26	8.74
19	60.4	11.6	0.471	1.230	0.574	0.508	2.26	8.74
20	52.4	11.4	0.532	1.230	0.563	0.507	2.96	8.90
					0.555	0.507	3.54	8.90

REFERENCES

1. Bergles, A.E., "Augmentation of Forced Convection Heat Transfer", *NATO Advanced Study Institute, Turbulent Forced Convection in Channels and Rod Bundles*, Istanbul, Turkey, July 20- August 2, 1978.
2. Elçi, N., "Investigation of Heat Transfer Augmentation by Roughness Elements in the Form of Dimples Under Forced Convection in Circular Tubes", B.S. in M.E., Robert College, 1971.
3. Bergles, A.E., "Heat Transfer Characteristics of Turbotec Tubing", *Engineering Research Institute*, Iowa State University, Ames, Iowa, 50010, USA.
4. Lawson, C.G., R.J. Kedl and R.E. McDonald, "Enhanced Heat Transfer Tubes for Horizontal Condensers with Possible Application in Nuclear Power Plant Design", *American Nuclear Society Transactions*, Vol. 9, 1966, pp. 565-566.
5. Blumenkratz, A., A. Yorden and J. Taburec, "Performance Prediction and Evaluation of Phelps Dodge Spirally Grooved Tubes. Inside Tube Flow Pressure Drop and Heat Transfer in Turbulent Regime", *Heat Transfer Research, Inc.*, 300-4, December 1969.
6. Kidd, G.J. "The Heat Transfer and Pressure Drop Characteristics of Gas Flow Inside Spirally Corrugated Tubes", *J. Heat Transfer*, Vol. 92, 1970, pp. 513-519.
7. Withers, J.G. and E.H. Young, "Steam Condensing on Vertical Rows of Horizontal Corrugated and Plain Tubes", *Ind. Eng. Chem. Process. Des. Develop.*, Vol. 10, 1971, pp. 19-30.
8. Kalinin, E.K. and C.A. Yarkho, "Study of Intensification of Heat Transfer to Liquids and Gases in Channels", *Journal of Engineering Physics*, Vol. 20, 1971, pp. 592-599.
9. Kramer, J.M. and R.A. Gater, "Pressure Loss and Heat Transfer for Non-Boiling Fluid Flow in Convolute Tubing", *ASME*, Paper No. 73-HT-23, 1973.

10. Newson, I.H. and T.D. Hodgson, "The Development of Enhanced Heat Transfer Condenser Tubing", *4th International Symposium on Fresh Water from the Sea*, Vol. 1, 1973, pp. 69-74.
11. Robles, H., "Pressure Loss and Forced Convection Heat Transfer Characteristics of Convolute Tubing", ME Thesis, University of Florida, 1973.
12. Hitachi Mechanical Engineering Research Laboratory, Tschuira-Chi, Japan, *Special Research Report*, 73B23-4-1, October 15, 1974.
13. Watkinson, A.P., L. Louis and R. Brent, "Scaling of Enhanced Heat Exchanger Tubes", *The Canadian Journal of Chemical Engineering*, Vol. 52, 1974, pp. 558-562.
14. Yashitami, H., K. Oba and Y. Arima, "Heat Transfer and Pressure Drop in Tubes with Embossed Spiral", *Karysku Genshirysku Hodsuden*, Vol. 27, 1976, pp. 171-182.
15. Cunningham, J. and H.K. Milne, "The Effect of Helix Angle on the Performance of Roped Tubes", *Heat Transfer 1978, Proceedings of Sixth International Heat Transfer Conference*, Vol. 2, Hemisphere, Washington, D.C., 1978, pp. 601-605.
16. Marto, P.J., R.J. Reilly and J.H. Fenner, "An Experimental Comparison of Enhanced Heat Transfer Condenser Tubing", *Advances in Enhanced Heat Transfer*, ASME, New York, 1979, pp. 1-9.
17. Mehta, M.H. and M.R. Rao, "Heat Transfer and Frictional Characteristics of Spirally Enhanced Tubes for Horizontal Condensers", *Advances in Enhanced Heat Transfer*, ASME, New York, 1979, pp. 11-21.
18. Technical Memorandum, "YIM Heat Exchanger Tubes: Matching the Product to the Duty", *Yorkshire Imperial Metals Limited*, P.O. Box 166, Leeds LS1 1RD England.
19. Technical Memorandum, "YIM Heat Exchanger Tubes: Design Data for Horizontal Roped Tubes in Steam Condensers", *Yorkshire Imperial Alloys, IMI Yorkshire Imperial Limited*, P.O. Box 166, Leeds LS1 1RD, England.
20. "Roped Tubes for Steam Condenser", *Yorkshire Imperial Metals Limited*, P.O. Box 166, Leeds, LS1 1RD England.

21. "The Bending Characteristics of Roped Tubes", Yorkshire Imperial Metals Limited, P.O. Box 166, Leeds LS1 1RD, England.
22. "Roped Tube Data", Yorkshire Imperial Metals Limited, P.O. Box 166, Leeds LS1 1RD, England.
23. "Design Data for Roped Tubes", Yorkshire Imperial Metals Limited, P.O. Box 166, Leeds LS1 1RD, England.
24. Bergles, A.E., A.R. Blumenkrantz and J. Taborek, "Performance Evaluation Criteria for Enhanced Heat Transfer Surfaces", *Heat Transfer 1974, Japan, Society of Mechanical Engineering*, Vol. 2, pp. 239-243.
25. Reuben, M.O. *Essentials of Engineering Fluid Mechanics*, International Textbook Company, Scranton, Pennsylvania.
26. Kays, W.M., *Convective Heat and Mass Transfer*, TATA McGraw-Hill Publishing Company, Ltd., New Delhi.
27. Massey, B.S., *Mechanics of Fluid*, 4th Edition, Van Nostrand Reinhold Company.
28. Dağsöz, A.K., *Isı Geçişi*, Arpaz Matbaacılık, Istanbul, 1977.
29. Holman, J.P., *Heat Transfer*, McGraw-Hill Kogakusha, Ltd.
30. Richter, H., *Rohr Hydraulik*, Springer-Berlin, 1958.
31. Maeda Iron Works Co., Ltd., Yoshida, Nagano-Ken, Japan, "Turbotec Spiral Tube Used in Heat Transfer-Technical Data:", April 1, 1975.